Mathematical Modelling of Induced Resistance to Plant Disease

A thesis presented in partial fulfilment of the requirements for the degree of

Doctor of Philosophy

in

Mathematics

at Massey University, Albany Campus,

New Zealand.

Nurul Syaza Abdul Latif

May 2014

Abstract

The underlying theory of induced resistance (IR) is concerned with the situation when there is an increase in plant resistance to herbivore or pathogen attack that results from a plant's response triggered by an agent such as elicitors (also known as "plant activators"). This mechanism has been well studied in plant pathology literature. In this thesis, a mathematical model of induced resistance mechanism using elicitors is proposed and analysed. An adaptation of traditional Susceptible-Infected-Removed (SIR) model, this proposed model is characterised by three main compartments, namely: susceptible, resistant and diseased. Under appropriate environmental conditions, susceptible plants (S) may become diseased (D) when it is exposed to a compatible pathogen or able to resist the infection (R) via basal host defence mechanisms. The application of an elicitor enables the signal activation of plant defence genes to enhance the basal defence responses and thereby affecting the relative proportion of plants in each of the S, R and D compartments. In literature, induced resistance is described as a transient response and this scenario is modelled using reversible processes to describe the temporal evolution of the compartments. The terms in the equations introduce parameters which are determined by fitting the model to matching experimental data sets using MATLAB "fminsearch". This then gives the model's outcome to predict the relative proportion of plants in each compartment and quantitatively estimates the elicitor effectiveness. Extensions of the model are developed, which includes some factors that affect the performance of IR such as elicitor concentration and multiple elicitor applications. This IR model is also extended to include a scenario of post-pathogen inoculation for elicitor treatment. Finally, an application of optimal control theory is derived to determine the best strategy for a continuous elicitor application. Numerical evaluations of this IR model provide a potential support tool for the development of more potent elicitors and its application strategies. The model is generic and will be applicable to a range of plant-pathogen-elicitor scenarios.

Acknowledgements

Praise be to the Almighty the most Gracious most Merciful.

It would not have been possible to write this thesis without the help and support of the people around me; to some of whom only it is possible to give particular mention here.

My sincere thanks go to my mother Kamariah Abu Bakar, for her patience and continuous support throughout my studies. Her love and encouragement kept me going amidst the challenges. My thanks go also to my brothers Naufal Syafiq, Naufal Syahir, and Nabil Syahmi and also to my fiancé Raja Farid Raja Aziz, all of whom have given me their support, as always.

This thesis would not have been possible without the help, support and patience of my supervisor, Professor Graeme Wake, not to mention his advice and especially his unsurpassed knowledge of mathematical modelling. I would like to express my gratitude to the people who have contributed their time and knowledge: Dr. Phillip Elmer and Dr. Tony Reglinski of Plant & Food Research Limited (Hamilton). Their good advice and critical comments have helped me a lot in understanding the biological background of this research.

I would like to acknowledge the sponsorship from Universiti Malaysia Kelantan (UMK) and the Ministry of Education (MoE) Malaysia. Thanks are also due to the staff at the Institute of Natural and Mathematical Sciences (INMS) for their support and assistance. Appreciation is also expressed to Plant & Food Research Limited (Hamilton) for providing the experimental data used in this research.

I offer my regards and appreciation to all of those who have supported me in any respect during the course of the research, and especially to Manara, Antesar, Eman, Maryan, Kataraina, Valerie, Kerri, Sumaira, Faith and other INMS mathematics students.

Contents

List of Figures

List of Tables

Abbreviations

IR	**I**nduced **R**esistance
SIR	**S**usceptible-**I**nfected-**R**emoved
HR	**H**ypersensitive **R**esponse
BCA	**B**iological **C**ontrol **A**gent
SAR	**S**ystemic **A**cquired **R**esistance
ISR	**I**nduced **S**ystemic **R**esistance
PAL	**P**henylalanine **A**mmonia **L**yase
MeJA	**M**ethyl **J**asmonate
SSE	**S**um of **S**quares of **E**rror

Notations

R	Proportion of plant population able to express resistance to infection.	dimensionless
D	Proportion of plant population being infected and becoming diseased.	dimensionless
S	Proportion of plant population which is susceptible.	dimensionless
t	Time	[days]
α	The specific rate at which untreated plants lose their resistance due to the pathogen attack.	[days^{-1}]
β	The specific rate at which the disease spreads.	[days^{-1}]
γ	The specific rate the resistant plant becomes susceptible.	[days^{-1}]
$e(t)$	The effectiveness of the elicitor at a single application.	[days^{-1}]
k	Determines the effectiveness of the elicitor.	dimensionless
L	The time where the elicitor effectiveness is at the peak.	[days]
t_p	The induction time of the pathogen i.e. the time interval between the elicitor application and the pathogen challenge.	[days]
R_i	The proportion of the plant population that exhibits natural resistance at the initial time $t = 0$.	dimensionless
D_i	The proportion of the plant population which becomes infected immediately after the pathogen challenge.	dimensionless
a	The scaled dimensionless elicitor concentration.	dimensionless
r	The parameter determines the sub-linear effect of elicitor concentration.	dimensionless

$E(t)$	The cumulative effectiveness of the elicitor at daily application.	[days]
$c(t)$	The continuous elicitor application.	[mass days^{-1}]

Chapter 1

Introduction

1.1 Background and Research Motivation

Plants have evolved remarkable defence mechanisms to protect themselves from insects, pests, and pathogens. However, when there is an epidemic outbreak, losses from plant diseases have a significant impact on the economics apart from hunger and starvation (Agrios, 2005).

Introduction and use of disease control measures have been successful in reducing losses caused by plant disease. Plant disease management has traditionally relied on the regular application of pesticides such as fungicides and insecticides. This is because pesticides are effective across a wide range of diseases and improve crop yields. Although the use of pesticides can be beneficial, there are still potentially short and long-term risks that can harm the environment and pose a risk to human health. Thus, there are increasingly stringent constraints on the chemicals used and pressure to remove the hazardous chemicals from the market (Muilerman, 2011).

Many alternatives are available to reduce the application of pesticides such as cultural control, use of host plant resistance and chemical control (Walters, 2009). In the last 30 years biological controls have attracted increasing attention. These include induced resistance (IR), where the use of defence mechanisms that are inherent to plants is targeted. According to Cipollini & Heil (2010), IR can be defined as an

increase of resistance to a herbivore or pathogen that results from a plant's response to prior attack by the same or another attacker or to chemical or mechanical factors that mimic enemy attack. A better understanding of this IR phenomenon has led to the discovery of natural and synthetic compounds called "elicitors" that can trigger plant defence mechanisms. Unlike pesticides that are used to kill pathogens, elicitor compounds were primarily designed to improve plant resistance to pathogens. Various studies have confirmed the effectiveness of IR in suppressing diseases with a general agreement that an application of elicitor can provide between 4% and 90% disease control (Walters, 2010). This big range and the incompleteness of disease control is not a surprise since IR can be regarded as a plant response and is affected by many factors such as the environment and the aggressiveness of disease causing agents. This variable efficacy is a major hurdle affecting the implementation of IR in the current crop protection programmes. As pointed out by Walters in his published papers (Walters et al., 2005; Walters, 2010), it is important to consider the optimal timing of application, the optimal dosage for treatment and frequency of application. These considerations are crucial in order to gain a better understanding of the performance of IR before it can be potentially implemented as a practical tool for growers. The development of a mathematical model is one component in this process.

van Maanen & Xu (2003) quotes

> *"a mathematical model can be described as a simplification of reality and attempts to summarise the main process, to put forward hypotheses and to verify their coherence and consequences."*

A mathematical model allows one to investigate how complex an IR system is connected. The numerical and analytical evaluations of such model will then enable the researchers to systematically analyse the perturbations of the system and develop hypotheses to guide the design of new experimental tests. While there has been much research on modelling the biological control system, very little information is available in understanding the dynamics between the plants, pathogens and elicitors. Improved knowledge of the plant-pathogen-elicitor interaction is important in order to maximise the efficacy of elicitors used for the plant treatment to induce resistance to pathogen attacks. Thus, this proposed IR model serves as a basis for

decision-making tools for further experiments using elicitor-mediated induction of plant defence.

Therefore, the objectives of this study are:

- to develop a generic mathematical model that describes the interaction between plants, pathogens and elicitors
- to fit the model with experimental data in a custom-made case study
- to extend the generic model to include effects of elicitor treatment to manipulating IR mechanisms such as varying the elicitor concentrations applied, multiple elicitor applications and elicitor treatment after pathogen attacks
- to extend the model further to apply optimal control theory to optimise the use of elicitor application.

1.2 Outline of the Thesis

This thesis presents details of the development of the proposed IR model as outlined above. Chapter 2 provides an overview of plant pathology. The first part of the chapter is devoted to the general view of plant defence mechanism against pathogen attacks, and also plant protection technologies. The second part of the chapter focusses on the general concept of IR and its use as a plant disease management tool. Lastly, an overview of the pine system and its potential for IR to control pine diseases is presented. Common pine disease, Diplodia blight (*Diplodia pinea*), that causes pine stem canker and tip dieback to Monterey pine seedlings (*Pinus radiata*) is the case study used for this proposed IR model.

Chapter 3 is devoted to the mathematical background of modelling a biological control system. Although mathematical modelling of IR using elicitors to induce a host response specifically is lacking, some examples of mathematical models of biological control systems are presented in this chapter. Generic mathematical models by Jeger et al. (2009) and Xu et al. (2010) are discussed in this chapter, as the IR model developed for this thesis is an adaptation from these two models. This chapter also

features the method used in this thesis to estimate the unknown parameter for the proposed IR model, and an overview of Pontryagin's maximum principle.

Chapter 4 contains a full derivation of the IR model. Brief assumptions are described and the equations chosen are discussed. The experimental data set on the IR of pine seedlings is also described here. The model was derived from ordinary differential equations, and adaptations of the traditional susceptible-infected-removed (SIR) model. The IR experimental observations play an important role in choosing the suitable equations to represent IR mechanisms. The unknown parameters introduced in this model are then estimated in the next chapter.

Chapter 5 introduces the IR model for fitting the model to the matching experimental IR observations. Thus, the unknown parameters in this model can be determined. These values are then used to solve the IR model numerically, and results of the dynamical system are plotted. In Chapter 6, this IR model is extended to include the effect of IR in response to elicitor concentration, multiple elicitor applications and the post-pathogen inoculation challenge for the elicitor treatment. In each case, the numerical solutions to the models are presented.

The thesis is drawn to a close in Chapter 7 by applying Pontryagin's maximum principle to the IR model. The goal was to determine the optimal control strategy of the continuous elicitor application. Despite the fact that a continuous application might cause phytotoxicity to the plants, it is reasonable for plants that may be already infected. Thus, the model assumes that the elicitor application and pathogen challenge are introduced simultaneously, and elicitor is applied continuously until a desirable level of disease control is achieved. Attention to this optimal control problem is restricted to the case when the objective functional to be defined in a quadratic term for the control variable.

Finally, the thesis concludes in Chapter 8, with a summary of the main points from the development and analysis of the models in chapters 4–7, and offers some suggestions for future research.

Chapter 2

Plant Disease Management

All species of plants are subject to disease. In the past, major plant disease outbreaks among food crops have led to famines and mass migrations (e.g. the "Irish Potato Blight"). Therefore there is a need to ensure the disease control strategies for all economically important crops are robust enough to sustain crop yield. In this chapter, the mechanisms of plant defence are introduced. The impact of plant disease and disease control management systems are also briefly covered. The use of externally applied elicitors as a means of inducing a disease resistance response in plants are described and this chapter also includes an overview of the pine system and its IR potential to control pine disease.

2.1 Plant Defence Mechanism

Plants are very capable of defending themselves against dangers from the environment and pathogen attacks. They have evolved constitutive and inducible defence mechanisms (Walters, 2011). Constitutive defences are pre-existing physical barriers, such as thick cuticles, rigid cell walls, as well as aggressively looking thorns, needles and trichomes. In addition, plants contain pre-formed chemicals to protect themselves such as toxic and repellent compounds. An inducible defence mechanism is the second layer of plant defence, which many require gene activation. Inducible defence can be of two types: physical and biochemical responses. The physical form

of inducible defence is the strengthening of cell walls such as lignification. The biochemical response corresponds to the synthesis of antimicrobial chemicals, enzyme induction and hypersensitive response (HR).

Generally, plant defence mechanisms against the pathogen can be described as an ordered process:

1. When receptors located in the cell wall and plasma membrane detects the pathogen, it will alert via a chemical signal the surrounding cells to activate their defences (see Figure 2.1).

2. The alerted cells then release an oxidative burst that serves to create toxic environment within the cell and also to release signalling molecules to alert neighbouring cells. One of the outcomes of the oxidative burst can be cell death at the infection site; this is called the hypersensitive response (HR).

3. HR will result in sacrificing some of the plants' cells at the site of the infection in order to stop the pathogen spreading throughout the plant (Figure 2.2). This action may prevent the pathogens from getting access to water and nutrients necessary for them to survive.

The plant defence system is very complicated and only a small amount of information is currently known. The plant defence system is coordinated via a complex network of interdependent signalling pathways. Many of the mechanisms associated with the induction of plant defence are similar in many plant species.

2.2 Plant Disease Development in Agricultural Systems

Although plants have evolved a remarkable defence system, there are some pathogen populations can evolve to overcome resistance mechanisms and to cause disease. Historically, plant disease epidemics have resulted in severe economic losses where no disease control management has been applied. Frequently cited examples include the "Irish Potato Famine" between 1845 and 1852. Consequences of this catastrophic

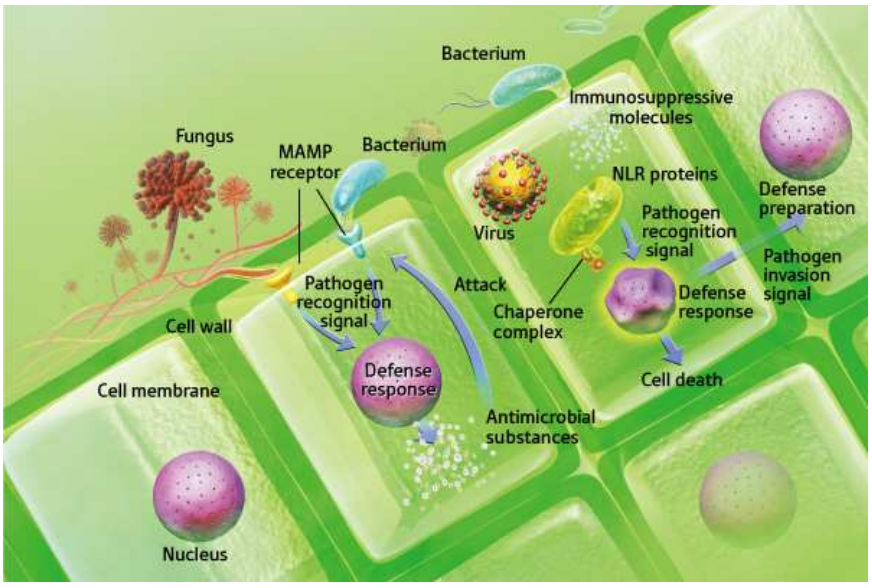

FIGURE 2.1: The schematic diagram of how the pathogen invades the plant's cells (source from: http://www.rikenresearch.riken.jp/eng/frontline/6025). When the pathogens are able to penetrate a cell, the infected plants cells release intercellular signals that prime defence mechanisms in neighbouring cells.

FIGURE 2.2: One of the signs of a plant activating their inducible defence called the hypersensitive response (HR).

Estimated Annual Crop Losses Worldwide in 2002	
Attainable crop production (2002 prices)	USD$1.5 trillion
Actual crop production (-36.5%)	USD$950 billion
Production without crop protection	USD$455 billion
Losses prevented by crop protection	USD$415 billion
Actual annual losses to world crop production	USD$550 billion
Losses caused by diseases only (14.1%)	USD$220 billion

TABLE 2.1: Crop losses due to plant disease. Numbers taken from Agrios (2005).

plant disease caused a deficit in the food supply where a million people died of starvation and almost two million migrated (Strange & Scott, 2005).

In recent years, 14.1% of the global harvest was estimated to have been lost to plant diseases caused by bacteria, fungi and viruses, at a cost of USD220 billion in 2002 (Table 2.1). The goal of disease management is to reduce this economic and aesthetic damage caused by plant disease. Thus, to ensure the economics of continuity of food supplies, significant research effort has been targeted at the development of more efficient plant disease management practices.

Plant Protection Using Old Technologies

The most common method of disease control is based on the regular application of fungicides. Globally, the use of fungicides as protection to the crop to increase crop yield has steadily increased. Issues (2011) reported that in 1970 the amount of fungicides applied globally was four million tonnes; five million tonnes in 1985; and in 2001 the tonnage had increased to six million tonnes with 85% of all fungicides used in agriculture. In India, an estimated 59 million kg of pesticides are applied annually (as cited in Pimentel (2002)).

Modern societies demand nutritious food, but at the same time they want their food to be damage-free with no disease symptoms. This is arguably difficult without pesticides. However, serious questions have been raised about the environmental and human health safety of prolonged use of synthetic agrochemicals. This has led to considerable changes in peoples' attitude towards pesticides. Today, there are increasingly stringent constraints on chemical pesticides used and there is pressure

to remove the most hazardous chemicals from the market (Muilerman, 2011) and a need for alternatives to synthetic agrochemicals.

Disease Management Based on Alternatives Technologies: Biological Control

Biological control has attracted attention as an alternative to pesticides. Biological control is a more environmentally sound strategy for reducing or mitigating disease development through the use of selected anti-microbial microorganisms. Some biological control agents (BCAs) are effective at reducing disease development and several have been commercialised (Elmer & Reglinski, 2006; Jacometti et al., 2010). In general, there are four mechanisms by which BCA's bring about a reduction of disease development (McSpadden Gardener & Fravel, 2002):

- competition
- parasitism
- antibiosis
- induced resistance (IR).

The aim of this thesis research was to explore the applicability of induced resistance in plant disease management, and this will be discussed in the next section.

2.3 Induced Resistance: A General Concept

The general concept of IR is taken to mean as the phenomenon of induced changes in resistance after attack by herbivores or pathogens. This observations of IR in plants were reported over 100 years ago (Hammerschimdt, 2007). Chester (1933) analysed these early works and concluded that this IR discovering phenomenon might play an important role in sustainability of plants in nature. In his early published paper, Chester (1933) describes IR as

> *"The vaccination of plants resulting in an increased resistance of variable duration, to subsequent infection."*

There has been some confusion in the literature about the definition of IR, and this has been confounded by different authors using the terms interchangeably. Chester (1933) used the term "vaccination" which is often compared to vaccination or immunisation in animals, but this term can be misleading; Van Loon (1997) points out there is a difference in the mechanism of immunisation between animals and plants as, unlike animals, plants possess neither a circulatory system nor immune surveillance. In recent years, there has been a general understanding about the definition of IR, and it is best described as (Cipollini & Heil, 2010)

> *"an increase in resistance to a herbivore or pathogen that results from a plant's response to a prior attack by the same or another attacker or to chemical or mechanical factors that mimic enemy attack".*

There are now two generally recognised forms of IR:

1. Systemic acquired resistance (SAR)
    - Initially characterised as a type of IR induced in response to pathogens that cause a localised, necrotic lesion. This necrotic lesion can be a result of HR.
    - Involves salicylic acid (SA) signalling pathways and is also associated with pathogenesis-related (PR) proteins.
    - SAR becomes evident to the subsequent attack.
2. Induced systemic resistance (ISR)
    - Develops systemically in response to the colonisation of roots by bacteria and fungi.
    - ISR is regulated by jasmonate acid (JA) or ethylene signalling pathways.
    - May result in the ability of the host to enhanced defence response on infection.

Figure 2.3 illustrates SAR and ISR. Although different signalling pathways are used for SAR and ISR, these two forms of resistance can be simultaneously activated in the same plant leading to enhanced resistance. Moreover, both SAR and ISR are effective against a broad spectrum of plant pathogens. In all cases of IR, SAR and ISR have a similar mechanism where IR is expressed on subsequent "challenge" inoculation. There is a time interval between the first treatment and "challenge" inoculation which is a prerequisite for effective expression of IR. This span of time is necessary for signals to be translocated to non-treated tissues and for the triggering and development of defence potential in these tissues.

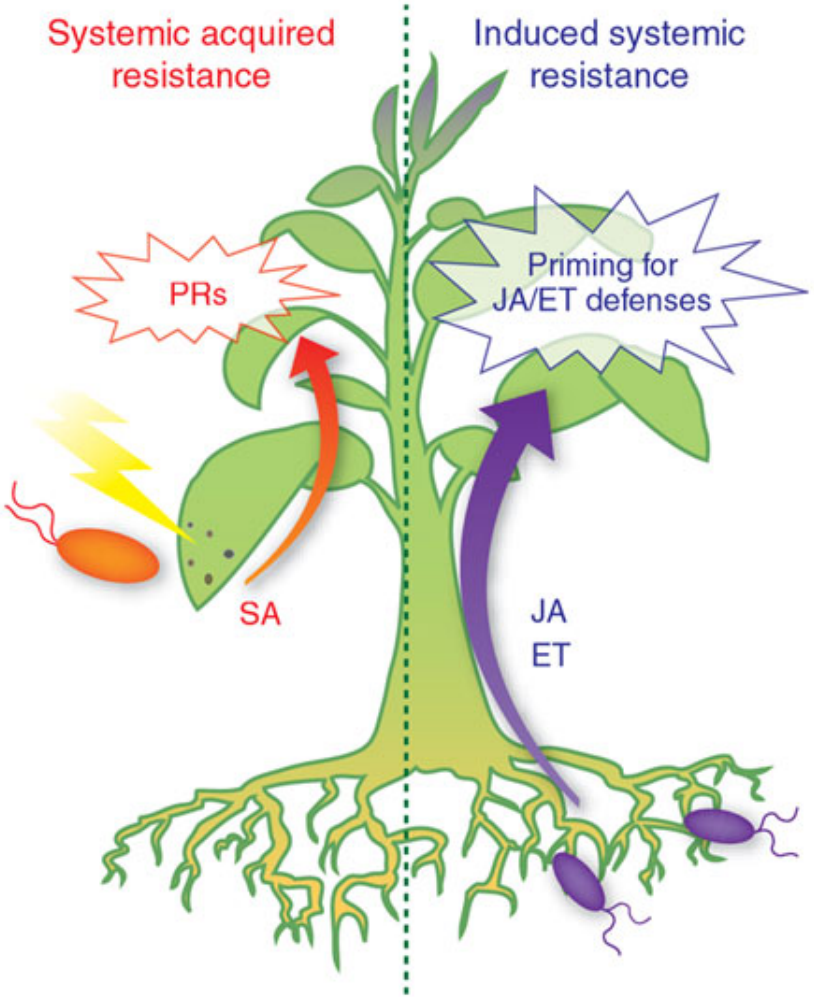

FIGURE 2.3: SAR is triggered by local infection that causes HR and involves the SA and PR signalling. ISR is induced by root colonising by bacteria and it is regulated by JA or ethylene signalling. This diagram is from Pieterse et al. (2009).

Since 1933, many studies have been developed to discover further exploitation on IR. The pioneering works by Kuć et al. (1959), Loebenstein (1963), and Ross (1966) have led to a new concept of IR in plants and its application (as cited in Kuć (2000)). IR as a plant protection strategy may assist with reduction of the use of environmentally toxic chemicals for disease control, and thus could be proposed as an alternative and more environmentally benign eco-friendly approach for plant protection. Many publications in the literature have described IR as a successful tool in plant protection. As pointed out by Walters (2010) however, one major drawback of IR is that it rarely leads to complete protection, with levels of disease control ranging from 4% to greater than 90%. IR is a host response influenced by a number of factors (see Figure 2.4), including the host plant, the virulence of the pathogen and the environment. The understanding of the interrelationship between these variables might contribute to more effective IR as a tool to control disease development. The development of a mathematical model could be one part of the process.

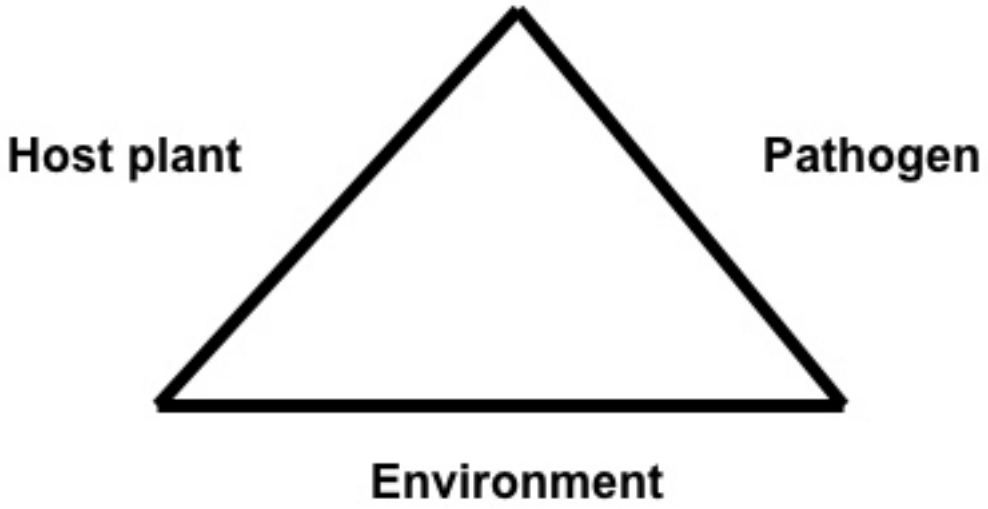

FIGURE 2.4: The disease triangle. The three necessary causal factors of disease: a host plant, a favourable environment conditions, and a pathogen to cause the disease.

2.3.1 Induced Resistance for Pathogen Control using Elicitors

The past decade has seen a rapid development in exploiting IR mechanisms. An appealing method of IR is the application of plant "activators" or elicitors to replace fungicides. In broad biological terms, an elicitor is defined as any compound that, when introduced, signals the activation or synthesis of another compound. In plant pathology, the elicitor is an important component in IR, and plays a key role in activating the plant's resistance to disease. Plant disease resistance relies on the activation of various physical and chemical defences, described in Section 2.1, and therefore this is where the elicitor application stimulate the resistance genes. By referring to Figure 2.4, elicitors develop resistance in plants as elicitors are not antimicrobial *per se* but operate instead by activating defences signalling cascades which culminate in an enhanced resistance to pathogen attack.

Elicitors can be divided into two groups (Radman et al., 2003):

1. Biotic
    - Biological origin, derived from the pathogen or from the plant itself.
2. Abiotic
    - Not of biological origin and derived from organic chemical compounds.

One biochemical response associated with resistant induction in plants is the Phenylalanine ammonia lyase (PAL) (Nicholson & Hammerschmidt, 1992). Many studies have measured PAL activity as a potential biochemical marker for elicitor activity. For example Reglinski et al. (1998); Mandal (2010); El Modafara et al. (2012) investigated PAL activity for elicitor-treated plants and they reported a transient induction of PAL where PAL activity increased then decreased back to pre-elicitation concentrations (see Figure 2.5). However, some chemical elicitors such as methyl jasmonate (MeJA) caused inhibition of PAL activity (Reglinski et al., 2012). Nevertheless, some studies in the literature suggest that the elicitors can induce a broad spectrum and long lasting resistance (Walters et al., 2013); however more commonly

it has been shown that the effectiveness of the elicitor is transient and lasts for a few weeks only.

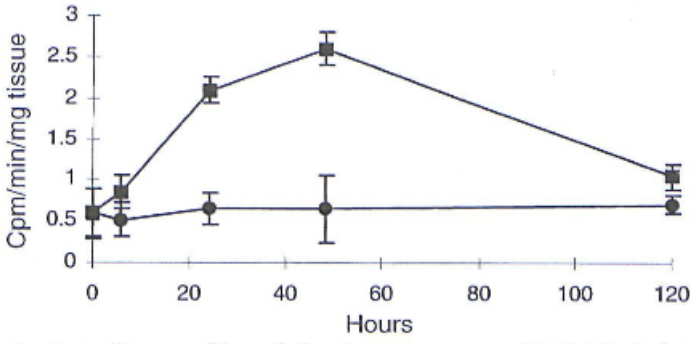

FIGURE 2.5: PAL activity of *Pinus radiata* seedlings following treatment with elicitor 2 mM 5CSA (squares) and untreated (circles). Figure is from Reglinski et al. (1998).

If IR is to be used in disease management using appropriate elicitors, the timing of the elicitor application prior to pathogen challenge plays an important role in order to be effective as a potential disease control strategy. As previously described, IR is a transient response. Therefore many studies have focused on the onset and duration of the IR response (i.e. varying the time between the initial elicitor treatment and the subsequent challenge inoculation with the pathogen). Experimental works by Soylu et al. (2003), Gould et al. (2008), and Hindumathy (2012) studied the optimum time required. They found that if the time lag between elicitor treatment and challenge inoculation is too long, the elicited or induced response is no longer effective against pathogen attack; that is, a longer induction period provided no statistically significant increase in disease control.

In spite of the fact that the elicitors can enhance a plant's defence mechanism, there is also a drawback to the use of elicitors. In greenhouse studies (e.g. Godard et al. (1999); Gould et al. (2008); Hindumathy (2012); Vivas et al. (2012)), it was shown that applications of elicitors at higher concentrations caused phytotoxicity, a toxic effect by a compound on plant growth (see Figure 2.6). Identification from these studies indicated that IR is dependent on the dose of elicitor used. There is an optimal concentration for the elicitor that maximises induction of plant defensive responses and does not cause toxic effects to the plants. In practical disease control, the frequency of elicitor application is a crucial consideration as pointed out

by Walters et al. (2013). Studies by Gould et al. (2008) and Dinh et al. (2008) found that more frequent elicitor applications appear to be phytotoxic to the plants despite the fact it suppressed disease development. A greenhouse experiment by Gould et al. (2008) showed that weekly MeJA applications did not improve disease control efficacy but reduced pine seedlings' growth and health. While a study by Dinh et al. (2008) on pre-harvest multiple MeJA treatment with three-day intervals did not show any significant difference from the water control. This is contradictory to a field study by Huang & Vallad (2012), where application of an elicitor (Acibenzolar-S-Methyl (ASM)) weekly was capable of managing bacterial spot on tomatoes compared to the bi-weekly applications.

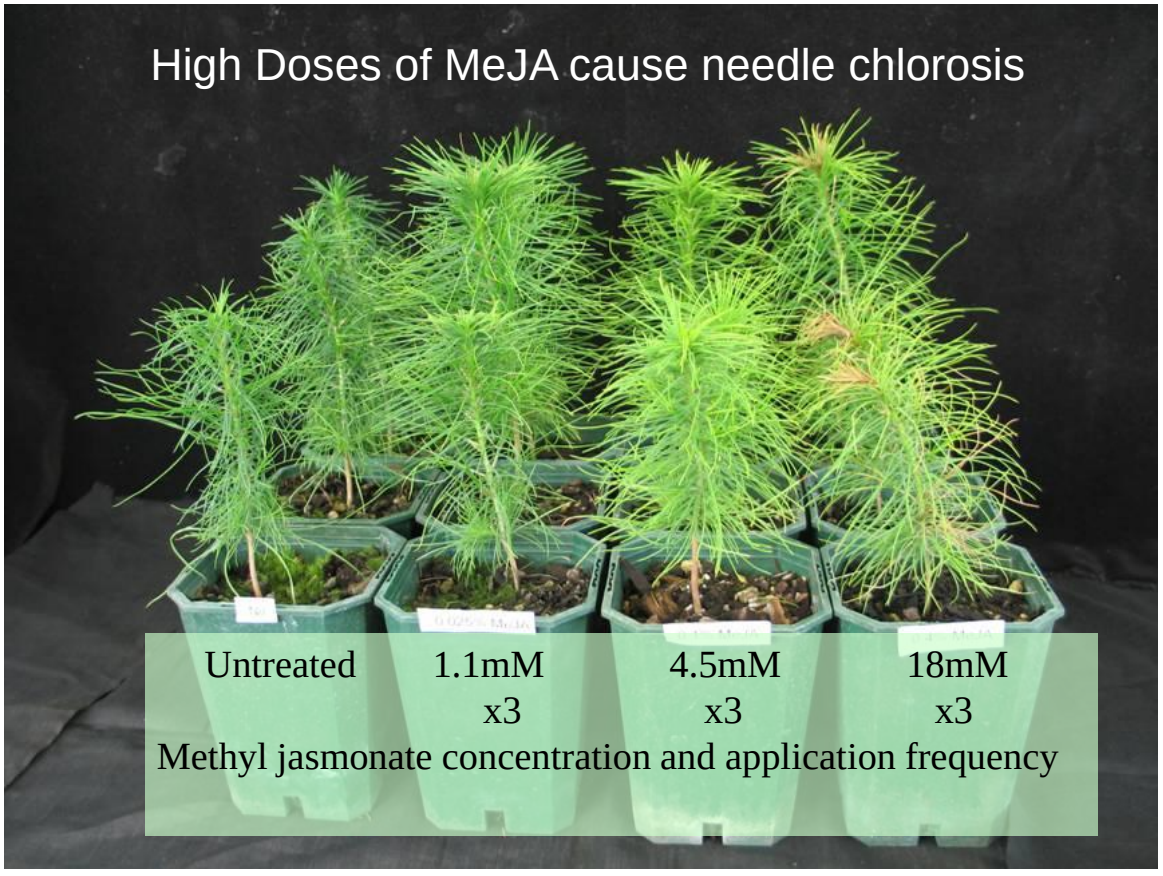

FIGURE 2.6: The phytotoxicity effects on pine seedlings after being treated with elicitor MEJA. Lab studies showed that MeJA treatment did not improve disease control efficacy and also reduced pine seedlings growth and health.

The awareness of IR, as a method for controlling plant diseases has resulted in increasing volumes of research assessing the efficacies of IR under field or commercial

production conditions (Reglinski et al., 2007). These studies have laid a foundation for the current comprehension of IR as a tool in plant protection, and therefore has led to the development of crop protectants. Some elicitor compounds (Table 2.2) have been commercially released in some countries as a plant health promoter of annual crops (Elmer & Reglinski, 2006; Reglinski et al., 2007; Walters et al., 2013; Thakur & Sohal, 2013). These elicitors have provided significant benefits (Hill et al., 1999; Walters et al., 2013):

- Reduction in the usage of pesticides and increased environmental sustainability
- Broad-spectrum disease control using plant's own resistance
- Prospect of durability where induced resistance relies on a range of plant defences and so development of pathogen resistance is unlikely
- Elicitor treatment is compatible to be integrated with other disease control methods.

Elicitor	Product Name
Acibenzolar-s-methyl	Actigard® Bion®
Chitosan	ARMOUR-Zen® Chitoplant®
Glucan and related oligosaccharides	PELIOIGV® Iodus40® Vacciplant®
Extract from giant knotweed (*Reynoutoria sachalinensis*)	Milsana®
Salicylic acid + others	Spotless Treet™

TABLE 2.2: Some example of commercial elicitors (Reglinski et al., 2011)

Despite the fact that elicitors can reduce disease severity, some questions have been asked about the safety of consuming food treated with elicitors. This dilemma has been discussed in Lyon & Newton (1997). Under European Union legislation, resistance elicitors are subject to the same requirements as other pesticides and must achieve all the required safety standards. Although some application of elicitors may cause phytotoxicity to plants, so far there is no evidence to suggest that this will have any harm effect on human or animal. This aspect is supported by the fact

that many resistance components that are increased by the elicitor treatment are normal components of plants that exist before the treatment. Conversely, there is also interest in the potential for elicitors to increase the content of bioactives with perceived human health benefits (e.g. antioxidants) (García-Mier et al., 2013).

2.4 Pine Trees: A Case Study for IR Model

2.4.1 Pine Disease and Disease Control Practice

Pines, scientifically known as *Pinus*, are conifer trees native to most of the Northern Hemisphere. There are approximately 115 species of pines worldwide. The most widely planted pine in the world is the Monterey Pine also known as *Pinus radiata*. This specific pine type, *Pinus radiata*, is commercially important for its valued timber and pulp. In New Zealand, forest nurseries produce over 50 million *Pinus radiata* annually in order to meet the demand (Reglinski & Dick, 2005).

Pine trees are large and long-lived plants, but are also exposed to pathogen attack which ultimately causes death, or disease to the point where they need to be cut. The forestry sector suffers substantial economic losses due to pine diseases. Nix in his article (Nix, 2013) listed some virulent pine diseases, and the list includes Diplodia blight of pines. This common disease affects pines worldwide, especially *Pinus radiata*, and has seriously damaged extensive plantings of this species in New Zealand. Pine blight is caused by the fungus *Diplodia pinea*. The most evident sign of a *Pinus radiata* infected with Diplodia blight is that the tree has brown, stunted new shoots with short, brown needles (Figure 2.7). Mostly younger and healthy needles of newly formed candles are infected by this fungus. Infections of *Diplodia pinea* reduce growth, deform trees, and ultimately kill them.

Some disease control management for Diplodia blight includes removing the infected twigs to reduce the amount of fungus in the tree. In addition, it is recommended not to plant young, healthy two-needle and three-needled pines near older, infected pines (Moorman, 2013). Infection of new shoots has been traditionally controlled by applying fungicide to pines. This method has reduced the infection significantly.

FIGURE 2.7: Top dieback caused by *Diplodia pinea*. Figure is from Wikipedia.

Concerns about the adverse effects of pesticides have increased interest in biological control methods.

2.4.2 The Potential of IR in Controlling Pine Disease

Induced resistance has been well studied in many agricultural systems and its application has proved effective, yet less is known for forestry. While trees and crop plants share common features, trees have certain unique features such as their larger size and much longer life spans.

In the last 15 years, there has been increasing interest in investigating IR in pine trees. Although tree protection strategies based on IR are in the early stages of conceptual development (Bonello et al., 2006; Eyles et al., 2010), there is potential for the use of IR in the management of forest systems, particularly pine trees forests. Studies in the literature have shown that biological induction in pine trees have provided effective control of pine diseases (e.g. Moreira & Zas (2009); Fitza et al. (2011); Vivas et al. (2012)).

Much work on *Pinus radiata* has been undertaken by Reglinski and his co-workers (Reglinski et al., 1998; Gould et al., 2008, 2009; Reglisnki et al., 2012). These studies found that foliar applications of chemical compounds have been shown to enhance resistance against *Diplodia pinea*. The same crucial points (e.g. timing of the applications, elicitor concentration and multiple applications) have been taken into account in these studies to investigate the efficacy of IR in suppressing Diplodia blight.

Several biological elicitors have been demonstrated to be effective for inducing resistance to a range of pathogens in *Pinus* and other coniferous species (Eyles et al., 2010). MeJA is one of the most commonly studied elicitors on pine trees, as a tool to simulate a similar response to wounding and herbivory (Holopainen et al., 2009).

2.5 Summary

Plants have evolved defence mechanisms to protect susceptible tissues from the impact of browsing by animals and loss of photosynthetic, structural and root tissues by pathogen and insect feeding. However, plants can still get infected and become diseased because some pathogen population has subsequently evolved and overcome plant resistance mechanisms. Plant disease epidemics in the past have caused severe economic losses and have even led to food shortage and famine. There are many strategies for effective disease management but the most common practice is based on the application of pesticides. Serious questions have been raised about the adverse effect of pesticides on the environment and human health. Therefore, alternative disease control strategies have been developed as synthetic pesticides are withdrawn from the market. Biological control is an alternative strategy that has gained greater acceptance by food producers in the last 20–30 years. In the last 10 years, IR as a viable, biologically based strategy has become more prominent.

The underlying theory of IR is when plant defence mechanisms are triggered by an agent prior to infection by a plant pathogen resulting in a reduction in disease infection. This agent is known as the elicitors which, via a complex cascade of resistance inducing mechanisms is capable of transforming susceptible plant tissues

into tissues with elevated levels of resistance when specific treatments are applied to the plants prior to infection. Typically, there is a lag of several days between elicitor application and the onset of IR. Some studies suggest that elicitors can induce a broad spectrum of resistance which can be long lasting; however, more commonly it has been shown that IR is transient and lasts for a few weeks only. The plant protection based on IR provides incomplete disease control, and the extent of this variability is a function of the dynamic relationship between the plant, the pathogen and the environment

The understanding of IR in crop plants has been well observed, but little is known about its use for trees as it is still in the early stages of conceptual development. In spite of this, greenhouse studies have shown that IR can contributes to the suppression of pine diseases and would fit into an integrated management strategy. Development of a prototype mathematical model of IR using pine trees as a case study, which will be discussed in Chapter 4, might help to gain better understanding of IR in trees.

Studies have shown that the efficacy of the IR using elicitors is dependent on the concentration applied and the right timing for the treatment. A new approach in exploiting IR is the frequency of elicitor treatment to reduce disease infection. These factors that affect the efficacy of the elicitor to induce plant resistance to diseases will be taken into account for modelling IR. This is further discussed in Chapter 6.

Chapter 3

Mathematical Background

This chapter outlines previous mathematical models on biological control agents (BCA) for controlling plant diseases, and an overview of parameter estimation. Lastly, the background of Pontryagin's maximum principle, used later in this thesis, is covered.

3.1 Previous Mathematical Models

3.1.1 Modelling Biological Control System

Mathematical modelling is an important tool used in studying agricultural problems. The application of mathematical theory to the problem allows a qualitative and quantitative evaluation of the interested case. Nowadays, there is a rapid expansion of studies of mathematical modelling applied to the biological control system. To have a better understanding of the dynamical system of the biological control system, one needs to investigate the interactions within the system and understand the mechanisms involved.

Researchers have usually modelled interactions within biological control systems using predator-prey theory, such as in the Lotka-Volterra model. For example, studies by Xiao & van den Bosch (2003); Kessel et al. (2005); Liu et al. (2009);

Rafikov & de Holanda Limeira (2012) used Lotka-Volterra equations to investigate the dynamics of BCA population and the success of biological control mechanisms. These methods are not restricted to the predator-prey theory; some authors (e.g. Pathak & Maiti (2012)) formulated the biological control system using equation such as Michaelis-Menten type. Moreover, authors such as Jeger et al. (2009) and Gilligan & van den Bosch (2008) conducted their studies using the susceptible-infected-removed (SIR) model, a well-known work first introduced by Kermack & Mckendrick (1927), to model the efficacy of the BCA mechanisms that suppress plant diseases.

There is a large volume of published studies describing the biological control model, but there are limits in the literature review that consider plant-pathogen-elicitor dynamics. Nevertheless, Jeger et al. (2009) developed a generic mathematical model framework in which a compartmental SIR model for plant-pathogen dynamics was coupled with BCA-pathogen dynamics (see Figure 3.1). This study was extended by Xu et al. (2010) for further numerical computations. The authors considered four main BCA mechanisms as discussed in Chapter 2: induced resistance (IR), antibiosis, competition and mycoparasitism. Each BCA mechanism had their key parameter values in order to replicate the mechanisms involved. Another study by Liu et al. (2009) presented a model of tritrophic interactions mediated by the IR (Figure 3.2), using the Lotka-Volterra model and the modified An-Liu-Johnson-Lovett model. Underwood (1999) published an article on a model describing inducible plant-herbivore systems with a quantitatively induced response. This model was designed to examine the effect of IR on herbivore population dynamics. A delay time was included in this model, which incorporates the time interval for herbivore damage and the induction response. However, it was less clear how the plants were able to become resistant against the attack by herbivores whether by pre-damage or elicitor treatment prior to subsequent attack.

The existing models fail to show the modelling of IR mechanism using elicitors. Although elicitors can be treated as a BCA, the scope for this thesis is beyond the model by Jeger et al. (2009) and Xu et al. (2010), where BCA is assumed to be part of the plant population (see Figure 3.1). Moreover, Gilligan & van den Bosch (2008) and Xiao & van den Bosch (2003) introduced the effect of the control agent to suppressed disease at a constant rate to their model which is simply not true

for the elicitor effectiveness since elicitor response is transient (as discussed in the previous chapter).

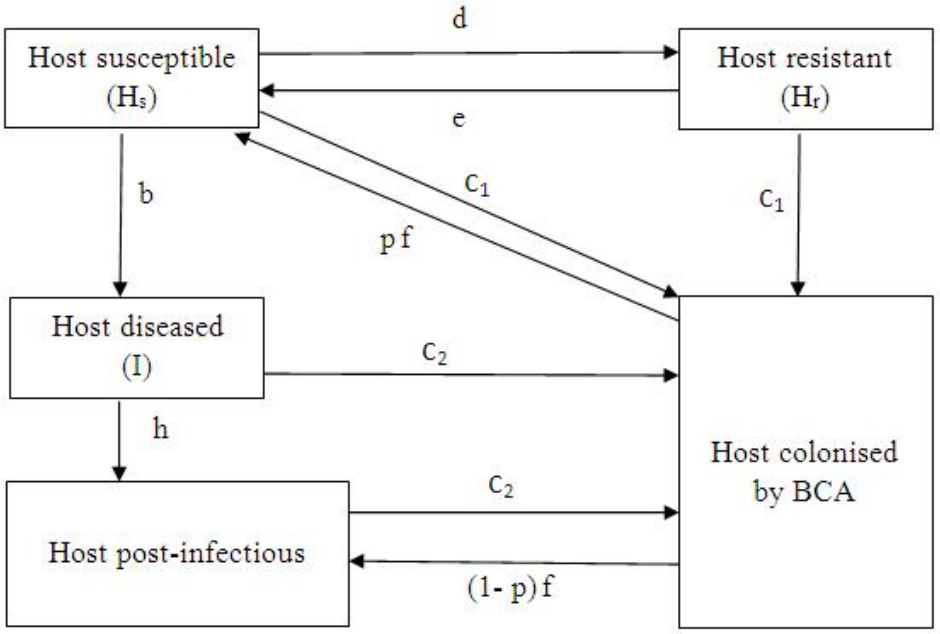

FIGURE 3.1: A simplified flow diagram describing the model by Jeger et al. (2009). The parameters correspond to the specific rates of movement between the linked compartments.

In spite of this, there are a few papers discussing a conceptual model of the length of IR (Underwood, 1998; Bonello et al., 2006). The hypothesis for IR dynamics proposed by these authors (Figure 3.3 and Figure 3.4) would be useful to formulate the IR mechanism.

3.1.2 Application of Pontryagin's Maximum Principle

There is an increasing interest in the application of Pontryagin's maximum principle in the field of agriculture. An early example is the article by Schaffer (1983). He discussed an example of a plant that can allocate the energy to leaves or seeds or stores the energy, which can be recalled at some cost to the following season (see Figure 3.5). In this simple example, Schaffer's analysis showed there exists switching

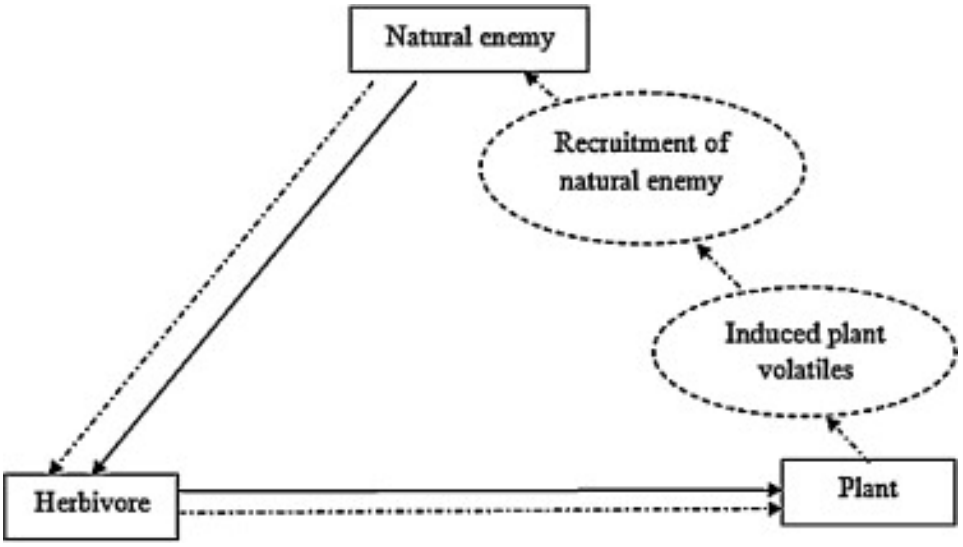

FIGURE 3.2: A schematic diagram of the conventional tritrophic system (solid lines) and induced volatiles-mediated tritrophic interactions (dotted lines). The arrows are the predation or the food web relationships interaction in the tritrophic system. When the natural enemies of the herbivore at the trophic level are attracted to the plant-herbivore system by induced volatiles, plants activate their induced chemical defensive system when they are attacked by herbivorous insects. Figure is from Liu et al. (2009).

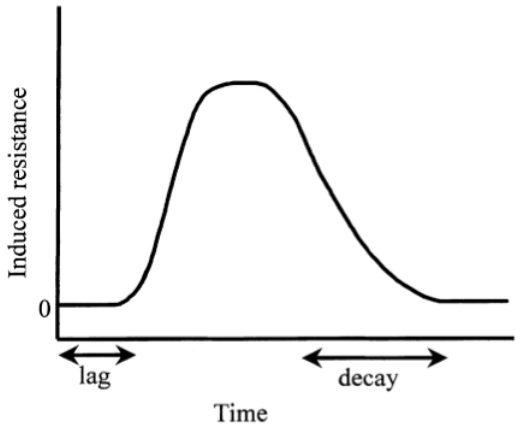

FIGURE 3.3: The conceptual model of the time course of IR presented by Underwood (1998) based on previous theoretical studies on the effect of IR on herbivore population dynamics. There is a time lag between damage and the induced response, and later IR is expected to decay over some period of time.

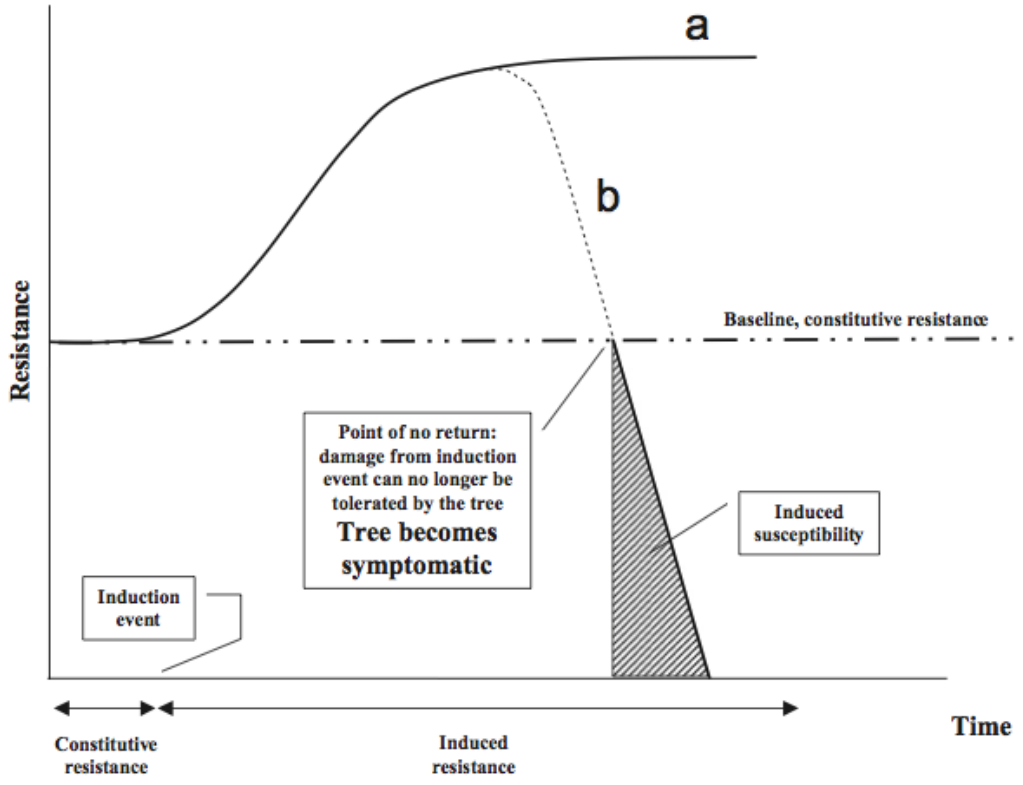

FIGURE 3.4: Diagram represents the IR hypothesis by Bonello et al. (2006). The baseline level of constitutive resistance exists in all plants, but an induction event is predicted to induce resistance against pathogens. IR is predicted to remain sustained for a period of time and this situation is described by curve **a**. If the plants are severely damaged by the pathogens and becoming visibly diseased, the resistance begins to decline and results in the plants become highly exposed to the pathogen (described by curve **b**).

functions independent of the controls. This means that in each year the plant either stores its energy for next season or for reproduction. Another example is a work published by Whittle et al. (2007) where they formulated a simple mathematical model to find the optimal solution to control an invasive plant species. The objective functional is defined to minimise the area covered by the invasive species at the end of the time period which is coupled with the control variable. The term for the control variable was chosen to be in a quadratic form for simplicity of the analysis. Although the author made several assumptions on the biological background in order to simplify the process associated with this model, the study of optimal control theory application is potentially still useful and applicable.

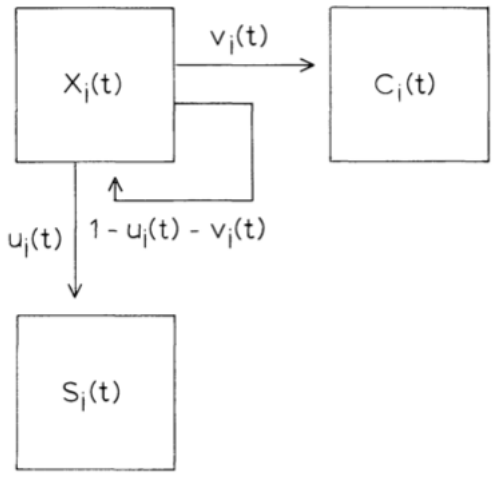

FIGURE 3.5: Schematic representation of the Schaffer (1983) model where it corresponds to a plant at age i. The energy, Carbon (calories), fixed at time t can be allocated to leaves ($X_i(t)$), stores ($C_i(t)$), or seeds ($S_i(t)$). The control variables are defined as: $u_i(t)$ is the fraction of newly fixed carbon allocated to seeds; $v_i(t)$ is the fraction allocated to stores.

Forster & Gilligan (2007) and Ndeffo Mbah & Gilligan (2013) addressed a problem of optimisation of plant disease control on a lattice with a spatial model for the spread of a plant pathogen over an agricultural region. Their goal was to minimise the total level of infection during a single agricultural season at the least possible cost of treatment. In the Forster & Gilligan (2007) study, the objective was to minimise the number of lattice sites receiving treatment. Two cases were considered in this study; those where the objective functionals are defined for short and long time scales. The difference in the objective functionals for both cases is the introduction of the discount rate in the long time scale to represent the rate which the policymaker is willing to pay. This is a trade-off between the value of treatment today against the ensuing cost of increased infection in the future. Ndeffo Mbah & Gilligan (2013) extended Forster & Gilligan (2007)'s idea to include the action of the control agent (protectant or eradication) and assume a lattice with periodic boundary conditions where each site of lattice exists in one of the following two states, healthy or infectious. Ndeffo Mbah and Gilligan assumed that if control is applied to a healthy site, the protectant action reduces the force of infection, whereas, if applied to an infected site, the eradicant action decreases the period of infection of the site. Both studies by Forster & Gilligan (2007) and Ndeffo Mbah & Gilligan (2013) used Pontragin's

maximum principle, and the optimal strategy obtained was a bang-bang type of control. Both authors agreed the main challenge with such a control strategy is the optimal switching times are generally unknown. They made some assumptions in order to determine the switching time analytically. Unfortunately, there is a risk of missing the optimal switching time which may drastically affect the outcome.

One simple optimal control problem quite relevant to this thesis is the example presented by Graves (2010) in her thesis. This concerned a fungus infestation controlled by the periodic application of fungicide and the model is formulated in discrete time. The objective of this control problem was to minimise the concentration of fungus at the final time and the cost of applying the control. For simplification, the author fixed the number of control applications and the final time in advance. The objective functional is the sum of the cost of fungus infestation which is proportional to the concentration of fungicide at the final time. Graves also defined the control function in a quadratic form, thus eliminating the possibility of a bang-bang type of control. This example would have been more interesting if the optimal control problem was adapted to the continuous time with the discount rate included in the objective functional.

3.2 Parameter Estimation: Least-squares Method

Normally, biological processes are modelled using ordinary differential equations (ODEs) which describe the evolution, over time, of certain quantities. A special feature of biological models is that they usually contain a numbers of parameters (such as reaction rates, production rates and decay coefficients) that have a physical meaning. Most of the parameters are unknown and it might be feasible to measure them experimentally; but in many cases this is either difficult, expensive, time consuming or otherwise impossible. However, these unknown parameters may possibly be determined from the experimental data, using parameter estimation methods.

According to Gibbs (2011), the problem of estimating parameters in a model can be visualised as a study of inverse modelling (see Figure 3.6). A parameter estimation method could help to determine adequate values for the most uncertain model input

parameters that cannot be deduced routinely through experimentation or expert judgment. It is crucial to have the knowledge of these parameter values for the mathematical model whenever one wants to obtain quantitative or even qualitative information from the model.

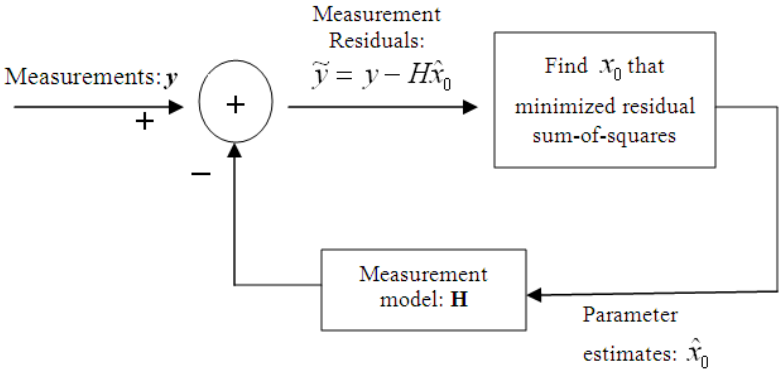

FIGURE 3.6: Least-squares solution to inverse modelling (from Gibbs (2011)).

Least-squares Method

Parameter estimation problems are often formulated as an optimisation problem. There are many ways of estimating parameters but the least-squares method is the most widely applied. This is because of its practicality in analysing various types of experimental data. In this method, estimation is accomplished by solving an optimisation problem in which the objective function containing the unknown parameters is being minimised. The results are the set of parameters that produce the best fit between simulations and experimental data.

Johnson & Faunt (1992) stated that there are six assumptions which must be made to implement the parameter estimation by the least-squares method. The assumptions are:

1. All the experimental uncertainties can be attributed to the dependent variables.

2. The experimental errors of the data follow a normal distribution.

3. No systematic error exists in the data.

4. The functional form of the selected model is correct.

5. There are enough data points to provide a good sampling of the experimental data.

6. The observations (data points) are independent of each other.

Least-squares methods are divided into two categories :

- linear / ordinary least-squares method
- non-linear / total least-squares method.

The ordinary least-squares method is based on minimising the vertical distance between the experimental measurements and the model's curve, whereas the total least-squares method is based on minimising the orthogonal distance between the measurement to the curve (see Figure 3.7). In this thesis, the ordinary least-squares method was used to estimate the unknown parameters in the IR model (see later in Chapter 5).

If given a data set consisting of a set of N points, and a vector $\mathbf{p} = (p_1, p_2, ..., p_n)$ of unknown parameters, then the least sum of squares of error (SSE) is minimised to obtain the parameter estimates:

$$SSE = \sum_{i=1}^{N} [y(t_i) - f(t_i; \mathbf{p})]^2, \tag{3.1}$$

where

- t_i is the independent variable that is treated as the observation time
- y_i is the dependent variable or the experimental measurement

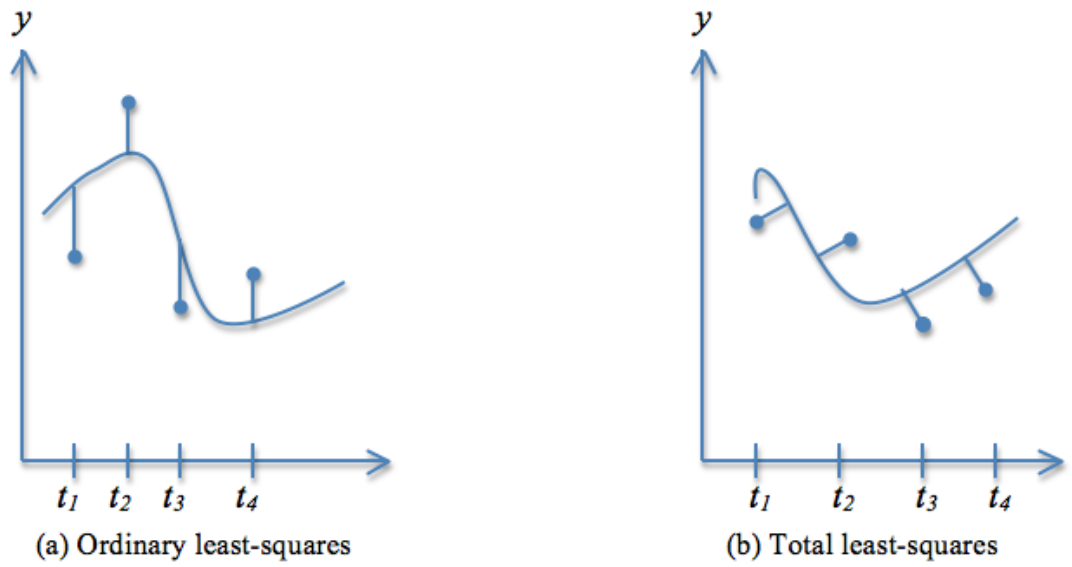

FIGURE 3.7: Graphical comparison between ordinary least-squares and total least-squares methods. The ordinary least-squares is based on minimising the vertical distance between the experimental data and the model simulation, whereas the total least-squares estimate minimises the orthogonal distance.

- $f(t_i; \mathbf{p})$ is a function of the independent variable that is the model simulation curve
- $\mathbf{p}$ vector of unknown parameters which needs to be evaluated.

The least-squares minimisation for linear models can usually be done analytically. On the other hand, for a nonlinear model it is done using iterative numerical algorithm (such as Nelder-Mead simplex method and Gauss-Newton method) to evaluate the "optimal values" for $\mathbf{p}$. For this study, a MATLAB built-in tool called "fminsearch" which is an application of Nelder-Mead simplex method, was used to estimate the unknown parameters. In this case, the SSE is used, as the objective function and initial guesses of each parameter need to be provided. The function "fminsearch" will find the optimal value of each parameter to achieve the best model fit.

For nonlinear problems, there is a possibility that multiple local minima of the SSE exists. This means there may be more than one set of the parameters; each will yield a relative minimum in the SSE (see Figure 3.8). The values of the SSE for

the multiple minima may or may not have the same value. Once "fminsearch" have converged to a minimum, there is no guaranteed means of determining whether it is a unique or even the global minimum. To check the minimum value attained is the global minimum; start the "fminsearch" procedure at several different estimates for the parameters. If the final results are independent of the initial values, there is more confidence that the final parameter values describe a global minimum.

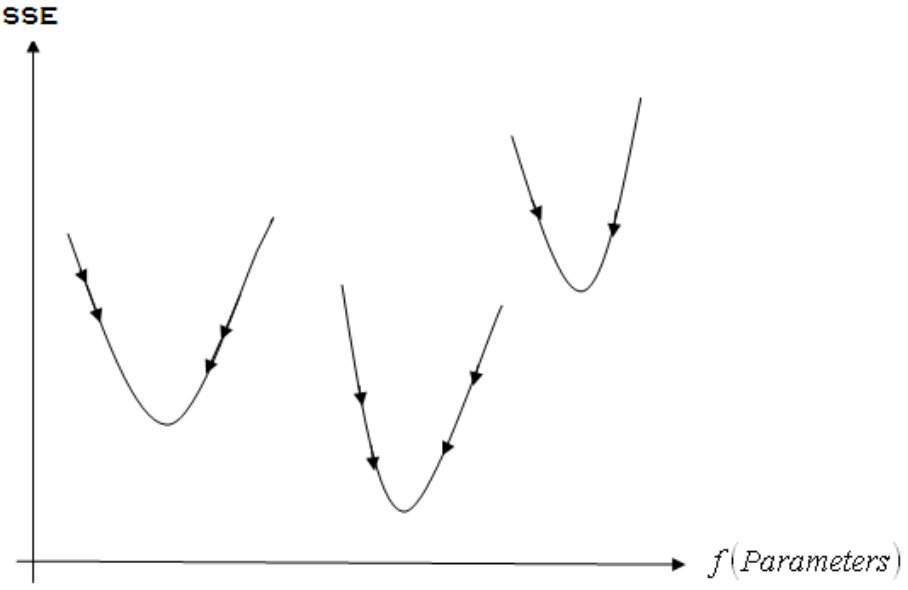

FIGURE 3.8: Illustrative of multiple minima for non-linear parameter estimation.

3.3 Maximum Principle of Pontryagin: An Introduction

The well-known work by Russian mathematician Lev Semenovich Pontryagin and his student (Boltyanskii et al., 1956) [translated into English (Pontryagin et al., 1962)] has been a powerful method for the computation of optimal control. This method is essentially an extension of the classical variational techniques of Euler, Lagrange, Legendre, Weierstrass, Hamilton and Jacobi (Clark, 1990). Pontryagin's maximum (or minimum) principle is used in optimal control theory to find the best

manner of control to take a dynamical system from one state to another. This is particularly so in the presence of constraints for the state of input controls.

3.3.1 The Optimal Control Problem

From Clark (1990), the optimal control problem of one-dimensional ordinary differential equations (ODEs) with real values consists of $u(t)$ as the control variable and $x(t)$ as the state variable. The state equation describes the evolution of the system from its initial state x_0 resulting from the application of a given control $u = u(t)$. That is to say,

$$\frac{dx}{dt} = f(t, x(t), u(t)), \quad 0 \leq t \leq T, \tag{3.2}$$

with initial condition

$$x(0) = x_0. \tag{3.3}$$

Where $f(x, t, u)$ is the state function and T is the terminal time (suppose here that T is finite).

Then, there is an objective functional

$$J\{u\} = \int_0^T g(t, x(t), u(t))\ dt \tag{3.4}$$

where $g(x, t, u)$ is a given, continuously differentiable function and $x(t)$ denotes the response to $u(t)$. The fundamental problem in optimal control theory is to determine a feasible control $u(t)$ that maximises $J\{u\}$. Such a control, if it exists, is called an *optimal control*. The Pontryagin's maximum principle gives certain necessary conditions that must be satisfied by an optimal control. Pontryagin introduced the "adjoint" functions to append the differential equation to the objective functional (Lenhart & Workman, 2007).

The Necessary Condition

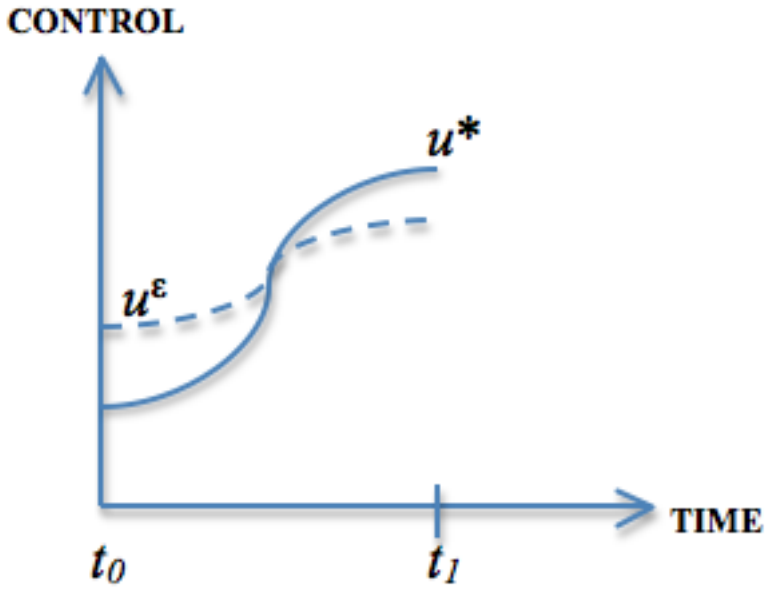

FIGURE 3.9: The optimal control u^* plotted together with u^ε.

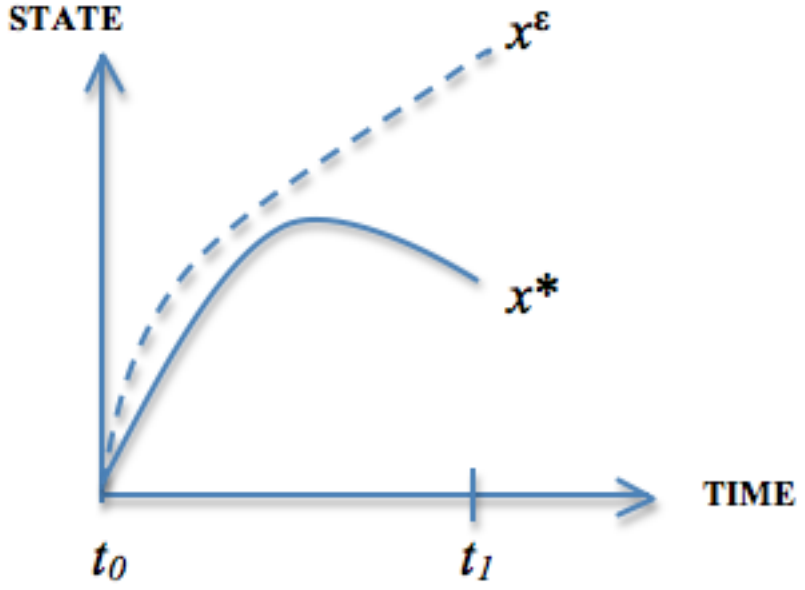

FIGURE 3.10: The optimal control x^* plotted together with x^ε.

To derive this necessary condition (following Lenhart & Workman (2007)), assume there exists a piecewise continuous optimal control in which u^* is a control and x^* is the corresponding state. Suppose that $J(u) \leq J(u^*) < \infty$ for all controls u. Next, let $h(t)$ be a piecewise continuous function and $\varepsilon \in \Re$ a constant. Then

$$u^{\varepsilon}(t) = u^*(t) + \varepsilon h(t) \tag{3.5}$$

is a piecewise continuous control function (see Figure 3.9).

Let $x^{\varepsilon}(t)$ be the state corresponding to the control $u^{\varepsilon}(t)$, then $x^{\varepsilon}(t)$ satisfies

$$\frac{d}{dt}x^{\varepsilon}(t) = f(t, x^{\varepsilon}(t), u^{\varepsilon}(t)). \tag{3.6}$$

It is easily seen that $u^{\varepsilon}(t) \to u^*(t)$ for all t as $\varepsilon \to 0$. Furthermore, for all t

$$\left.\frac{\partial u^{\varepsilon}(t)}{\partial \varepsilon}\right|_{\varepsilon=0} = h(t).$$

The same reasoning is true for $x^{\varepsilon}(t)$ because of the assumptions made on f where that it is a continuously differentiable function. If $\varepsilon \to 0$, then it follows that

$$x^{\varepsilon}(t) \to x^*(t)$$

for each fixed t. Further, the derivative

$$\left.\frac{\partial x^{\varepsilon}(t)}{\partial \varepsilon}\right|_{\varepsilon=0}$$

exists for each t.

The objective functional at u^{ε} is

$$J(u^{\varepsilon}) = \int_{t_0}^{t_1} g(t, x^{\varepsilon}(t), u^{\varepsilon}(t))\ dt. \tag{3.7}$$

The maximum of J with respect to ε occurs at $\varepsilon = 0$. Let $\lambda(t)$ be a piecewise differentiable function on $[t_0, t_1]$. By the fundamental theorem of Calculus,

$$\int_{t_0}^{t_1} \frac{d}{dt}[\lambda(t)x^{\varepsilon}(t)]\ dt = \lambda(t_1)x^{\varepsilon}(t_1) - \lambda(t_0)x^{\varepsilon}(t_0)$$

which implies

$$\int_{t_0}^{t_1} \frac{d}{dt}[\lambda(t)x^{\varepsilon}(t)]\ dt - \lambda(t_1)x^{\varepsilon}(t_1) + \lambda(t_0)x^{\varepsilon}(t_0) = 0. \tag{3.8}$$

Here, $\lambda(t)$ is a Lagrange multiplier (or called the *adjoint variable*).

Then adding the left-hand side of Equation (3.8) to Equation (3.7) gives

$$J(u^{\varepsilon}) = \int_{t_0}^{t_1} \left[g(t, x^{\varepsilon}(t), u^{\varepsilon}(t)) + \frac{d}{dt}\lambda(t)x^{\varepsilon}(t) \right]\ dt - \lambda(t_1)x^{\varepsilon}(t_1) + \lambda(t_0)x^{\varepsilon}(t_0).$$

By the product rule, and from Equation (3.6), the above expression can be written as

$$\begin{aligned} J(u^{\varepsilon}) \quad = \quad & \int_{t_0}^{t_1} [g(t, x^{\varepsilon}(t), u^{\varepsilon}(t)) + \lambda'(t)x^{\varepsilon}(t) + \lambda(t)f(t, x^{\varepsilon}(t), u^{\varepsilon}(t))]\ dt \\ & -\lambda(t_1)x^{\varepsilon}(t_1) + \lambda(t_0)x^{\varepsilon}(t_0). \end{aligned}$$

Since the maximum of J with respect to the control u occurs at u^*, the derivative of $J(u^{\varepsilon})$ with respect to ε (in the direction h) is zero.

$$0 = \left.\frac{dJ(u^{\varepsilon})}{d\varepsilon}\right|_{\varepsilon=0} = \lim_{\varepsilon \to 0} \frac{J(u^{\varepsilon}) - J(u^*)}{\varepsilon}. \tag{3.9}$$

Therefore,

$$\begin{aligned} 0 \quad = \quad & \left.\frac{dJ(u^{\varepsilon})}{d\varepsilon}\right|_{\varepsilon=0} \\ = \quad & \left[\int_{t_0}^{t_1} \frac{\partial}{\partial \varepsilon}[g(t, x^{\varepsilon}(t), u^{\varepsilon}(t)) + \lambda'(t)x^{\varepsilon}(t) + \lambda(t)f(t, x^{\varepsilon}(t), u^{\varepsilon}(t))]\ dt \right] \Bigg|_{\varepsilon=0} \\ & -\left.\frac{\partial}{\partial \varepsilon}\lambda(t_1)x^{\varepsilon}(t_1)\right|_{\varepsilon=0} + \left.\frac{\partial}{\partial \varepsilon}\lambda(t_0)x^{\varepsilon}(t_0)\right|_{\varepsilon=0}. \end{aligned}$$

From Figure 3.10, take $x^{\varepsilon}(t_0) = x_0$ yields

$$\frac{\partial}{\partial \varepsilon}\lambda(t_0)x^{\varepsilon}(t_0) = \frac{\partial}{\partial \varepsilon}\lambda(t_0)x_0 = 0,$$

Then,

$$\begin{aligned} 0 \;=\; & \left[\int_{t_0}^{t_1} \frac{\partial}{\partial \varepsilon}[g(t, x^{\varepsilon}(t), u^{\varepsilon}(t)) + \lambda'(t)x^{\varepsilon}(t) + \lambda(t)f(t, x^{\varepsilon}(t), u^{\varepsilon}(t))]\, dt\right]\Big|_{\varepsilon=0} \\ & -\frac{\partial}{\partial \varepsilon}\lambda(t_1)x^{\varepsilon}(t_1)\Big|_{\varepsilon=0}. \end{aligned}$$

Applying the chain rule to g and f

$$\begin{aligned} 0 \;=\; & \int_{t_0}^{t_1} \left[g_x \frac{\partial x^{\varepsilon}}{\partial \varepsilon} + g_u \frac{\partial u^{\varepsilon}}{\partial \varepsilon} + \lambda'(t)\frac{\partial x^{\varepsilon}}{\partial \varepsilon} + \lambda(t)\left(f_x \frac{\partial x^{\varepsilon}}{\partial \varepsilon} + f_u \frac{\partial u^{\varepsilon}}{\partial \varepsilon}\right)\right]\Big|_{\varepsilon=0} dt \\ & -\frac{\partial}{\partial \varepsilon}\lambda(t_1)x^{\varepsilon}(t_1)\Big|_{\varepsilon=0} \end{aligned}$$

where the arguments of the g_x, g_u, f_x, f_u terms are $(t, x^*(t), u^*(t))$. Rearranging the above term and recalling Equation (3.5) gives

$$\begin{aligned} 0 \;=\; & \int_{t_0}^{t_1} \left[(g_x + \lambda(t)f_x + \lambda'(t))\frac{\partial x^{\varepsilon}}{\partial \varepsilon}\Big|_{\varepsilon=0} + (g_u + \lambda(t)f_u)h(t)\right] dt \\ & -\frac{\partial}{\partial \varepsilon}\lambda(t_1)x^{\varepsilon}(t_1)\Big|_{\varepsilon=0}. \end{aligned} \tag{3.10}$$

The adjoint function is chosen to simplify the above function by making the coefficient of $\dfrac{\partial x^{\varepsilon}(t)}{\partial \varepsilon}\Big|_{\varepsilon=0}$ vanish. So,

$$g_x + \lambda(t)f_x + \lambda'(t) = 0$$

Thus, the adjoint function $\lambda(t)$ satisfies

$$\lambda'(t) = -[g_x(t, x^*(t), u^*(t)) + \lambda(t)f_x(t, x^*(t), u^*(t))] \tag{3.11}$$

Also, the boundary condition $\lambda(t_1) = 0$.

Therefore, the Equation (3.10) reduces to

$$0 = \int_{t_0}^{t_1} \left[g_u(t, x^*(t), u^*(t)) + \lambda(t) f_u(t, x^*(t), u^*(t)) \right] h(t)\ dt.$$

Since $h(t)$ is an arbitrary variation, it holds in particular for

$$h(t) = g_u(t, x^*(t), u^*(t)) + \lambda(t) f_u(t, x^*(t), u^*(t))$$

for all $t_0 \leq t \leq t_1$. Then,

$$0 = \int_{t_0}^{t_1} \left[g_u(t, x^*(t), u^*(t)) + \lambda(t) f_u(t, x^*(t), u^*(t)) \right]^2\ dt,$$

which implies the *optimality condition*

$$g_u(t, x^*(t), u^*(t)) + \lambda(t) f_u(t, x^*(t), u^*(t)) = 0 \tag{3.12}$$

for all $t_0 \leq t \leq t_1$.

The Equations (3.11) and (3.12) form a set of necessary conditions that an optimal control and state variables must satisfy. These necessary conditions can be generated from the Hamilton, $\mathcal{H}$, which is defined as

$$\mathcal{H} = g(t, x(t), u(t)) + \lambda(t) f(t, x(t), u(t)). \tag{3.13}$$

If the optimal control $u(t)$ happens to be at $u^*(t)$, then the *optimality condition* is

$$\frac{\partial \mathcal{H}}{\partial u} = 0. \tag{3.14}$$

While the *adjoint equation* is defined as

$$\frac{d\lambda}{dt} = -\frac{\partial \mathcal{H}}{\partial x} = -\frac{\partial g}{\partial x} - \lambda(t)\frac{\partial f}{\partial x}. \tag{3.15}$$

There is a *transversality condition* which states that the adjoint variable is zero at every end point where the corresponding state variable is not specified; that is, if there is no terminal value (called the *terminal condition*) labelled as

$$x(t_1) = x_T \tag{3.16}$$

specified for the state variable, then the problem is referred to as a *free terminal-value problem*, and

$$\lambda(T) = 0. \tag{3.17}$$

3.3.2 Pontraygin's Maximum Principle

The above Equations (3.13)–(3.17), can be extended to Pontryagin's maximum principle (Pontryagin et al., 1962).

Theorem 3.1. (From Lenhart & Workman (2007))
If $u^*(t)$ and $x^*(t)$ are optimal for the system as in Equations (3.2)–(3.4), then there exists a piecewise differentiable adjoint variable $\lambda(t)$ such that

$$\mathcal{H}(t, x^*(t), u(t), \lambda(t)) \leq \mathcal{H}(t, x^*(t), u^*(t), \lambda(t))$$

for all controls u at each time t, where the Hamiltonian $\mathcal{H}$ is

$$\mathcal{H} = g(t, x(t), u(t)) + \lambda(t) f(t, x(t), u(t))$$

and

$$\begin{aligned} \frac{d\lambda}{dt} &= -\frac{\partial \mathcal{H}(t, x^*(t), u^*(t), \lambda(t))}{\partial x}, \\ \lambda(t_1) &= 0. \end{aligned}$$

Theorem 3.2. (From Lenhart & Workman (2007))
Suppose that $g(t, x, u)$ and $f(t, x, u)$ are both continuously differentiable functions in their three arguments and concave in u. Suppose u^* is an optimal control for problem in Equations (3.2)–(3.4), with associated state x^*, and λ a piecewise differentiable

function with $\lambda(t) \geq 0$ *for all* t. *Suppose for all* $t_0 \leq t \leq t_1$

$$0 = \mathcal{H}_u(t, x^*(t), u(t), \lambda(t)).$$

Then for all controls u *at each* $t_0 \leq t \leq t_1$ *implies*

$$\mathcal{H}(t, x^*(t), u(t), \lambda(t)) \leq \mathcal{H}(t, x^*(t), u^*(t), \lambda(t)).$$

The same argument applies for the minimisation problem to generate the necessary conditions. In a minimisation problem, the Hamiltonian is minimised point-wise. Therefore, the inequality above is defined in the reverse order with the functions g and f being convex in u. Hence,

$$\mathcal{H}(t, x^*(t), u(t), \lambda(t)) \geq \mathcal{H}(t, x^*(t), u^*(t), \lambda(t))$$

by the same argument as in Theorem 3.2.

The property of the Hamiltonian, $\mathcal{H}$, is very useful to find the necessary conditions in which one does not need to calculate the integral in the objective functional. The necessary condition can be calculated by the property of the Hamiltonian being maximised (or minimised) by an optimal control.

To determine the controls that maximise or minimise the objective functional, one can check using

$$\text{concavity condition} = \begin{cases} \dfrac{\partial^2 \mathcal{H}}{\partial u^2} < 0 & \text{at } u^* \quad \text{if the problem is maximisation,} \\ \dfrac{\partial^2 \mathcal{H}}{\partial u^2} > 0 & \text{at } u^* \quad \text{otherwise.} \end{cases} \tag{3.18}$$

To apply the Maximum Pontryagin Principle, one needs to determine three unknown functions: $x(t)$, $u(t)$ and $\lambda(t)$. Three equations are known i.e. the state equation [Equation (3.2)], the adjoint equation [Equation (3.15)] and the optimality condition [Equation (3.14)]. The Equations (3.2) and (3.15) are first order ODEs, their solution requires the specification of initial or terminal conditions which are included in

the problem: Equation (3.3) and Equation (3.17). This presents the problem as a boundary value problem (BVP). Analytical solutions can be found in various special cases but, generally, it is necessary to solve the BVP by numerical techniques.

Generally, if given a system of n state variables and m control variables, then the optimal control problem is:

$$\text{minimise} \qquad \int_0^T g(t, x_1, x_2, ..., x_n, u_1, u_2, ..., u_m)\ dt,$$

subject to

$$\frac{dx_i}{dt} = f_i\left(t, x_1, x_2, ..., x_n, u_1, u_2, ..., u_m\right) \qquad 0 \leq t \leq T,$$

with boundary conditions

$$x_i(t_0) = x_{i_0} \qquad x_i(T) = x_{i_T}$$

where $i = 1, 2, ..., n$. The functions g and f_i are continuously differentiable in all variables. Also, each component u is assumed to be a piecewise-continuous function of t. Using vector notation, let

$$\begin{aligned}
\vec{x} &= (x_1, x_2, ..., x_n), \\
\vec{u} &= (u_1, u_2, ..., u_m), \\
\vec{f} &= (f_1(t, \vec{x}, \vec{u}), f_2(t, \vec{x}, \vec{u}), ..., f_n(t, \vec{x}, \vec{u})), \\
\vec{x}(t_0) &= (x_{1_0}, x_{2_0}, ..., x_{n_0}), \\
\vec{x}(T) &= (x_{1_T}, x_{2_T}, ..., x_{n_T}),
\end{aligned}$$

The optimal control problem then can be written in a simplified vector form

$$\text{minimise} \qquad \int_0^T g(t, \vec{x}, \vec{u})\ dt, \tag{3.19}$$

subject to

$$\frac{d\vec{x}}{dt} = \vec{f}(t, \vec{x}, \vec{u}),$$

with boundary conditions

$$\vec{x}(t_0) = \vec{x}_0 \qquad \vec{x}(T) = \vec{x}_T.$$

Therefore, the Hamiltonian can be defined as

$$\mathcal{H} = g(t, \vec{x}, \vec{u}) + \vec{\lambda}(t) \cdot \vec{f}(t, \vec{x}, \vec{u}).$$

Here $\vec{\lambda}(t) = (\lambda_1(t), \lambda_2(t), ..., \lambda_n(t))$ is a piecewise differentiable vector-valued function where λ_i is the adjoint variable corresponding to x_i. The "$\cdot$" is the dot product for vectors. Let $\vec{u}^*$ and $\vec{x}^*$ be a vector of optimal control functions and a vector of the corresponding optimal state variables that minimises Equation (3.19), respectively. Then, by essentially the same arguments for the one-dimensional system, the adjoints vector $\vec{\lambda}$ satisfies:

$$\begin{aligned} \frac{d\lambda_j}{dt} &= -\frac{\partial \mathcal{H}}{\partial x_j} \qquad \text{for} \quad j = 1, 2, ..., n \ , \\ \frac{\partial \mathcal{H}}{\partial u_k} &= 0 \quad \text{at } {u_k}^* \qquad \text{for} \quad k = 1, 2, ..., m \ . \end{aligned}$$

3.4 Summary

Many studies in the field of agricultural, especially in biological control systems, have applied mathematical theory, such as the SIR model, as tools to investigate the dynamics of a biological control system. This is crucial to understand the mechanisms involved in biological control, how they interact and how they are demonstrated at different levels; that is from the infection area to the ecosystem scale. Moreover, Pontryagin's maximum principle has been widely used in agricultural fields; for example, to control the cost of production of the crop yield.

The mathematical models formulated obviously contain several numbers of parameters that have physical meanings. Most of the parameters are unknown and are sometimes impossible to measure experimentally. However, the unknown parameters can be determined using parameter estimation by fitting the model with the experimental measurements. This is done by minimising the distance between the measurements and the model. The method is known as least-squares. In this thesis, the ordinary least-squares method is used to estimate the parameter values.

Chapter 4

Mathematical Modelling of Induced Resistance

In this chapter, a mathematical model is formulated that represents the efficacy of elicitors in inducing resistance to pathogen infection as discussed in Chapter 2. The majority of this chapter covers a full derivation of the proposed IR model along with the descriptions of the experimental datasets.

This chapter is part of an article published in Journal Frontiers Plant Science (see Abdul Latif et al. (2013)).

4.1 Introduction

When constructing a mathematical model, there are many factors influencing the mechanism, such as natural biological processes, that can be realistically implemented into the model and that can mimic the dynamic behaviour within the biological system. However, a decision must be made about what to include in the model and what to exclude. While it is true that large, detailed models are easier to "sell" to a biological audience since it is more biologically realistic - the level of complexity in such a detailed model poses many problems. For instance, with a large number of parameters, it is not possible to determine the accuracy of the parameter

values, and a study of the parameter sensitivity is also a very difficult task. Recall that parameter values must be chosen carefully so that the model exhibits realistic behaviour.

Although simple models contain the essential mechanism of the interested process, they can often provide unforeseen insight into the biological process. With simple models, it is easier to see what mechanisms are driving the model's behaviour. Consequently, models can feed back directly into the biological understanding of a process.

In this study, a mathematical model is developed in order to include the key mechanism of induced resistance (IR) which is triggered by the elicitor treatment. Such a model has not been proposed in the literature.

4.2 Descriptions of the Experimental Datasets

This section contains a brief description of the IR experiment and full information on fitting the datasets will be in the next chapter. The available experimental datasets were provided by Plant & Food Research Ltd and the datasets were judged as appropriate for this proposed model. This experimental data was associated with the effect of an elicitor called methyl jasmonate (MeJA) on the pine seedling, *Pinus radiata*, to the causal agent of pine stem canker and tip dieback, *Diplodia pinea*.

To date various methods have been developed and introduced to measure IR. For this study, the IR experiment was prepared according to the procedure used by Gould et al. (2009). The pine seedlings were divided into groups of 20 plants and sprayed with 0.1% MeJA at few days before inoculation with *D. pinea*. There were also a group of 20 untreated seedlings as the control group for this experiment. For this experiment, the pathogen was introduced via a wound site, simulated by physically removing a pine needle.

Disease assessments for each treatment commenced one week after inoculation and continued at three-to-four day intervals thereafter for at least 20 days.

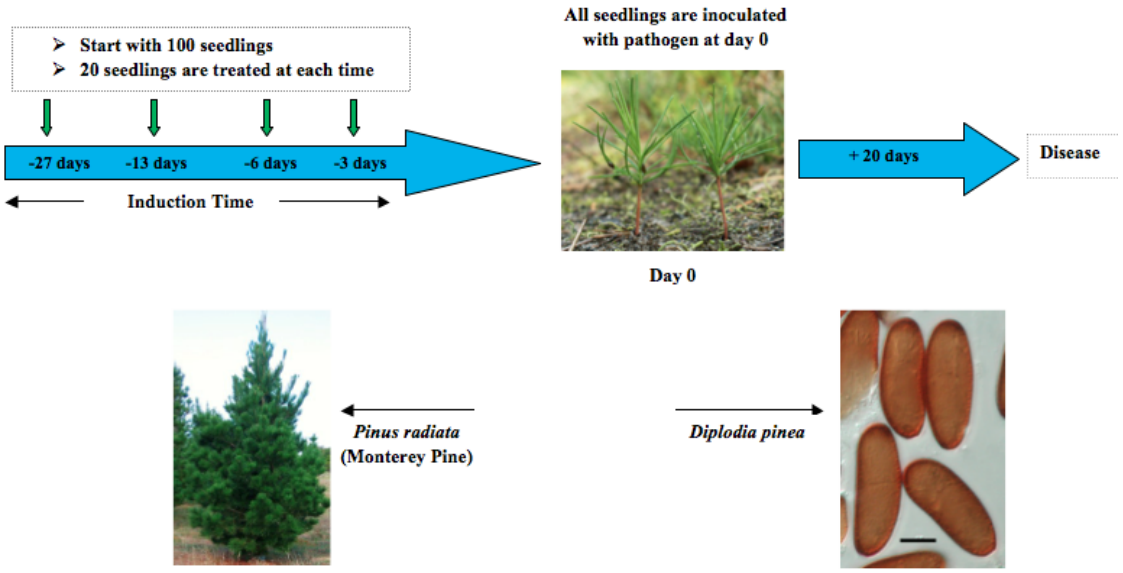

FIGURE 4.1: IR experiments: the pine seedlings were divided into groups and sprayed with 0.1% MeJA at few days before inoculation (e.g. 27, 13, 6 and 3 days) with *D. pinea*. There was also an untreated control group for this experiment. Disease assessments for each treatment commenced one week after inoculation and continued at three-to-four day intervals thereafter for at least 20 days.

This IR experiment was designed as in the Figure 4.1 in order to inoculate the pathogen at the same time for all the experiment groups. Figure 4.2 shows the IR experiment setup in the greenhouse. For the disease assessments, the observation was done on the disease symptoms of the seedlings as shown in Figure 4.3. The available datasets provided by Plant & Food Research Ltd are shown in Table 4.1 and Table 4.2.

FIGURE 4.2: Greenhouse experiment: Pine seedlings were treated with methyl jasmonate (MeJA) within a specific environmental condition (i.e. fixed temperature, moisture, light).

FIGURE 4.3: The difference between diseased (left) and healthy (right) seedlings.

	Disease Assessment Time (Days After Inoculation)								
Elicitor Treatment Time (Days Before Inoculation)	7	11	15	18	21	25	28	32	35
Untreated (0)	0.16	0.34	0.53	0.56	0.59	0.59	0.59	0.66	0.66
3	0.09	0.16	0.22	0.31	0.34	0.34	0.34	0.34	0.41
6	0.06	0.13	0.19	0.19	0.22	0.22	0.28	0.31	0.31
13	0.03	0.16	0.16	0.28	0.38	0.38	0.38	0.41	0.41
27	0.19	0.28	0.31	0.38	0.44	0.47	0.50	0.50	0.50

TABLE 4.1: First dataset: Shows the proportion of diseased seedlings. The seedlings were treated with 0.1% MeJA at different inoculation times t_p days, before the pathogen is introduced. The percentage of the healthy seedlings is determined by 1 - proportion of the diseased seedlings.

	Disease Assessment Time (Days After Inoculation)		
Elicitor Treatment Time (Days Before Inoculation)	12	20	27
7	0.125	0.25	0.25
14	0.0625	0.125	0.125
21	0.125	0.25	0.375
35	0.3125	0.5	0.5

TABLE 4.2: Second dataset: Shows the proportion of diseased seedlings. The seedlings were treated with 0.1% MeJA at different inoculation times t_p, days, before the pathogen is introduced. The percentage of the healthy seedlings is determined by 1 - proportion diseased seedlings.

4.3 Model Developments

In general, standard epidemiological models for plant disease development are based on the interactions between three critical components:

- the plant,
- the pathogen, and
- the environment.

When modelling the spread of a disease through a population, there is a physical contact for the infection of a susceptible by an infective; however, plants do not move

unless they are triffids. The spread of disease in plants is the result of migration of the pathogen. Dispersal is the movement of the pathogens dispersal units (e.g. spores) from the place where they are formed to the plant tissue they infect. Some referred to this dispersion as the "conquest of space" (Zadoks & Schein, 1979). There are many mechanisms of dispersal, such as leaf rubbing, rain splash, turbulent transfer (wind-borne), water-borne, animal or vertebrate-borne, insect (invertebrate-borne) and human-borne.

In disease conducive conditions, **susceptible** (S) plants become infected and develop **disease** (D) when inoculated with a compatible pathogen (a direct disease transmission). Here, D represents the proportion of plants that have become infected but are not infectious; therefore D is different from I in the SIR model. This is a dynamic relationship, and a subtle change to any one parameter may result in a proportion of the plant population being able to exhibit **resistance** (R) to an infection. In this study, a plant defence elicitor was applied to susceptible plants in order to elevate their basal resistance and hence enable a proportion of formerly susceptible plants to express IR, affecting a shift in the population from S to R.

This prototype IR model is an adaptation of the models by Jeger et al. (2009) and Xu et al. (2010). Their models were developed for a generic biological control system featuring a compartmental SIR model for host-pathogen dynamics coupled with the pathogen-BCA dynamics. An induced resistance mechanism has been included in their model; however, this is in a generic form where BCA is assumed part of the plant population. Here the models are extended to include the induced resistance as the specific biological control mechanism and to determine the effectiveness of the elicitor used as the agent to induce resistance in plants. Apparently, there are no mathematical models in the literature which specifically describe the interactions between the plant, pathogen and elicitor.

4.3.1 IR Model: Assumptions and Definitions

The assumptions underlying the model's formulation can be summarised as follows:

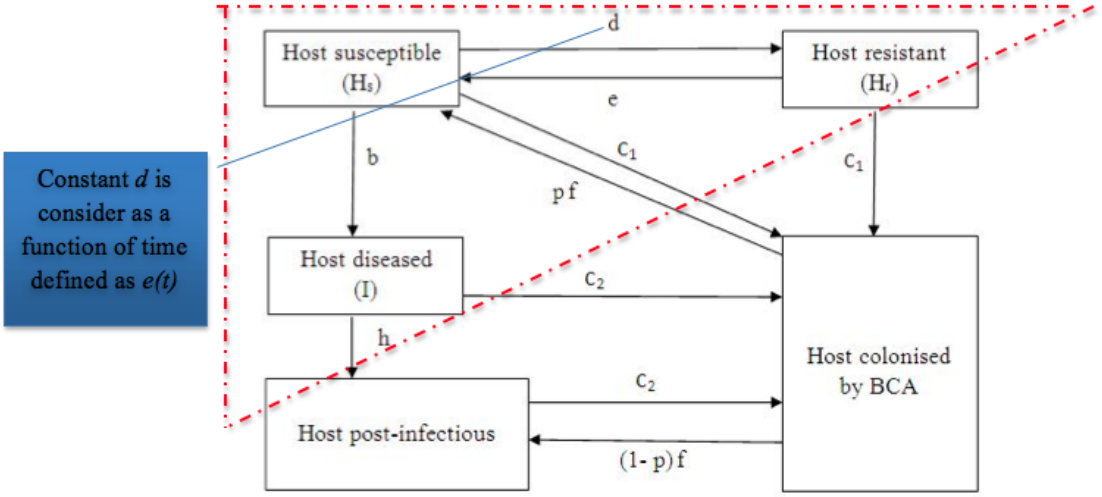

FIGURE 4.4: The adaptation from Jeger et al. (2009) to construct an IR model where the effectiveness of the elicitor used is defined as $e(t)$ for which converts some of the susceptible plants to become resistant.

1. Let S be the proportion of susceptible plants, R be the proportion of the resistant plants, and D be the proportion of the diseased plants at time t. These proportions are with total plant population which is assumed to be a constant, given by $S + R + D = 1$.

2. Immediately following the time when the plants are treated with an elicitor (at $t = 0$), a proportion of the plant population will exhibit natural resistance (R_i). This means that, on treatment, the plant is assumed to be utilising the elicitor effect immediately.

3. The induction period (t_p) describes the time interval (in days) between the elicitor treatment and pathogen inoculation. Upon inoculation, a proportion of plants (D_i) will become infected immediately. It is confirmed by the fact that for the pathogen to infect young-plants, it must be able to colonise the susceptible tissue quickly.

With a small sample size, as in the datasets in Table 4.1 and Table 4.2, the results must be interpreted with caution, as discussed in the IR experimental set up described in Section 4.2. Therefore, the timeline of the experiment is interpreted as

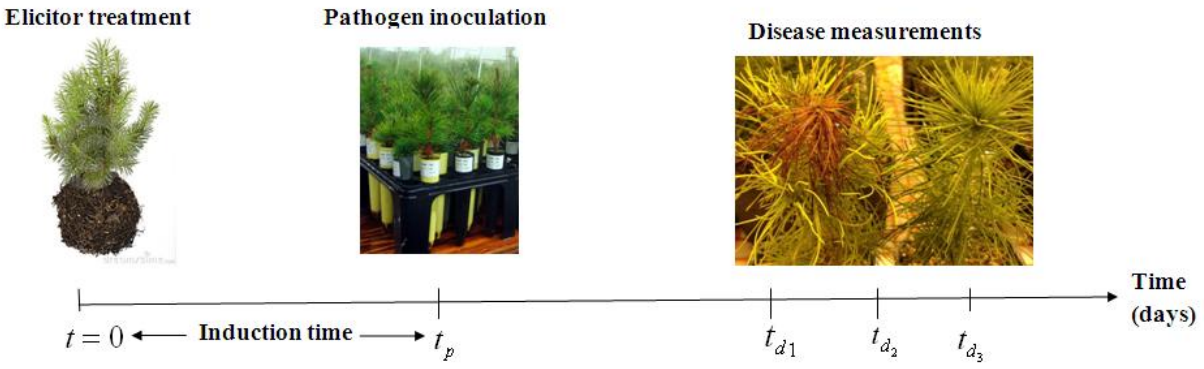

FIGURE 4.5: Time series for the IR model for treated plants.

in Figure 4.5 and for each induction time t_p, has a different dynamic (see later in Chapter 5 for further explanation).

4.3.1.1 The Treated Model

Typically, inducible defences are triggered in response to pathogen attacks. Therefore, the model is formulated with the elicitor treated plants divided into two regimes: i) pre-inoculation (before the pathogen arrives) and ii) post-inoculation (after the pathogen arrives). The model's equations for the **treated** plants are as follows:

Pre-inoculation: For $0 < t < t_p$

$$\frac{dR}{dt} = (e(t) - \gamma R)(1 - R) \qquad ; R(0) = R_i. \tag{4.1}$$

Post-inoculation: For $t_p < t < T$ (where T is sufficiently large)

$$\frac{dR}{dt} = (e(t) - \gamma R)(1 - R - D) \qquad ; R(t_p) = R_p, \tag{4.2}$$

$$\frac{dD}{dt} = \beta D(1 - R - D) \qquad ; D(t_p) = D_i. \tag{4.3}$$

and the elicitor effectiveness in the plants is defined to be:

$$e(t) = \frac{kt}{t^2 + L^2} \tag{4.4}$$

where $\frac{k}{2L}$ [days^{-1}] is the maximum elicitor effect and L [days] is the time when this is at its peak (see Figure 4.6). The parameter γ [days^{-1}] is the specific rate that resistant tissue becomes susceptible and β [days^{-1}] is the specific rate at which the disease spreads. It must be noted that the parameter β does not determine the upper limit for disease D. The value of R_p represents the degree of the resistance at the time of the pathogen inoculation obtained from Equation (4.1). For Equation (4.1), D is not in the equation because the pathogen is absent during this period. Pathogen is inoculated at time t_p, therefore the D term only occurs in equations (4.2) and (4.3).

The function $e(t)$ was assumed to be time-dependent, to reflects the fact that elicitor-induced changes in plant resistance is transient and the lasting effect may be short (as previously described in Section 2.3.1). Other functional forms for $e(t)$ were tried, and this one (Equation (4.4)) gave a best fit and matched the biological insight from experiments.

Note that Equations (4.1), (4.2) and (4.3) are based on the assumption that the rates of change of R and D are directly proportional to the amount of S available at a particular time (that is, $S = 1-R-D$) using the usual "mass-action-kinetics" (see Keener & Sneyd (1998)). This rate of change is also following Jeger et al. (2009). Furthermore, according to Vanderplank (1982), plant disease evolve through time and can be treated synthetically, where the rate of increase in disease is proportional to the amount of tissue that is uninfected and available for infection.

Consider the data given in Table 4.1 and Table 4.2; the fraction of diseased seedlings increased relatively fast until 20 days after pathogen inoculation, when the amount of diseased seedlings stopped increasing. This is not because there were no more healthy seedlings available, but because there was no inoculum left to infect it, and the pathogen ran out of spores. This obviously applies to Equation (4.3), but the situation is less clear for the R compartment. This problem has been taken into

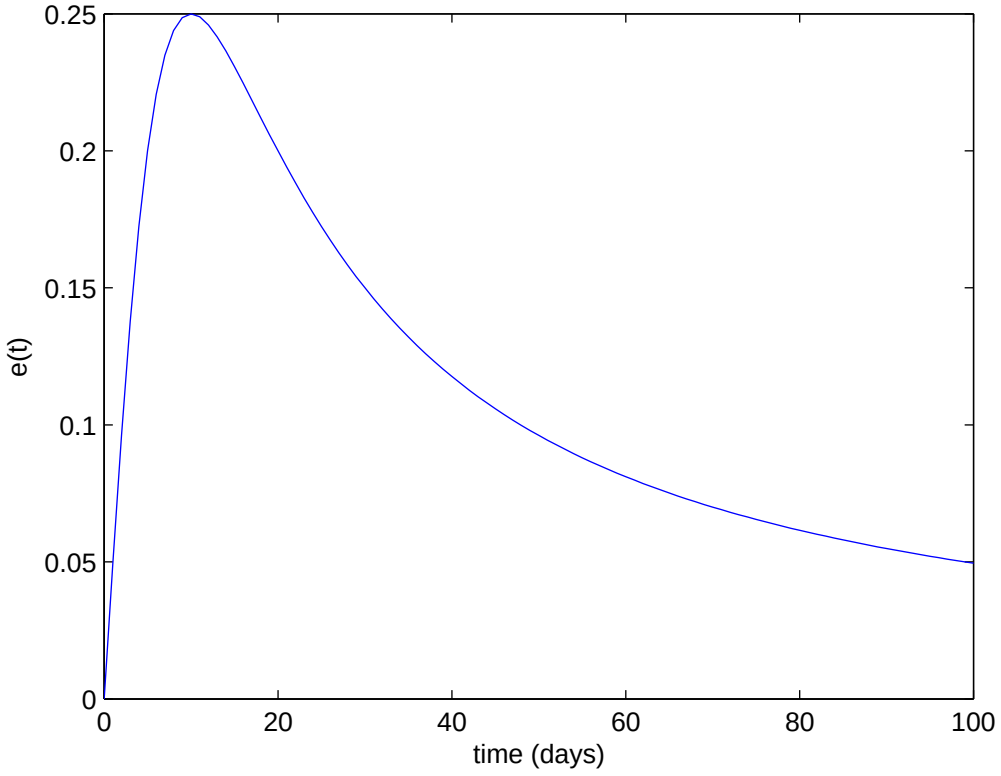

FIGURE 4.6: The diagram for equation $e(t) = \dfrac{kt}{t^2 + L^2}$ with $k = 5.3749$ and $L = 10.7607$ chosen arbitrarily.

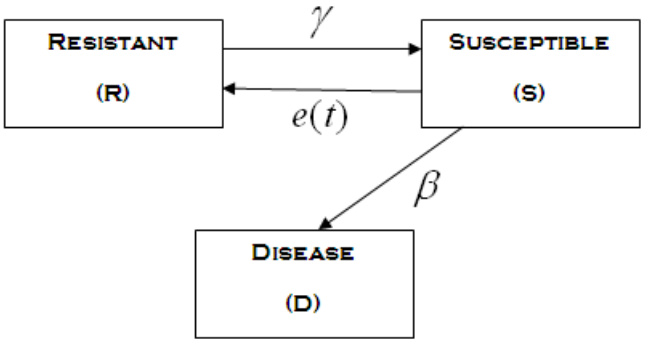

FIGURE 4.7: The schematic diagram for the treated model. Here S, R, D are the proportion of plants in the representative compartments and the parameters γ, β and $e(t)$ are the specific rates of movement between the linked compartments.

account where the rate of change of R is not proportional to S. If Equations (4.1) – (4.3) are redefined to be

$$\frac{d\hat{R}}{dt} = \begin{cases} e(t)(1-\hat{R}) - \gamma\hat{R} & \text{for } 0 < t < t_p, \\ e(t)(1-\hat{R}-D) - \gamma\hat{R} & \text{for } t_p < t < T. \end{cases}$$

and

$$\frac{dD}{dt} = \beta D(1-\hat{R}-D) \qquad \text{for } t_p < t < T.$$

Then, consider the second regime; that is $t_p < t < T$ and find the steady states for this system. Taking the limit $t \to \infty$, this becomes a coupled autonomous system:

$$\frac{d\hat{R}}{dt} = -\gamma\hat{R} = 0 \tag{4.5}$$

$$\frac{dD}{dt} = \beta D(1-\hat{R}-D) = 0. \tag{4.6}$$

This implies that the steady states for the above system are $(\hat{R}^*, D^*) = (0,0), (0,1)$ (see Figure 4.8); showing D eventually approaches unity which is not shown by the data. Note that the only mechanism that could cause this would be genetic in origin, and so is beyond the scope of this study.

By taking the same analysis approach as above, the equations (4.2) and (4.3) become:

$$\frac{dR}{dt} = -\gamma R(1-R-D) = 0 \tag{4.7}$$

$$\frac{dD}{dt} = \beta D(1-R-D) = 0. \tag{4.8}$$

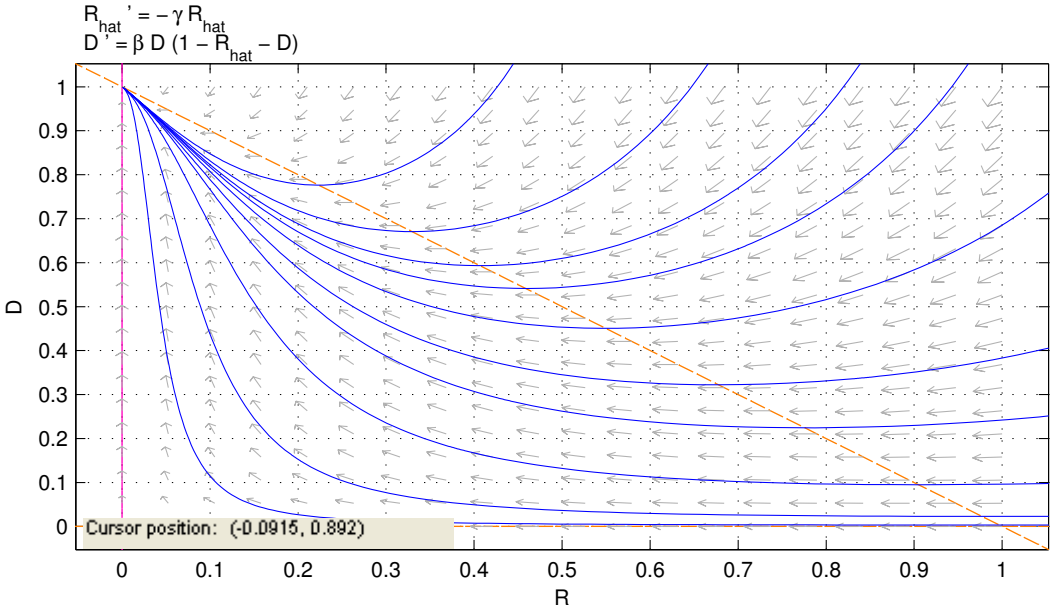

FIGURE 4.8: Phase plane for Equations (4.5) and (4.6). The diagram was plotted using pplane8.m (see Polking (2009) for more details) with arbitrary parameter values.

with steady states

$$\begin{aligned} \frac{dR}{dD} &= \frac{-\gamma R}{\beta D}, \\ \frac{dR}{R} &= -\frac{\gamma}{\beta}\frac{dD}{D}, \\ \ln R &= -\frac{\gamma}{\beta}\ln D + C \qquad ; \text{C is a constant.} \end{aligned}$$

Given that $R(t_p) = R_p$ and $D(t_p) = D_i$,

$$R(t) = R_p \left[\frac{D(t)}{D_i}\right]^{-\frac{\gamma}{\beta}}, \qquad \text{for } t_p < t < T.$$

This shows that the steady state attained is dependent on the initial condition and always attracting to the line $R + D = 1$ (see Figure 4.9). Therefore, Equations (4.1) and (4.2) were employed for this IR model.

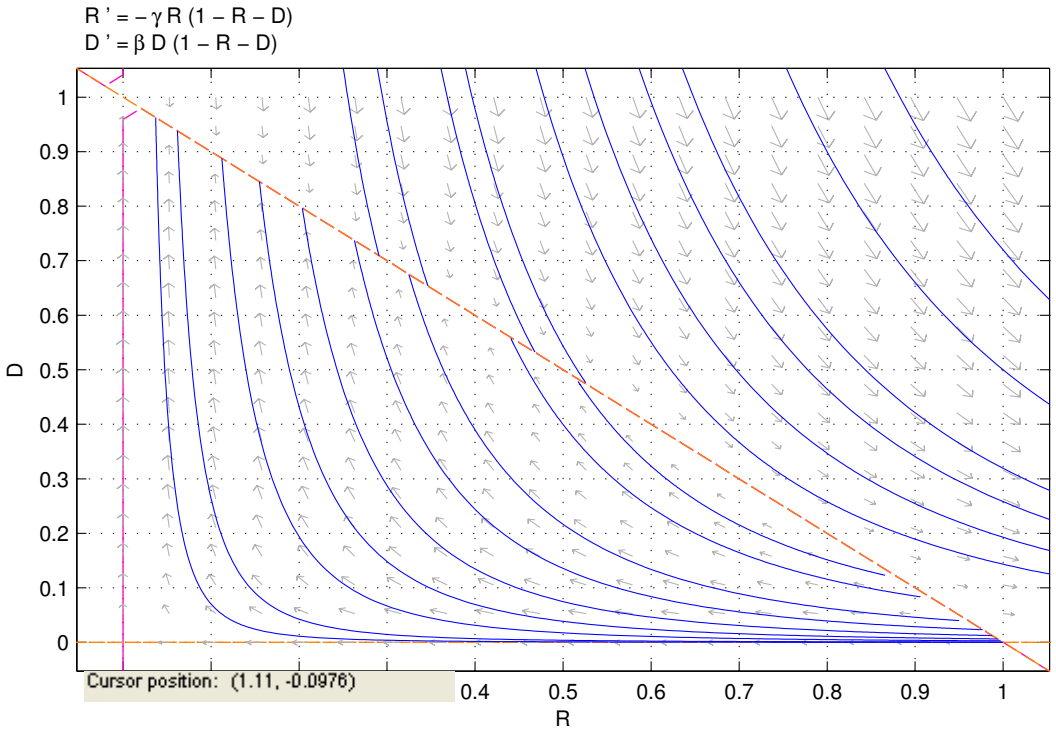

FIGURE 4.9: Phase plane for Equations (4.7) and (4.8). The diagram was plotted using pplane8.m (see Polking (2009) for more details) with arbitrary parameter values.

4.3.1.2 The Untreated Model

The equations for the **untreated** plants are as follows:

$$\frac{dR}{dt} = -\alpha R(1-R-D) \quad ; R(0) = R_i, \tag{4.9}$$

$$\frac{dD}{dt} = \beta D(1-R-D) \quad ; D(0) = D_i, \tag{4.10}$$

where α [days^{-1}] is the rate at which the untreated plants lose their resistance due to the pathogen attack. The untreated model shares the parameters β, R_i, D_i with the treated model as these untreated plants are a control group. This means that there is no elicitor treatment for the control group. Therefore the untreated model will not have the $e(t)$ term in its equations and so is autonomous. That is, the untreated is independent of time except implicitly. Note that the rates of change in R and D, for the untreated plants, are also directly proportional to the amount of S available. Also note that, if taken into consideration of no disease for the untreated model (i.e. consider Equation (4.9) without D), then the steady-states for this particular equation are $R = 0$ or $R = 1$. However, this scenario was not taken into account and there is no experimental data to support the argument. Thus, these Equations (4.9) and (4.10) were used in this proposed IR Model.

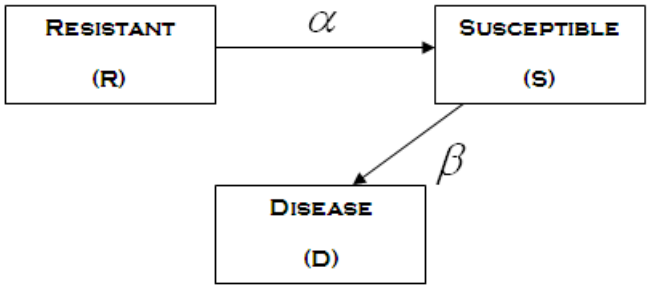

FIGURE 4.10: The schematic diagram for the untreated model. Here S, D, R are the proportion of plants in the respective compartments and the parameters are the specific rates of movement between the compartments.

4.4 Summary

In this chapter, the formulation of the proposed IR model has been presented. Table 4.3 shows the variables and parameters defined in equations (4.1)–(4.10). The unknown parameters are determined in the next chapter by matching the model's simulation with experimental observations (Table 4.1 and Table 4.2).

Variable / Parameter	**Description**	**Units**
R	Proportion of plant population able to express resistance to infection.	dimensionless
D	Proportion of plant population being infected and become diseased.	dimensionless
S	Proportion of plant population which is susceptible.	dimensionless
α	The specific rate at which untreated plants lose their resistance due to the pathogen attack.	days^{-1}
β	The specific rate at which the disease spreads.	days^{-1}
γ	The specific rate the resistant plant becomes susceptible.	days^{-1}
k	Determines the effectiveness of the elicitor.	dimensionless
L	The time where the elicitor effectiveness is at the peak.	days
t_p	The induction time of the pathogen; i.e. the time interval between the elicitor application and the pathogen challenge.	days
R_i	The proportion of the plant population that exhibits natural resistance at the initial time $t = 0$.	dimensionless
D_i	The proportion of the plant population which becomes infected immediately after the pathogen challenge.	dimensionless

TABLE 4.3: Description of variables and parameters used in the IR model.

Chapter 5

Model Fitting and Discussions

After formulating the model and gathering some indicative data, the next step in the model-building process is to estimate the unknown parameters. This process is known as model fitting or parameter estimation. This chapter discusses the process of making such estimations for the proposed IR model seen in Chapter 4.

5.1 Parameter Estimation Using Datasets Table 4.1

The general idea of the least-squares method for determining unknown parameters has been discussed in Chapter 3. In this chapter, the method is applied to determine the unknown parameters as in the IR model by comparing the model's simulation with an IR experiment on pine seedlings (more details in Chapter 4). The results and discussion in this section are part of an article in the Journal Frontiers Plant Science (see Abdul Latif et al. (2013)).

The parameterisation results presented in this section are based on Table 4.1. Since there is insufficient data to estimate all the parameters together, the parameterisation process is divided into 2 groups; i) parameterisation for data on the untreated seedlings, and ii) parameterisation for data on the treated seedlings. The flow charts

given in Figure 5.1 and Figure 5.2 are used to illustrate the process of parameter estimation for the IR model.

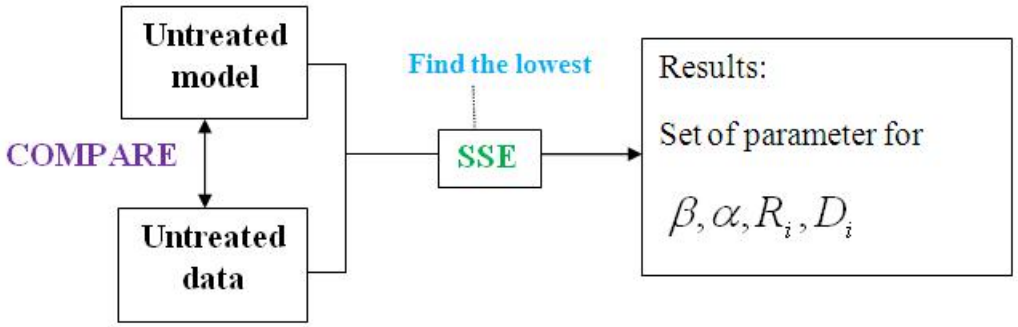

FIGURE 5.1: Parameter estimation using the untreated seedlings data in Table 4.1.

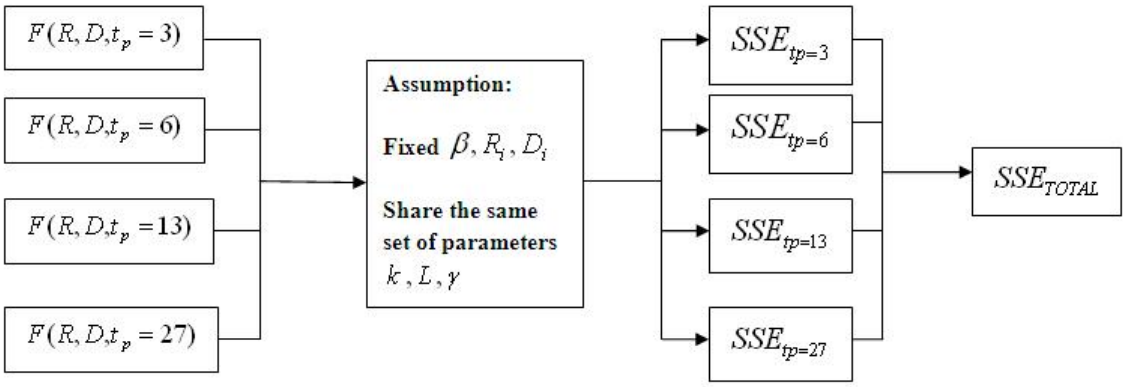

FIGURE 5.2: Parameter estimation using the treated seedlings data in Table 4.1.

The reason for separating the parameter estimation as mentioned above is because in the case for the untreated experimental data set, the parameters α, β, R_i and D_i appearing in the untreated model (Section 4.3.1.2) can be estimated and later fixed in the parameterisation for the treated model (Section 4.3.1.1), when the remaining parameters k, L, γ are estimated. This is acceptable based on the equations (4.1), (4.2), (4.3), (4.9) and (4.10). Other assumptions made are for each induction time t_p [days]; while different dynamics are displayed, it is important to assume that

these dynamical systems (both treated and untreated system) share the same set of parameters. For the treated cases, the dynamical system for each t_p was solved simultaneously, using the criterion of least-squares fit. The minimum values of SSE, for each t_p, were then totalled to give the overall SSE value to assess the quality of the fit. Supplementary to this parameter estimation, some artificial data was added to the data to make the estimation process more stable as the number of data points available was inadequate. Note that in Table 4.1, after a certain time (the last three columns), the number of diseased seedlings seem to reach a steady state. Therefore, artificial data points are added to the last five columns as shown in Table 5.1. This will make parameterisation become stable and more accurate in terms of taking more data points into account. Notice that, in the data sets (Table 5.1), there are only two compartments: diseased seedlings or healthy seedlings; thus, for parameter estimation, the healthy (H) compartment is evaluated as $H = S + R$ or $H = 1 - D$. This identification of the compartments of Resistant (R) and Susceptible (S) seedlings in the proposed IR model is a significant advantage over pure experimentation.

Mathematically, the least-squares fit criterion for the treated case is defined as:

$$\text{SSE} = \sum_{i=1}^{n} \sum_{j=0}^{m} [y_i(t_j) - f_i(t_j; \mathbf{a})]^2. \tag{5.1}$$

where

- i corresponds to the induction time t_p ($t_p = 3, 6, 13, 27$ days) (row),
- j corresponds to the number of observations and t_j corresponds to the disease assessment time (column),
- $y_i(t_j)$ corresponds to the experimental data points for a particular t_p at time t_j,
- $f_i(t_j; \mathbf{a})$ corresponds to the model's solution for a particular t_p at time t_j, with the vector of unknown parameters $\mathbf{a} = (k, L, \gamma)$.

	Disease Assessment Time													
Time for elicitor treatment	t_p+7	t_p+11	t_p+15	t_p+18	t_p+21	t_p+25	t_p+28	t_p+32	t_p+35	t_p+40	t_p+45	t_p+50	t_p+55	t_p+60
No elicitor ($t_p=0$)	0.16	0.34	0.53	0.56	0.59	0.59	0.59	0.66	0.66	0.66	0.66	0.66	0.66	0.66
$t_p=3$	0.09	0.16	0.22	0.31	0.34	0.34	0.34	0.34	0.41	0.34	0.34	0.34	0.34	0.34
$t_p=6$	0.06	0.13	0.19	0.19	0.22	0.22	0.28	0.31	0.31	0.31	0.31	0.31	0.31	0.31
$t_p=13$	0.03	0.16	0.16	0.28	0.38	0.38	0.38	0.41	0.41	0.41	0.41	0.41	0.41	0.41
$t_p=27$	0.19	0.28	0.31	0.38	0.44	0.47	0.50	0.50	0.50	0.50	0.50	0.50	0.50	0.50

TABLE 5.1: Artificial data points added to Table 4.1, given in red. The data shows the proportion of the diseased seedlings, where seedlings were treated with elicitor at different induction times t_p. The proportion of the healthy seedlings are determined by 1 - fraction of the diseased seedlings.

5.1.1 Results

5.1.1.1 Optimal Parameter Values

Table 5.2 shows the final optimal value of each parameter α, β, R_i and D_i based on the various initial guesses provided. It is apparent, from this table, that the global minimum SSE was not always reached and that the results indicate a dependency on starting values. In this case, the global minimum of SSE seems to be reached in four out of seven different sets of initial guesses. The lowest SSE recorded was 0.0151 for this untreated seedlings data parameterisation. The sets of initial guesses for (1), (3), (4) and (5) (Refer to Table 5.2) achieve the global minimum of SSE. However, the values of the other parameter sets (i.e. in (2), (6), (7)) show large variation. The results of those sets with lowest SSE show that the final optimal values are:

$$\begin{aligned} \alpha &= -0.1360 \text{ days}^{-1} \\ \beta &= 0.3346 \text{ days}^{-1} \\ R_i &= 0.0998 \\ D_i &= 0.0288. \end{aligned} \tag{5.2}$$

Hence, these parameters can be considered identifiable. By fixing the values in 5.2 the remaining unknown parameters in the treated case are estimated. Notice that parameter α has a negative final optimal value. This means that the susceptible seedlings (S) will build resistance, shifting towards the resistant (R) compartment in the model. Table 5.3 shows the final optimal value of each parameter k, L, γ based on various initial guesses provided. The output of the final value of each parameter and the final value of SSE are identical based on different sets of initial guesses used. This estimation reached a unique value, which suggests that the parameters are identifiable. Therefore the final optimal values obtained are:

$$\begin{aligned} k &= 0.6059 \\ L &= 1.8925 \text{ days} \\ \gamma &= 0.0571 \text{ days}^{-1}. \end{aligned} \tag{5.3}$$

Parameters	(1)		(2)		(3)		(4)		(5)		(6)		(7)	
	Initial	Final	Initial	Final	Initial	Final	Initial	Final	Initial	Final	Initial	Final	Initial	Final
α	-0.1300	-0.1360	1.000	0.8642	0.1000	-0.1360	-0.5000	-0.1360	0.0760	-0.1360	1.0000	-0.2517	5.0000	7.1119
β	0.3000	0.3346	3.000	1.4992	0.1000	0.3346	0.3000	0.3346	0.2399	0.3346	5.0000	6.8780	1.0000	0.0293
R_i	0.0200	0.0998	0.5000	0.8501	0.1000	0.0998	0.1000	0.0998	0.1233	0.0998	0.2000	0.3989	0.1000	-0.0955
D_i	0.0100	0.0288	0.030	0.1482	0.0100	0.0288	0.0100	0.0288	0.1839	0.0288	0.1000	0.0730	0.1000	0.3522
SSE		0.0151		0.0320		0.0151		0.0151		0.0151		0.5611		0.2338

TABLE 5.2: Parameter estimation for the untreated model using untreated experimental data in Table 4.1.

Parameters	(1)		(2)		(3)		(4)		(5)	
	Initial	Final	Initial	Final	Initial	Final	Initial	Final	Initial	Final
k	0.2599	0.6059	0.8693	0.6059	3.0000	0.6059	-9.7059	0.6059	0.1000	0.6059
L	0.8001	1.8925	0.5797	1.8925	10.000	1.8925	9.7059	1.8925	10.000	1.8925
γ	-0.1000	0.0571	0.5499	0.0571	0.1000	0.0571	0.4853	0.0571	0.5000	0.0571
SSE		0.6189		0.6189		0.6189		0.6189		0.6189

TABLE 5.3: Parameter estimation for the treated model using treated experimental data in Table 4.1.

5.1.1.2 Solution Graphs

In Figures 5.3 through 5.6 the parameter estimates given in (5.2) and (5.3) were used to plot the solutions of equations (4.1)–(4.10). The solution graphs for each t_p case are compared to the untreated model. The simulation given by our model is well fitted to the experimental data. It shows that some of the susceptible seedlings are being induced to become resistant by the elicitor to fight the pathogen attack. Furthermore, it clearly shows that all treated seedlings have a better disease control than the untreated seedlings.

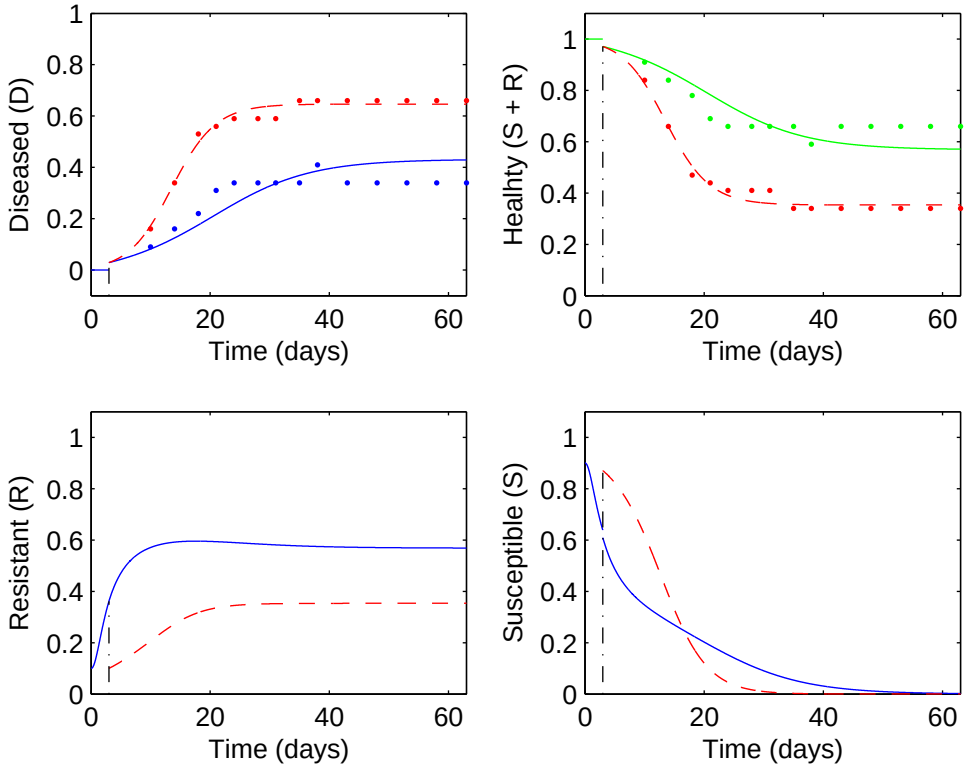

FIGURE 5.3: Solution graphs for each compartment with induction time $t_p = 3$ days. The solid lines (—) are describing the dynamics for the treated model and the dashed lines (– –) are indicating the untreated model. The blue (●) and green (●) dots are experimental data for the treated seedlings and the red (●) dots correspond to the untreated seedlings. The vertical line indicates the induction time t_p.

From the diagrams in Figure 5.3, it can be seen there is a discontinuity in the dynamics of diseased (D) and healthy (H) compartments due to the introduction of the pathogen after three days of elicitor treatment. That is to say the whole population of seedlings was healthy prior to the introduction of the pathogen. This proportion of healthy seedlings decreases as the number of diseased seedlings increases until it reaches the limiting disease growth. An interesting finding occurs in the dynamics of the resistant and susceptible populations. It can be seen that the susceptible population declines, meaning that the entire proportion of susceptible seedlings becomes resistant, limiting the spread of pathogen. This fluctuation results in the resistant population reaching a peak before declining to a steady state.

In general, this behaviour is comparable to all treated seedlings with a different induction time t_p (see Figures 5.4, 5.5, 5.6). The dynamics of resistant and susceptible populations are due to variations in induction time t_p. This scenario can be clearly seen in Figure 5.7.

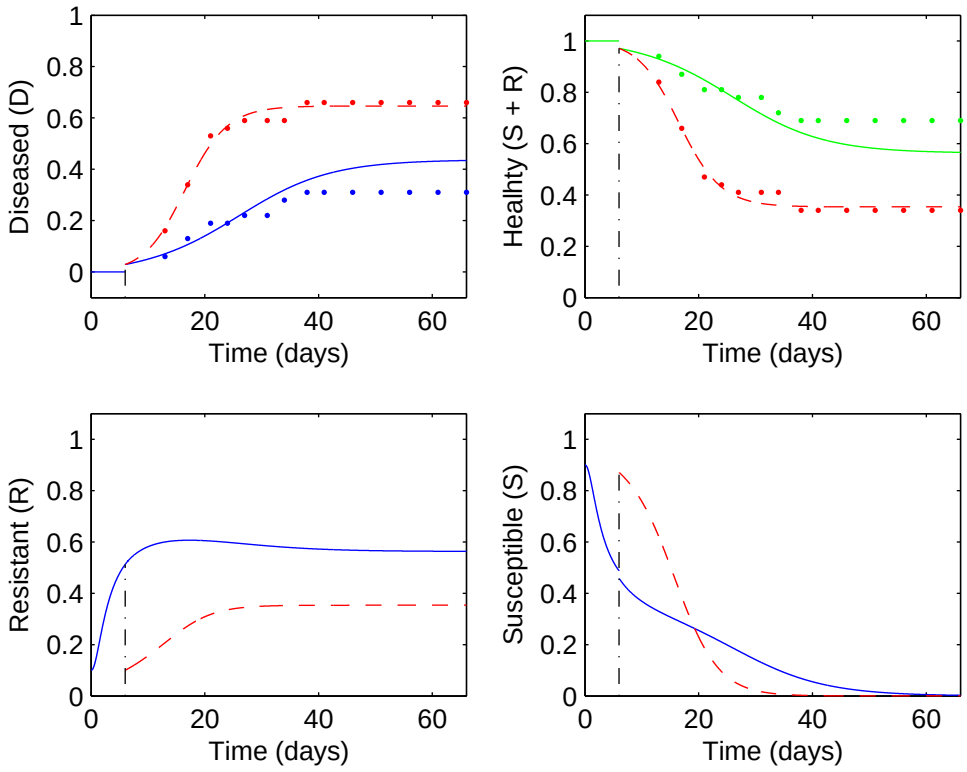

FIGURE 5.4: Solution graphs for each compartment with induction time $t_p = 6$ days. The solid lines (—) describe the dynamics for the treated model and the dashed lines (– –) indicate the untreated model. The blue (•) and green (•) dots are experimental data for the treated seedlings and the red (•) dots correspond to the untreated seedlings. The vertical line indicates the induction time t_p.

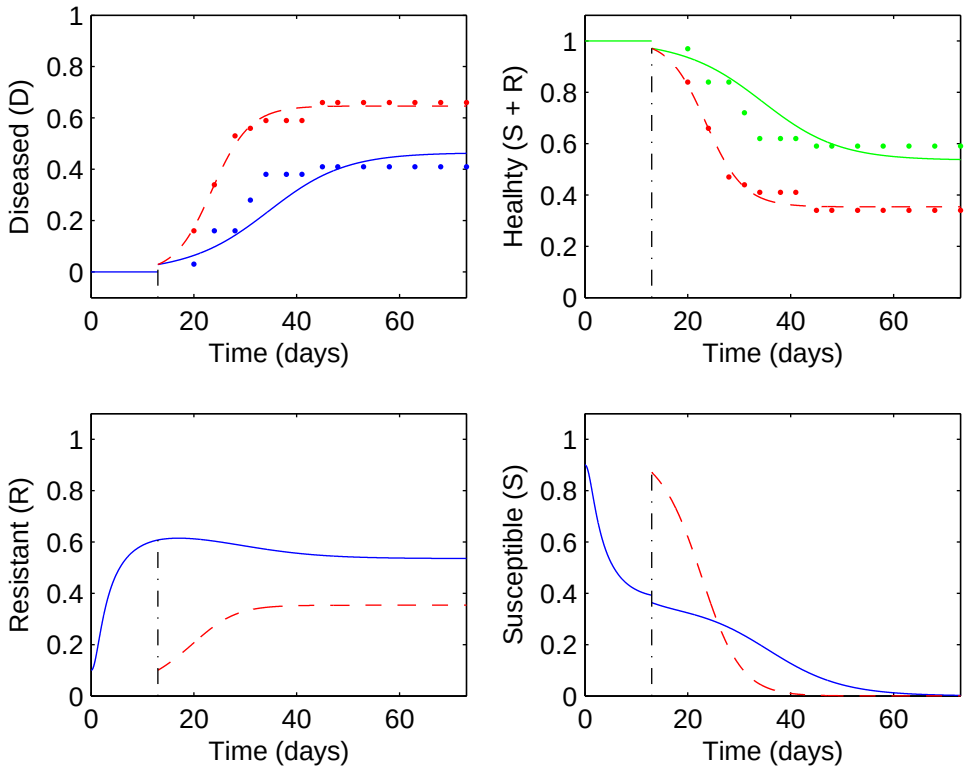

FIGURE 5.5: Solution graphs for each compartment with induction time $t_p = 13$ days. The solid lines (—) describe the dynamics for the treated model and the dashed lines (– –) indicate the untreated model. The blue (•) and green (•) dots are experimental data for the treated seedlings and the red (•) dots correspond to the untreated seedlings. The vertical line indicates the induction time t_p.

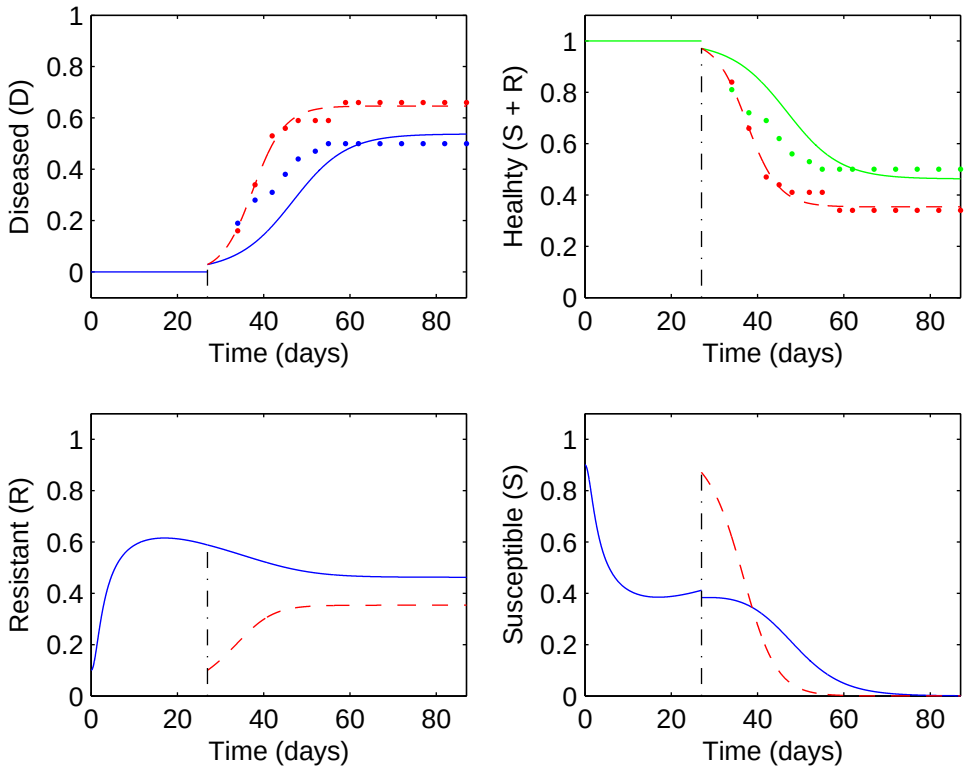

FIGURE 5.6: Solution graphs for each compartment with induction time $t_p = 27$ days. The solid lines (—) describe the dynamics for the treated model and the dashed lines (– –) indicate the untreated model. The blue (●) and green (●) dots are experimental data for the treated seedlings and the red (●) dots correspond to the untreated seedlings. The vertical line indicates the induction time t_p.

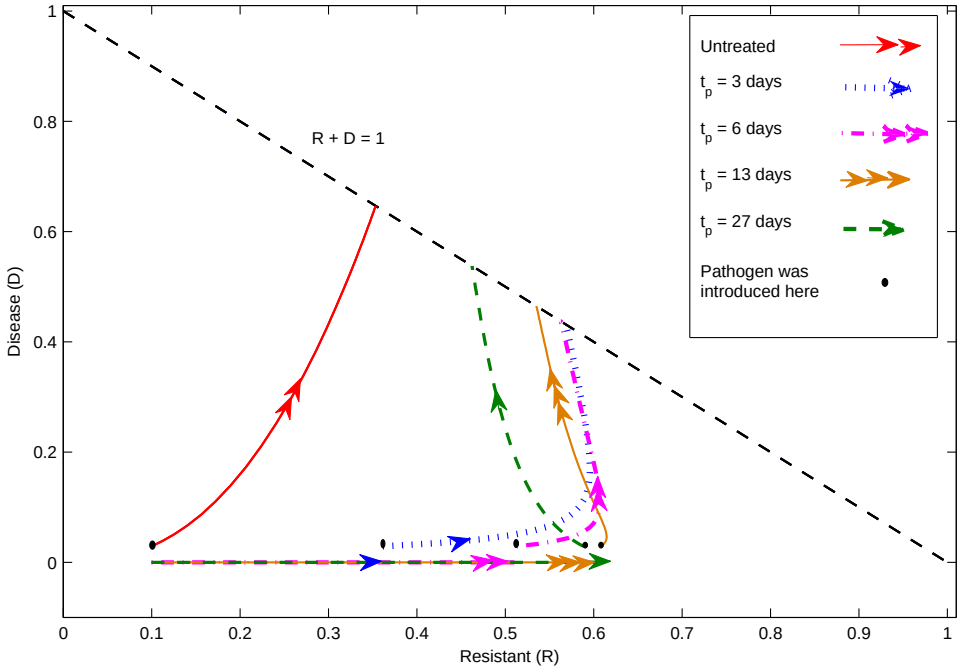

FIGURE 5.7: The phase plane for the IR model with trajectories of the R, D compartments plotted in the feasible region ($R, D > 0,\ R + D < 1$). The lines schematically correspond to the values of the two compartments R and D as time passes for the equations in previous chapter (see Chapter 4) based on each induction time t_p and the untreated case. When $D = 0$, the straight lines illustrate the dynamics of the R compartment in the absence of the pathogen. These lines then have a discontinuity when the seedlings are inoculated with pathogen that is being introduced at time $t = t_p$, and it shows the state of the R compartment at that particular time. Clearly there is a jump in the D values of D_i at $t = t_p$ and the trajectories of the R, D compartments will continue to approach the straight line $R + D = 1$. For the untreated case, the dynamics of the R, D compartments will depend on the initial condition of the systems; that is R_i and D_i.

The phase plane in Figure 5.7 illustrates the characteristics of the resistant (R) and diseased (D) compartments. The flows in the diagram indicate the time-evolution of the dynamical system, based on the different values of t_p and the untreated case. There is a significant result when the induction time t_p is between three and six days; the development of disease is less severe compared to the other induction times and with the untreated seedlings. The observed result can be attributed to the resistance induced by the elicitor treatment, attaining its peak to coincide with

the introduction of the pathogen. The figure also shows that the trajectories for each induction case will eventually approach the line $R+D=1$; which can be considered to be a line of neutrally stable (non-hyperbolic) equilibria.

5.2 New Parameterisation

The results and discussions in this section are part of a published article in the Journal of Theoretical Biology (Abdul Latif et al., 2014).

For the previous parameterisation result only the data set in Table 4.1 was used to fit the model. Now, consider another experimental data set given by Plant & Food (Table 4.2) and incorporate it into the data set of Table 4.1, producing a more robust parameterisation.

Since there is a disparity in the disease assessment time for both of the experimental data sets (Table 4.1 and Table 4.2), a logistic equation was used to interpolate the numbers to fill in the gaps;

$$P(t) = \frac{A}{1 + Be^{-Ct}}$$

where A, B, C are real valued positive constants. It can be seen from Table 4.1 and Table 4.2 that the numbers for diseased seedlings are monotonically increasing and will reach a constant number after some time has passed. Therefore, the logistic equation above is suitable to interpolate the data as:

1. $P(t)$ is monotonic increasing

2. $\lim_{t\to\infty} P(t) = A$, meaning $P(t)$ approaches the steady state, A, as time gets large.

	Disease Assessment Time											
Time for elicitor treatment	$t_p + 7$	$t_p + 11$	$t_p + 12$	$t_p + 15$	$t_p + 18$	$t_p + 20$	$t_p + 21$	$t_p + 25$	$t_p + 27$	$t_p + 28$	$t_p + 32$	$t_p + 35$
No elicitor ($t_p = 0$)	0.1600	0.340	0.3900	0.5300	0.5600	0.5900	0.5900	0.5900	0.5900	0.5900	0.6600	0.6600
3 days	0.0900	0.1600	0.1800	0.2200	0.3100	0.3200	0.3400	0.3400	0.3400	0.3400	0.3400	0.4100
6 days	0.0600	0.1300	0.1300	0.1900	0.1900	0.2100	0.2200	0.2200	0.2700	0.2800	0.3100	0.3100
7 days	0.0000	0.0600	0.1250	0.2400	0.2500	0.2500	0.2500	0.2500	0.2500	0.2500	0.2500	0.2500
13 days	0.0300	0.1600	0.1300	0.1600	0.2800	0.3200	0.3800	0.3800	0.3800	0.3800	0.4100	0.4100
14 days	0.0000	0.0300	0.0625	0.1200	0.1250	0.1250	0.1250	0.1250	0.1250	0.1250	0.1250	0.1250
21 days	0.0700	0.1100	0.1250	0.1700	0.2100	0.2500	0.2700	0.3400	0.3750	0.3900	0.4500	0.4800
27 days	0.1900	0.2800	0.2800	0.3100	0.3800	0.4100	0.4400	0.4700	0.4800	0.5000	0.5000	0.5000
35 days	0.0100	0.2100	0.3125	0.4800	0.5000	0.5000	0.5000	0.5000	0.5000	0.5000	0.5000	0.5000

TABLE 5.4: Experimental data used in the new parameterisation process to determine the seven unknown parameter values. Since there are gaps in the disease assessments time for both experimental data sets (Table 4.1 and Table 4.2), logistic equation was used to interpolate the numbers to fill in the gaps. This is given by the numbers in red; while the numbers in black represent the actual experimental data.

Therefore a "new" data set is used for the parameterisation, as seen in Table 5.4. These new parameterisation results are also based on the equations in Chapter 4. For this parameterisation, the least-squares criterion is calculated as:

$$\begin{aligned} \text{SSE} &= \text{SSE treated} + \text{SSE untreated} \\ \text{SSE} &= \sum_{i=1}^{n}\sum_{j=0}^{m}[y_i(t_j) - f_i(t_j;\mathbf{p})]^2 + \sum_{j=0}^{m}[z(t_j) - h(t_j;\mathbf{p})]^2 \end{aligned} \tag{5.4}$$

where:

- i corresponds to the induction time t_p ($t_p = 3, 6, 7, 13, 14, 21, 27, 35$ days) (rows),
- t_j corresponds to the disease assessment time (columns),
- $y_i(t_j)$ corresponds to the treated experimental data points for a particular t_p at a particular time t_j,
- $z(t_j)$ corresponds to the untreated experimental data points at a particular time t_j,
- $f_i(t_j;\mathbf{p})$ corresponds to the treated model's solution with a particular t_p,
- $h(t_j;\mathbf{p})$ corresponds to the untreated model's solution at a particular time t_j,
- $\mathbf{p} = (k, L, \gamma, \beta, \alpha, R_i, D_i)$ is a vector of unknown parameters.

The flow chart in Figure 5.8 illustrates how the SSE in Equation (5.4) is calculated.

Note that the experimental data sets (without the interpolation) can be used for parameterisation, but more data points are hypothetically will ensure the parameterisation process become stable.

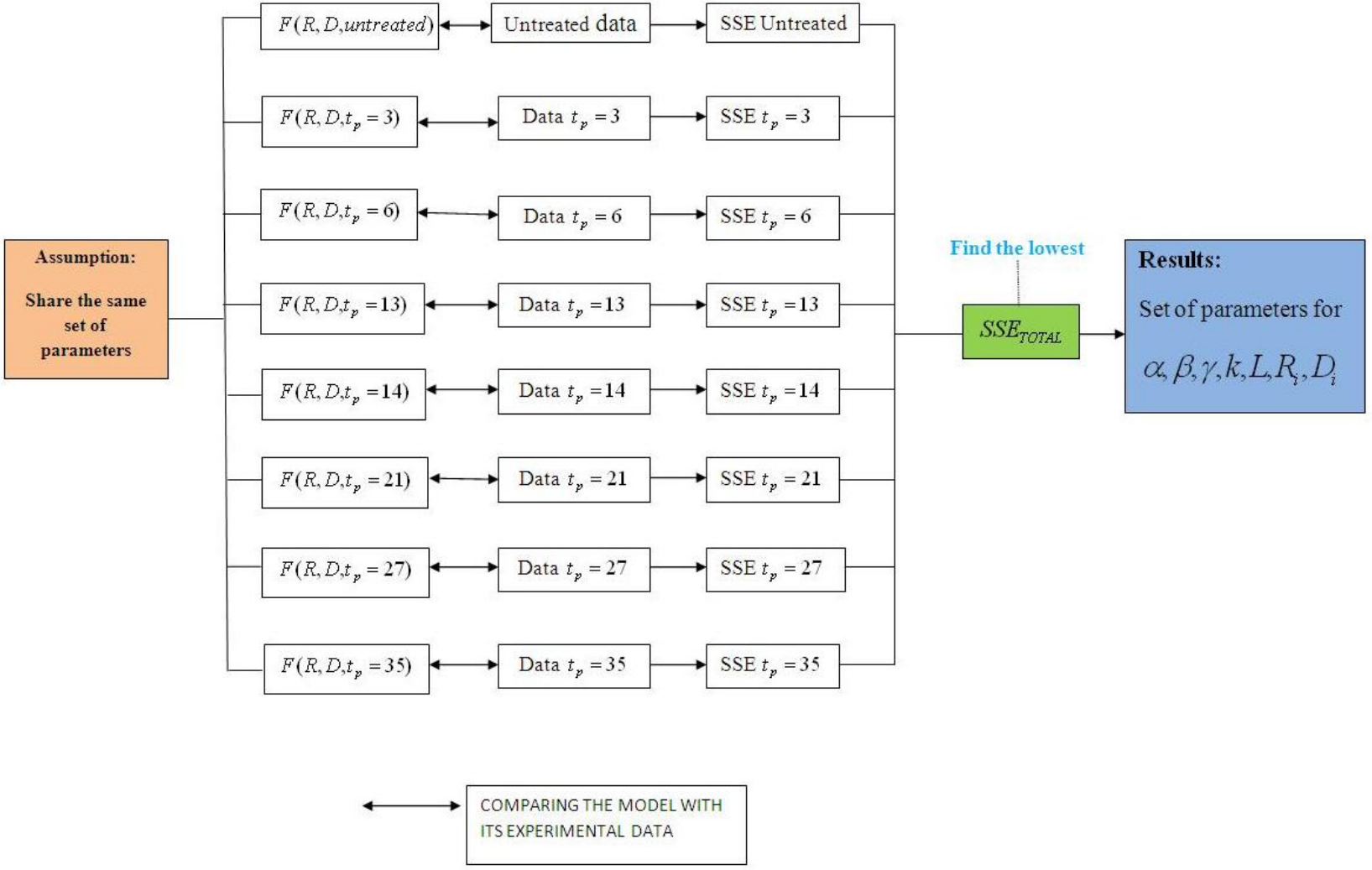

FIGURE 5.8: Parameter estimation using the experimental data in Table 5.4.

5.2.1 New Results

5.2.1.1 New Optimal Parameter Values

The results in Table 5.5 show that the global minimum value of the final SSE is achieved at 0.8968, based on the initial guesses (1), (2), (3), (4) and (7). For those initial guesses which reach the global minimum of SSE, the final value of each parameter is identical. In this case, the model parameters can be uniquely estimated. It can be concluded that this model is identifiable, and the values of the unknown parameter are:

$$\begin{aligned} \alpha &= 0.0908 \text{ days}^{-1} \\ \beta &= 0.7379 \text{ days}^{-1} \\ \gamma &= 0.2801 \text{ days}^{-1} \\ k &= 5.3749 \\ L &= 10.7607 \text{ days} \\ R_i &= 0.6118 \\ D_i &= 0.0168. \end{aligned} \tag{5.5}$$

In contrast to earlier findings, the value for α is positive, which means, from Equation (4.9), the dynamics involve compartment R moving towards compartment S. In other words the basal resistant seedlings lose their resistance and become susceptible. The divergent of the empirical result for the α can only be attributed physiologically to the effect of the elicitor. The non-treated cohort could, in principal behave differently.

Parameters	(1)		(2)		(3)		(4)		(5)		(6)		(7)	
	Initial	Final	Initial	Final	Initial	Final	Initial	Final	Initial	Final	Initial	Final	Initial	Final
k	0.4468	5.3749	0.5108	5.3749	0.1712	5.3749	0.1712	5.3749	1.0000	2.1291	1.0000	1.0968	3.0000	5.3749
L	0.3063	10.7607	0.8176	10.7607	0.7060	10.7607	10.0000	10.7607	1.0000	2.1632	1.0000	3.4517	10.0000	10.7607
γ	0.2801	0.2801	0.3000	0.2801	0.2801	0.2801	0.2000	0.2801	0.1419	0.2472	0.8147	0.0926	0.2000	0.2801
β	0.7379	0.7379	0.6000	0.7379	0.7379	0.7379	0.6000	0.7379	0.4218	0.0925	0.9058	0.6499	0.6000	0.7379
α	0.5085	0.0908	0.7948	0.0908	0.0908	0.0908	0.1000	0.0908	1.0000	1099.3665	1.0000	-0.0127	0.1000	0.0908
R_i	0.6118	0.6118	0.2000	0.6118	0.6118	0.6118	0.5000	0.6118	0.9157	-409.8927	0.1270	0.3852	0.5000	0.6118
D_i	0.0164	0.0164	0.0164	0.0164	0.1000	0.0164	0.1000	0.0164	0.0186	0.1480	0.0186	0.0186	0.1000	0.0164
SSE		0.8968		0.8968		0.8968		0.8968		1.6746		1.0201		0.8968

TABLE 5.5: Parameter estimation for the data in Table 5.4.

5.2.1.2 New Solution Graphs

The estimated parameter values given in (5.5) were used to plot the optimal solution graphs. Figures 5.9– 5.16 show how well the model fits to the corresponding experimental data (Table 5.5). The red lines describe the untreated model and the blue lines indicate the treated model. In each figure, the behaviours of the treated seedlings to the untreated seedlings, and corresponding to the inoculation time t_p, were compared. It is clearly demonstrated that all treated seedlings have a better disease resistance than the untreated seedlings. The findings of the new parameterisation are consistent with those in the old parameterisation; the difference is the quality of fit for each parameterisation, which arises from the greater number of data points used in this new fitting. The fitted model for $t_p = 13, 14$ are not particularly satisfactory, but this could be the result of the variability in the experimental observations - this experimental variability is beyond our control.

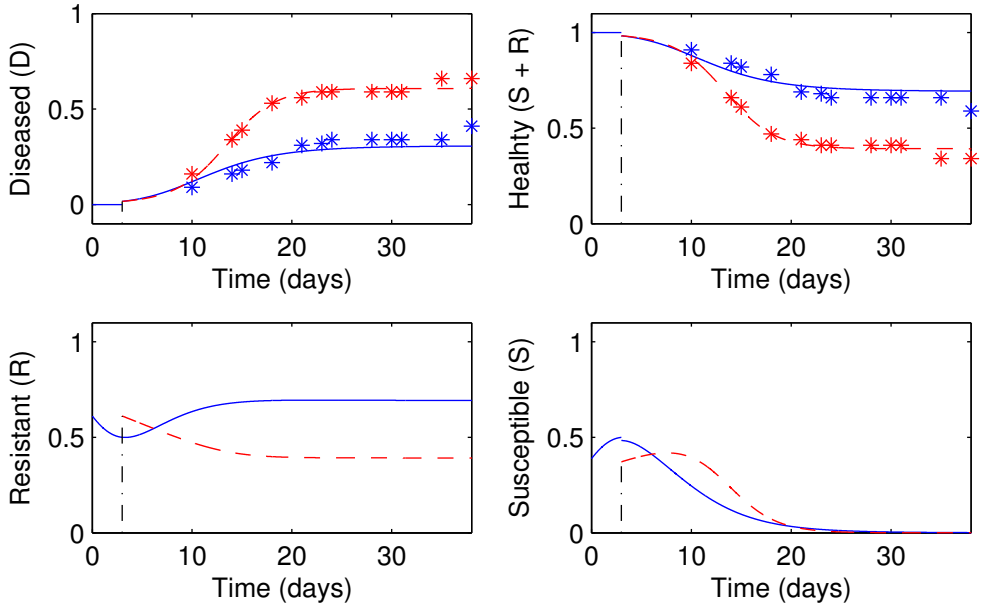

FIGURE 5.9: New solution graphs for each compartment with induction time $t_p = 3$ days. The solid lines (—) describe the dynamics for the treated model and the dashed lines (– –) indicate the untreated model. The marked points are the experimental data. The vertical line indicates the induction time $t_p = 3$.

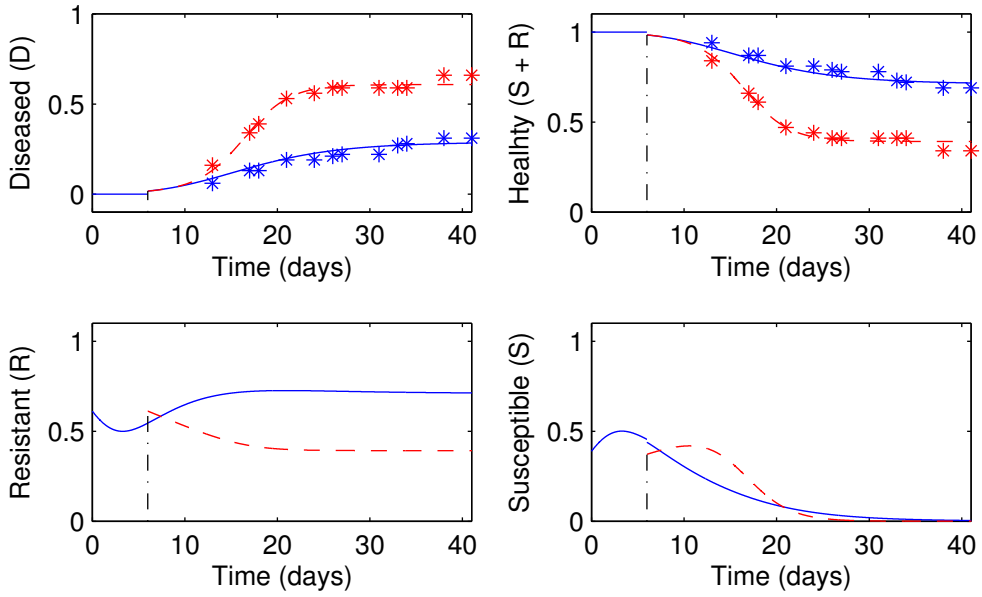

FIGURE 5.10: New solution graphs for each compartment with induction time $t_p = 6$ days. The solid lines (—) describe the dynamics for the treated model and the dashed lines (– –) indicate the untreated model. The marked points are the experimental data. The vertical line indicates the induction time $t_p = 6$.

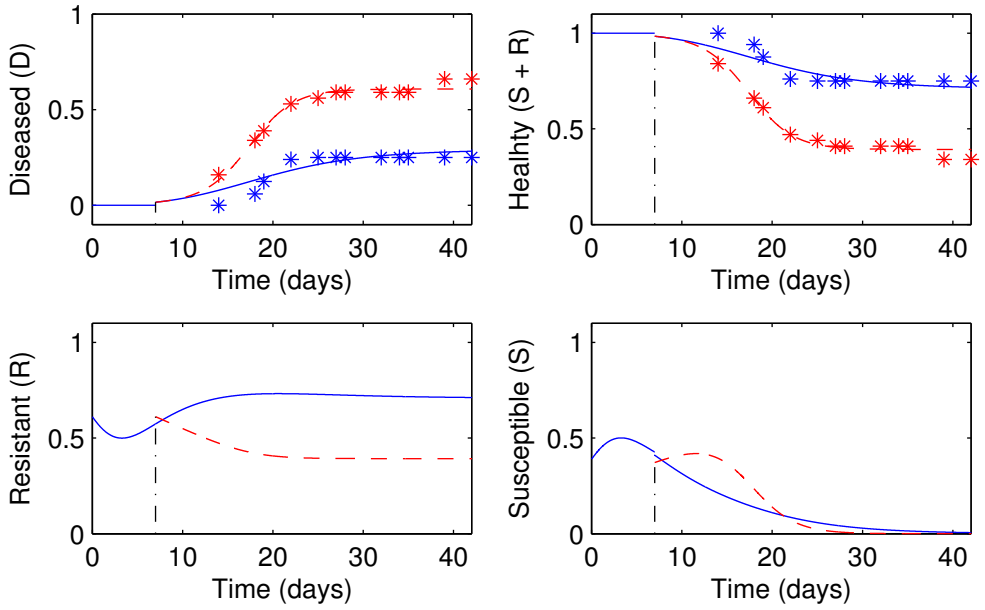

FIGURE 5.11: New solution graphs for each compartment with induction time $t_p = 7$ days. The solid lines (—) describe the dynamics for the treated model and the dashed lines (– –) indicate the untreated model. The marked points are the experimental data. The vertical line indicates the induction time $t_p = 7$.

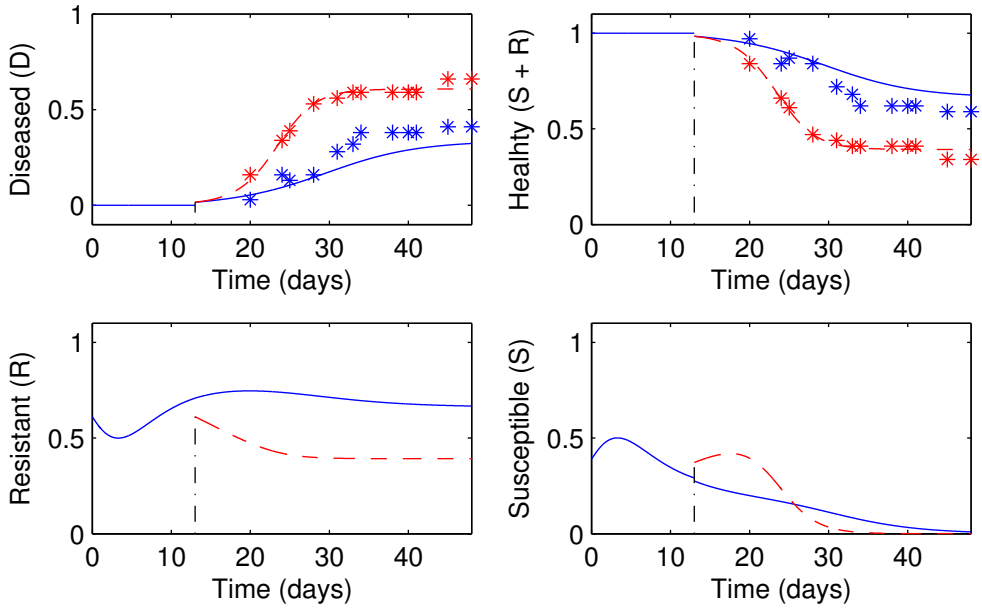

FIGURE 5.12: New solution graphs for each compartment with induction time $t_p = 13$ days. The solid lines (—) describe the dynamics for the treated model and the dashed lines (– –) indicate the untreated model. The marked points are the experimental data. The vertical line indicates the induction time $t_p = 13$.

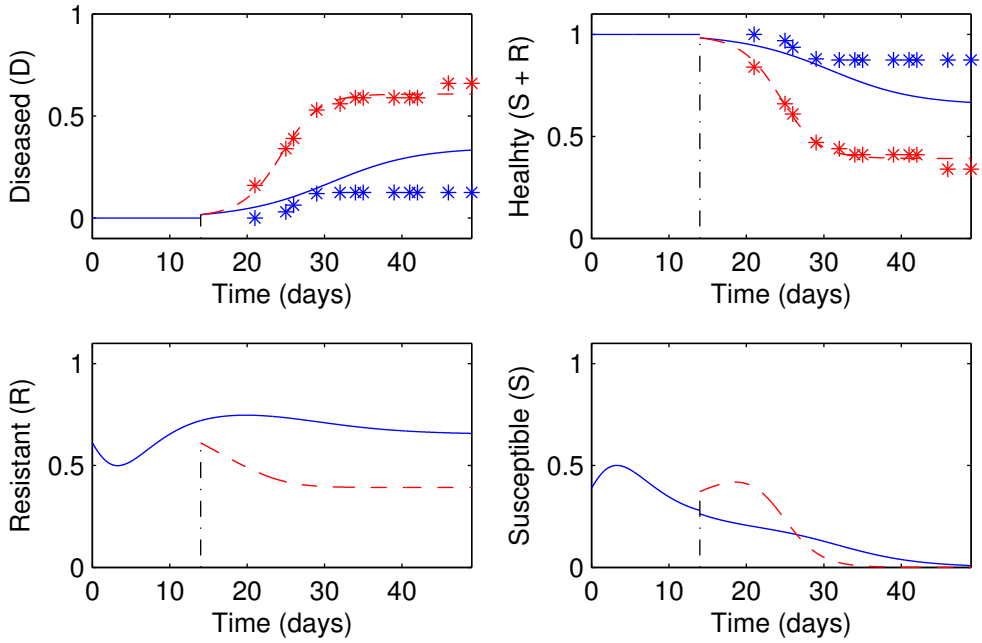

FIGURE 5.13: New solution graphs for each compartment with induction time $t_p = 14$ days. The solid lines (—) describe the dynamics for the treated model and the dashed lines (– –) indicate the untreated model. The marked points are the experimental data. The vertical line indicates the induction time $t_p = 14$.

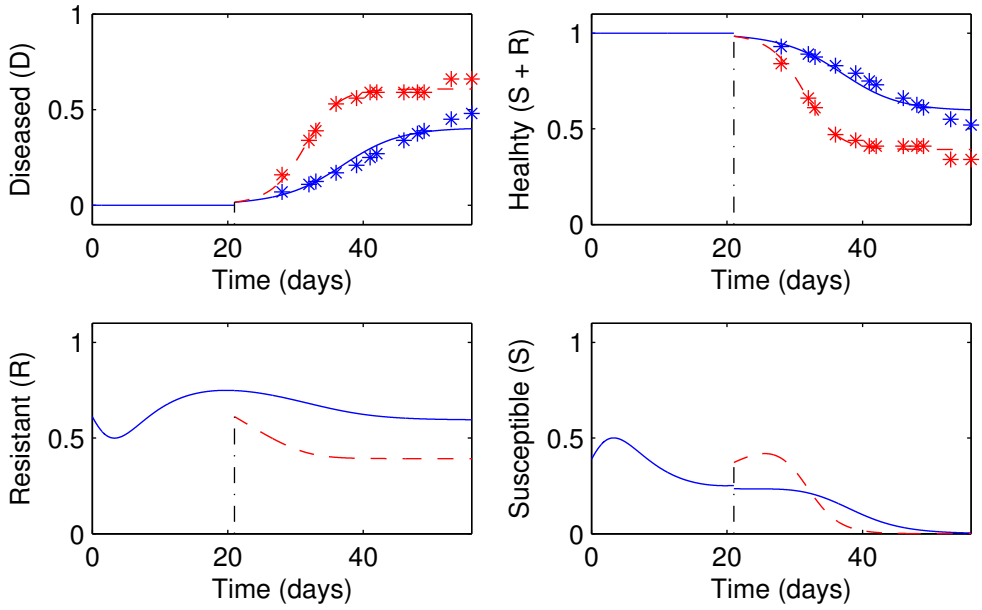

FIGURE 5.14: New solution graphs for each compartment with induction time $t_p = 21$ days. The solid lines (—) describe the dynamics for the treated model and the dashed lines (– –) indicate the untreated model. The marked points are the experimental data. The vertical line indicates the induction time $t_p = 21$.

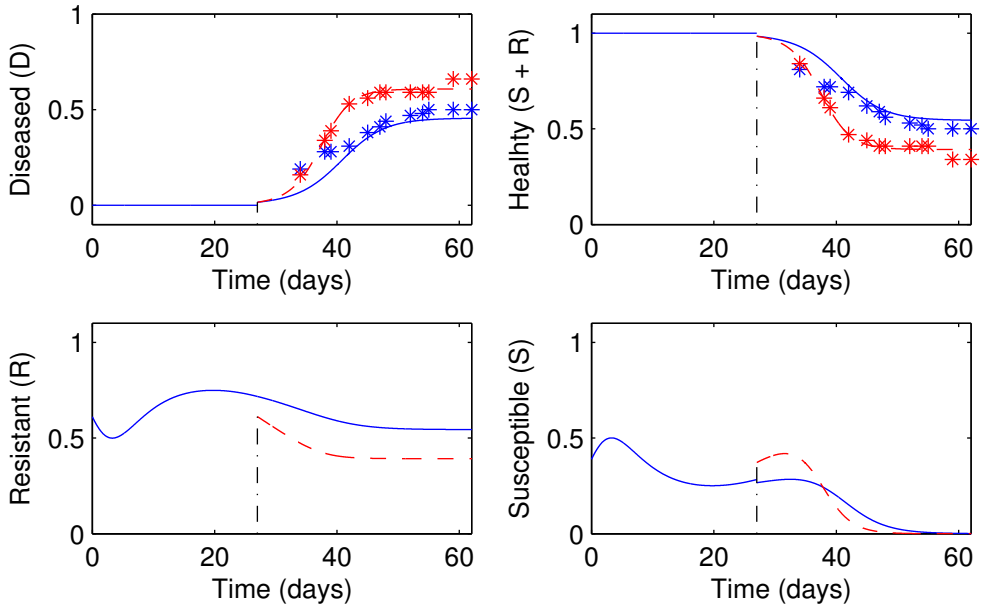

FIGURE 5.15: New solution graphs for each compartment with induction time $t_p = 27$ days. The solid lines (—) describe the dynamics for the treated model and the dashed lines (– –) indicate the untreated model. The marked points are the experimental data. The vertical line indicates the induction time $t_p = 27$.

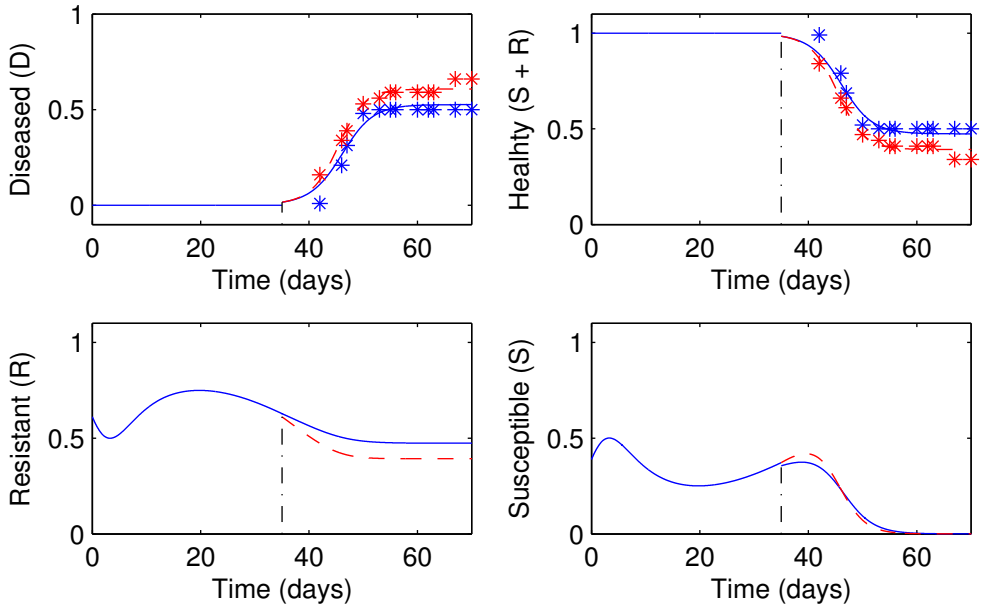

FIGURE 5.16: New solution graphs for each compartment with induction time $t_p = 35$ days. The solid lines (—) describe the dynamics for the treated model and the dashed lines (– –) indicate the untreated model. The marked points are the experimental data. The vertical line indicates the induction time $t_p = 35$.

It can be seen in Figures 5.9–5.16 that there is a discontinuity in the dynamics of diseased (D) and healthy ($H = S + R$) compartments, which is again due to the introduction of the pathogen. This means that in the absence of a pathogen attack the entire seedling population is healthy. Later, the proportion of these healthy seedlings decreases as the disease spreads until it stops at the limiting diseased value. The most striking result to emerge from this new parameterisation result is the description of the dynamics between the resistant R and susceptible S compartments. It shows that almost half of the seedling population is susceptible and the remainder resistant. From the figures at the initial phase, the resistant compartment is decreasing until, after some time, it increases to reach the steady state. This is probably because of the delay effect of the elicitor treatment. In general, this dynamical behaviour is comparable to all treated seedlings with different induction time t_p. This can be clearly seen in Figure 5.17.

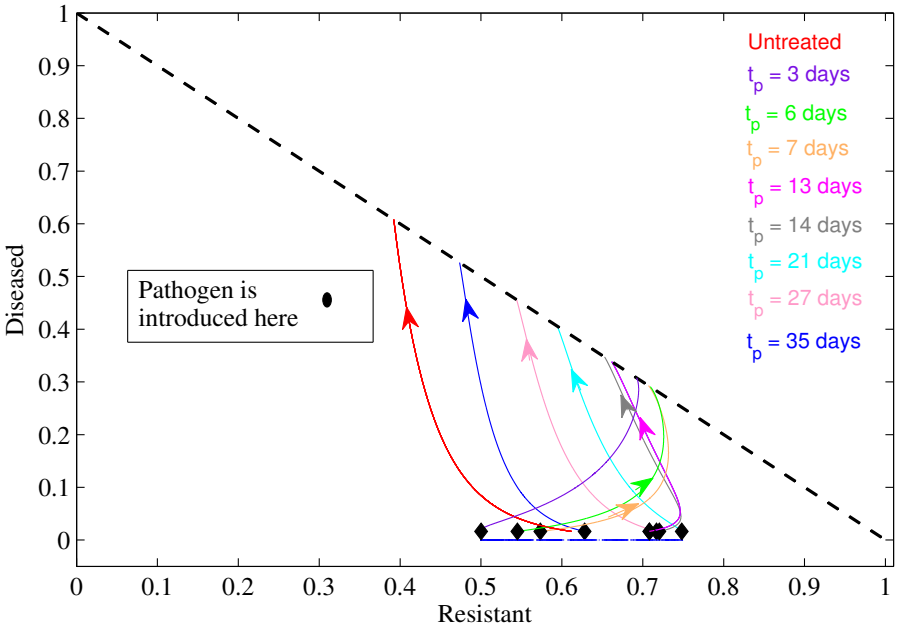

FIGURE 5.17: The phase-plane for the induced resistance (IR) model with trajectories of the R, D compartments plotted in the feasible region ($R, D > 0, R + D < 1$) using new parameter estimation as in (5.5). The lines schematically represent the values of the two compartments R and D as time passes for the equations (1)–(5) based on each induction case t_p and the untreated case. When $D = 0$, the straight lines illustrate the dynamics of the R compartment before the pathogen inoculation. These lines will have a discontinuity when the pathogen is introduced at time $t = t_p$, and show the state of the R compartment at that particular time. As can be seen in the figure, there is a jump in the D values of D_i at $t = t_p$ and the trajectories of the R, D compartments will continue to approach the straight line $R + D = 1$. For the untreated case, the dynamics of the R, D compartments will depend on the initial condition of the systems i.e. R_i and D_i.

Figure 5.17 illustrates the characteristics of the two compartments R and D. The flows in the figure indicate the time-evolution of the system of the differential equations based on the different values of t_p and the untreated case. It shows that when t_p is between three and seven days, the development of disease is less severe compared with the other induction times and with the untreated control plants. The figure shows that the trajectories for each induction case will eventually approach the straight line $R + D = 1$. The model has a line of equilibrium states in the R, D plane which are neutrally stable (non-hyperbolic), and predicts that disease development depends on the induction time t_p.

An interesting result shown here in Figure 5.17 is that the best disease control attained when pathogen inoculation occurs at the time of lowest resistance. The reason of such scenario happened is beyond of this thesis scope and there is no available experimental data to support the statement.

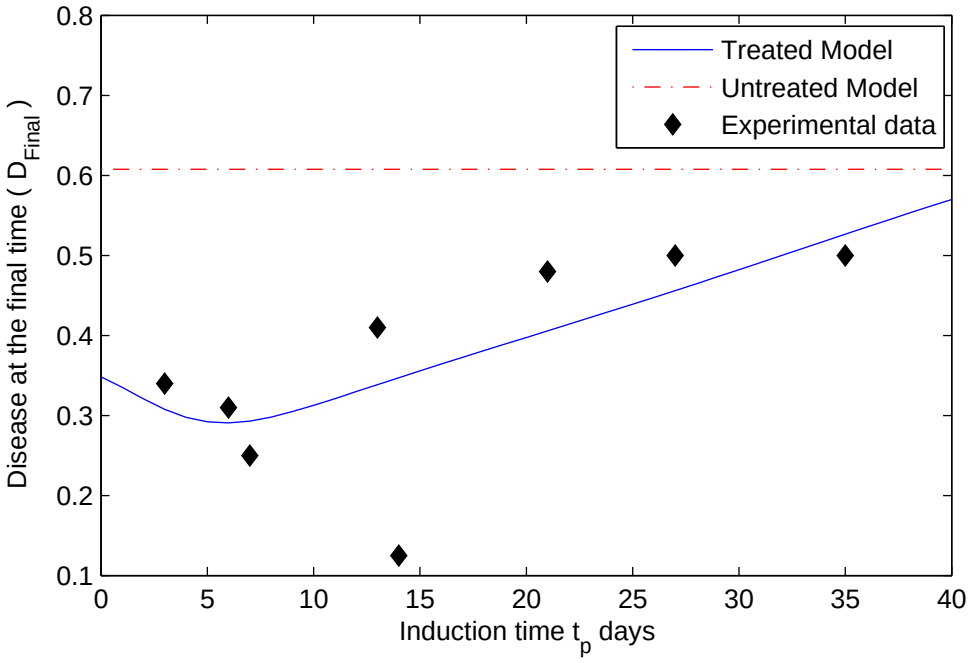

FIGURE 5.18: The proportion of the diseased seedlings which were treated at a fixed final time against the inoculation time t_p

Figure 5.18 shows the proportion of diseased seedlings which were treated at the final time against the induction time t_p. The IR model can determine the optimal induction time t_p that gives the best outcome for disease control for the treated pine seedlings. This can be done by taking the point at the final time t_f as a fixed variable, e.g. let $t_f = t_p + 35$, and minimise the trajectories of $D_{final} = D(t = t_f)$. For $t_p = 0$ days, it means the elicitor treatment and the pathogen inoculation were introduced at the same time. Experimental data for diseased seedlings, measured at $t_p + 35$ days for each t_p case, is taken into account to compare with the model outcome. This numerical experiment shows that induced resistance was greatest when MeJA was applied to pine seedlings six days before pathogen inoculation. Although the error gaps between the model outcomes and the experimental data are noticeable,

especially for the case $t_p = 14$ days, it can be attributed to either the variability of the data sets or experimental error. Also note that it is assumed that for every induction time t_p, the dynamics share the same parameter values.

5.2.2 Model's Validation

To validate this proposed IR model, consider the experimental data except the data points for $t_p = 21$ (in Table 5.5) and redo the parameterisation. The results are as below:

$$\begin{aligned} \alpha &= 0.1028 \text{ days}^{-1} \\ \beta &= 0.8239 \text{ days}^{-1} \\ \gamma &= 0.2689 \text{ days}^{-1} \\ k &= 5.1561 \\ L &= 10.8161 \text{ days} \\ R_i &= 0.6434 \\ D_i &= 0.0124. \end{aligned} \tag{5.6}$$

These parameter values in (5.6) were then used to plot the model when $t_p = 21$ and the results compared with the experimental data. Based on Figure 5.19, it can be seen that the IR model with the parameters values in (5.6), fits well with the experimental data. The most striking result from this numerical experiment is the similarity of parameter values both in (5.6) and (5.5).

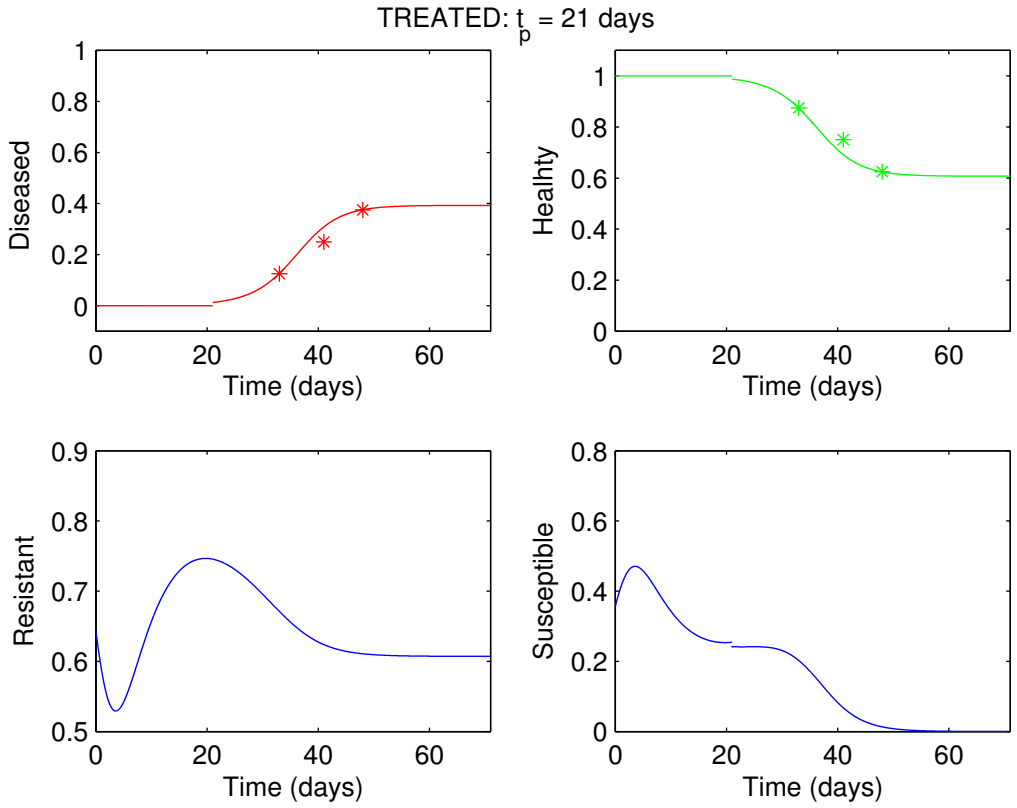

FIGURE 5.19: The treated model with the inoculation time $t_p = 21$ days. The marked points are the experimental data $t_p = 21$ as in Table 4.2. The calculated coefficient of determination $R^2 = 0.8917$ shows this optimal parameter values in (5.6) is well fitted to the IR model.

5.3 Summary

In this chapter, the results of the parameter estimation for our proposed IR model have been presented. The least-squares method is used as the objective function to optimise the parameters for the IR model. The results suggest that the parameterisation will become more robust if we take into account the data sets both in Table 4.1 and Table 4.2. The model parameters are identifiable with any initial guesses used and suggest that it is stable; always achieving the global minimum value of SSE to get the optimal value of parameters with the best model fitting. Moreover, even though the experimental data required consists of two compartments

only, which is (H, D), this model has the ability to determine the H compartment defining $H = S + R$. In other words, the susceptible cohort can be determined by $S = 1 - R - D$ and can be separated out by this model.

In summary, the table below shows the parameter values which are used in this thesis:

Parameter	**Description**	**Value [Units]**
α	The specific rate at which untreated plants lose the resistance due to the pathogen attack.	0.0908 [days^{-1}]
β	The specific rate at which the disease spreads.	0.7379 [days^{-1}]
γ	The specific rate the resistant plant becomes susceptible.	0.2801 [days^{-1}]
k	Determines the effectiveness of the elicitor.	5.3749 [dimensionless]
L	The time where the elicitor effectiveness is at the peak.	10.7607 [days]
R_i	A proportion of the plant population exhibit natural resistance at the initial time $t = 0$.	0.6118 [dimensionless]
D_i	A proportion of the plant population which becomes infected immediately after the pathogen challenge.	0.0168 [dimensionless]

TABLE 5.6: Parameter values obtained from parameterisation using experimental data of IR for pine seedlings with elicitor MeJA.

Biologically, the potential for using a plant-defence elicitor to induce resistance against plant disease is evaluated through the use of this IR compartment model, which in turn is based on a SIR-type model. The model enables the likely long-term effect of the disease to be examined. The attracting steady states in this model are dependent on the initial conditions and not, as is usually the case, asymptotically stable (the phase-plane in Figure 5.17). Of particular interest is the optimal induction time t_p, which leads to a minimisation of the long-term effect for elicitor application before the inoculation of the plants by the pathogen. The knowledge of this optimal t_p is crucial for an effective elicitor to enhance IR as pointed out by Walters et al. (2013).

In conclusion, based on the parameterisation in Section 5.2, this IR model suggests that the model does exhibit all the characteristics observed in the data provided to

us. Further analysis on extending this IR model using the same parameter values in Table 5.6 will be presented in the following chapters.

Chapter 6

IR Model Extensions

In the previous chapter, the unknown parameters for this IR model were determined by the least-squares method. Here, the mathematical model is extended to include the concentration effect, multiple elicitor applications and post-inoculation treatment.

The discussions in this chapter are part of the article submitted to the Journal of Theoretical Biology (Abdul Latif et al., 2014).

6.1 Varying the Elicitor Concentration

Holopainen et al. (2009); Teniente et al. (2010); Thakur & Sohal (2013) reviewed that various studies have been measured where exogenous application of elicitor, specifically methyl jasmonate (MeJA), can enhance the levels of certain defensive compounds of plants, and in consequence be used to trigger the defence mechanism. Some experimental studies have reported that there is an effect of different elicitor concentrations on the capability to induced resistance (Godard et al., 1999; Boughton et al., 2006; Gould et al., 2009; Vivas et al., 2012; Hindumathy, 2012). This has led to an increased interest in extending the proposed IR model to include a measure of elicitor concentration.

Plant & Food Research Ltd set up an experiment for this purpose and provided relevant experimental data. Different concentrations of elicitor MeJA at 1.1, 4.5, 18 mM were sprayed onto pine seedlings and these seedlings were inoculated with pathogen after seven days of seed treatment (i.e. $t_p = 7$). Various levels of protection over the control can be seen in Table 6.1.

Unpublished data from Plant & Food Research Ltd (sent Oct 2011)			
Elicitor Concentration	Disease Assessment Time		
	$t_p + 14$	$t_p + 22$	$t_p + 28$
1.1mM = 0.025%	0.10	0.25	0.30
4.5mM = 0.10%	0.05	0.10	0.15
18mM = 0.40%	0.00	0.15	0.15
Untreated Control 0%	0.30	0.65	0.70

Unpublished data from Plant & Food Research Ltd (sent Apr 2013)			
Elicitor Concentration	Disease Assessment Time		
	$t_p + 14$	$t_p + 21$	$t_p + 35$
1.1mM = 0.025%	0.250	0.313	0.250
4.5mM = 0.10%	0.125	0.250	0.250
18mM = 0.40%	0.429	0.571	0.770
Untreated Control 0%	0.500	0.625	0.625

TABLE 6.1: The proportion of the diseased *Pinus radiata* seedlings following treatment with applications of 0, 1.1, 4.5,18 mM methyl jasmonate (MeJA) and subsequent inoculation of all seedlings with *Diplodia pinea*. This experimental data is used to estimate the value of parameter r in Equation (6.1).

Data in Gould et al. (2009))	
Elicitor Concentration	Disease Assessment Time
	$t_p + 35$
1mM = 0.023%	0.25
4.5mM = 0.10%	0.25
18mM = 0.40%	0.80

TABLE 6.2: The proportion of the diseased *Pinus radiata* seedlings at five weeks following treatment with applications of three different concentrations of methyl jasmonate (MeJA) and subsequent inoculation of all seedlings with *Diplodia pinea*. This data is also used in order to estimate r.

The data suggests that the effect of the different concentration is not linearly dependent on the elicitor dose. Hence, to replicate this experimental data measurement, the elicitor effect is formulated as

$$f(a) = a^r e^{1-a}, \tag{6.1}$$

where a is the elicitor concentration and r is a constant to describe the sub-linear effects of the elicitor concentration with the elicitor effectiveness for induced resistance. Note that $f(a)$ is maximised at $a = r$.

Thus, the elicitor term will be:

$$\text{concentration} \times \text{elicitor effectiveness to the plant} = a^r e^{1-a} \times \frac{kt}{t^2 + L^2}. \tag{6.2}$$

As mentioned in Chapter 4, k determines the effectiveness of the elicitor used for treatment and L corresponds to the time when the effectiveness is at the peak. The newly introduced parameter r needs to be determined while the parameter a is deduced from the experimental data. To parameterise r, the same least-squares method was used and another dataset (Table 6.2) is also included in this process.

To simplify the parameterisation process, the values of a, percentage (%) concentration, were scaled as

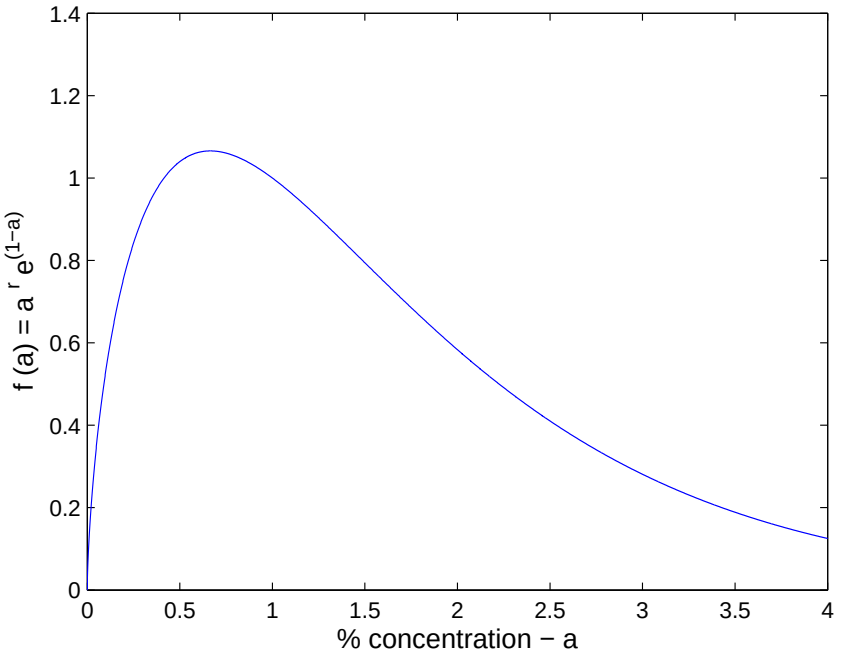

FIGURE 6.1: Graph for Equation (6.1) with $r = 0.6650$.

$$a = [0.23, \quad 0.25, \quad 1, \quad 4].$$

This approach is taken in order to use the same parameter values $(\alpha, \beta, \gamma, k, L, R_i, D_i)$ determined in Chapter 5 (Table 5.6) since the datasets in Table 4.1 and Table 4.2, the elicitor concentration used was 0.1% and the parameter estimation is done using this data. The biological assumption is that the dynamics of the physiological response was assumed to remain the same, except for the elicitor effect when the dose is changed. Therefore, the elicitor percentage concentration can be taken as a scaled factor of 1. Hence, the term in Equation (6.1) is applicable for this scale assumption, for which if $a = 1$ implies $f(a = 1) = 1$, and this becomes the original equation as in Chapter 4 (see Equation (4.1)–Equation (4.3)). Moreover, for the 0% concentration (or "water treatment") this implies $a = 0$ which gives $f(a = 0) = 0$, which suggests that the "water treatment" seedlings should be evaluated as the untreated model (see Equation (4.9)–Equation (4.10)).

This varying elicitor concentration scenario can be formulated as:

- For 0% elicitor concentration assume as untreated case

  For pre-inoculation: $0 < t < t_p$

$$\frac{dR}{dt} = -\alpha R(1-R) \quad ; R(0) = R_i. \tag{6.3}$$

  For post-inoculation: $t_p < t < T$

$$\frac{dR}{dt} = -\alpha R(1-R-D) \quad ; R(t_p) = R_{p_{\text{unt}}} \tag{6.4}$$

$$\frac{dD}{dt} = \beta D(1-R-D) \quad ; D(t_p) = D_i. \tag{6.5}$$

- For other elicitor concentration

  For pre-inoculation: $0 < t < t_p$

$$\frac{dR}{dt} = (a^r e^{(1-a)} \frac{kt}{t^2+L^2} - \gamma R)(1-R) \quad ; R(0) = R_i \tag{6.6}$$

  For post-inoculation: $t_p < t < T$

$$\frac{dR}{dt} = (a^r e^{(1-a)} \frac{kt}{t^2+L^2} - \gamma R)(1-R-D) \quad ; R(t_p) = R_p \tag{6.7}$$

$$\frac{dD}{dt} = \beta D(1-R-D) \quad ; D(t_p) = D_i. \tag{6.8}$$

where $R_{p_{\text{unt}}}$ and R_p are obtained from Equation (6.3) and Equation (6.6) respectively.

These equations (Equation (6.3)–(6.8)) were used to determine the value of r, by matching the model with the experimental data in Table 6.1 and Table 6.2. From this numerical computation, it was obtained that $r = 0.6650$. This is shown in Table 6.3 where the global minimum value of the final SSE seems to be achieved at 4.6725, based on any initial guesses; thus parameter r is identifiable and it converges to a unique value.

Parameters	(1)		(2)		(3)		(4)		(5)	
	Initial	Final	Initial	Final	Initial	Final	Initial	Final	Initial	Final
r	10.0000	0.6650	1.9048	0.6650	0.9134	0.6650	8.1472	0.6650	2.5397	0.6650
SSE		4.6725		4.6725		4.6725		4.6725		4.6725

TABLE 6.3: Parameter estimation for the parameter r using treated experimental data as given in Table 6.1 and Table 6.2.

This r value has been used to plot the solutions to Equations (6.3)–(6.8); and Figures 6.2 – 6.6 show the model simulation for each elicitor concentration and exhibits the characteristics of the experimental data given in the Table 6.1 and Table 6.2. Although it is not well fitted, this is likely the result of the variability in the experimental observations, or the quantity of experimental data is not sufficient to estimate r accurately.

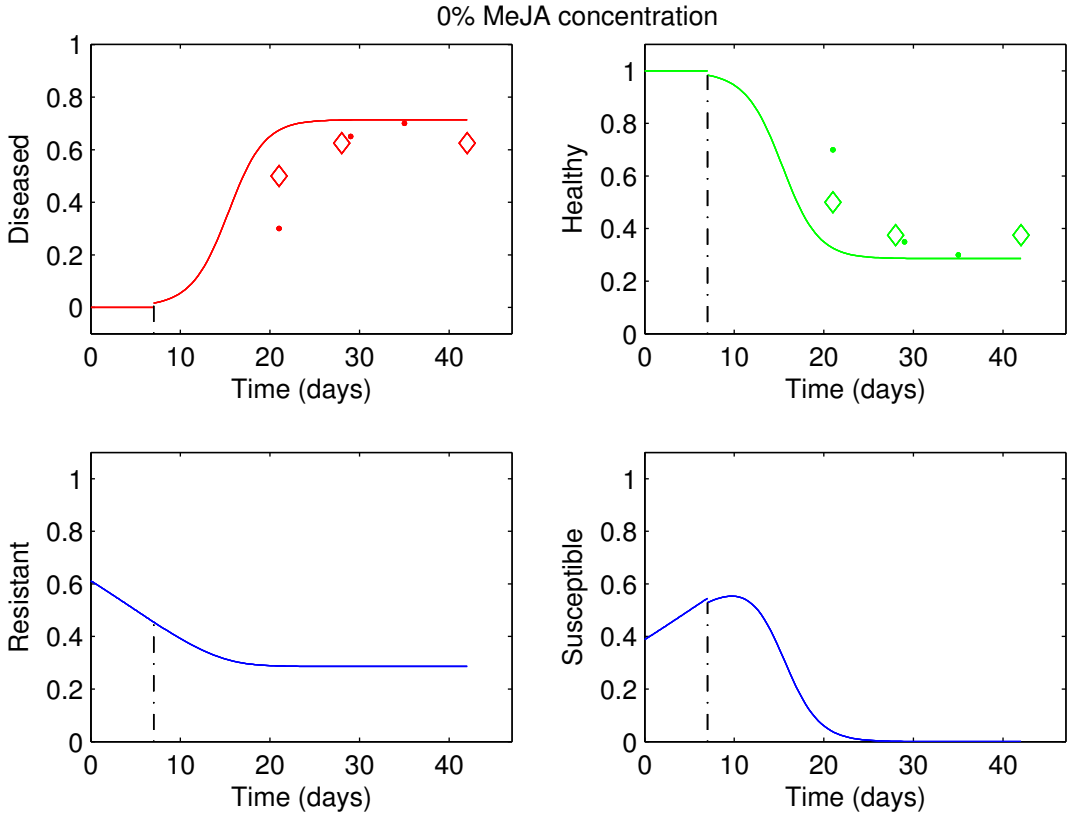

FIGURE 6.2: Solution graphs for each compartment with its elicitor 0 % concentration for the untreated control seedlings group. The vertical line (- -) corresponds to the inoculation time $t_p = 7$ days. The marked points are the experimental observations: $\diamond$ (April 2013 data) and $\bullet$ (October 2011 data).

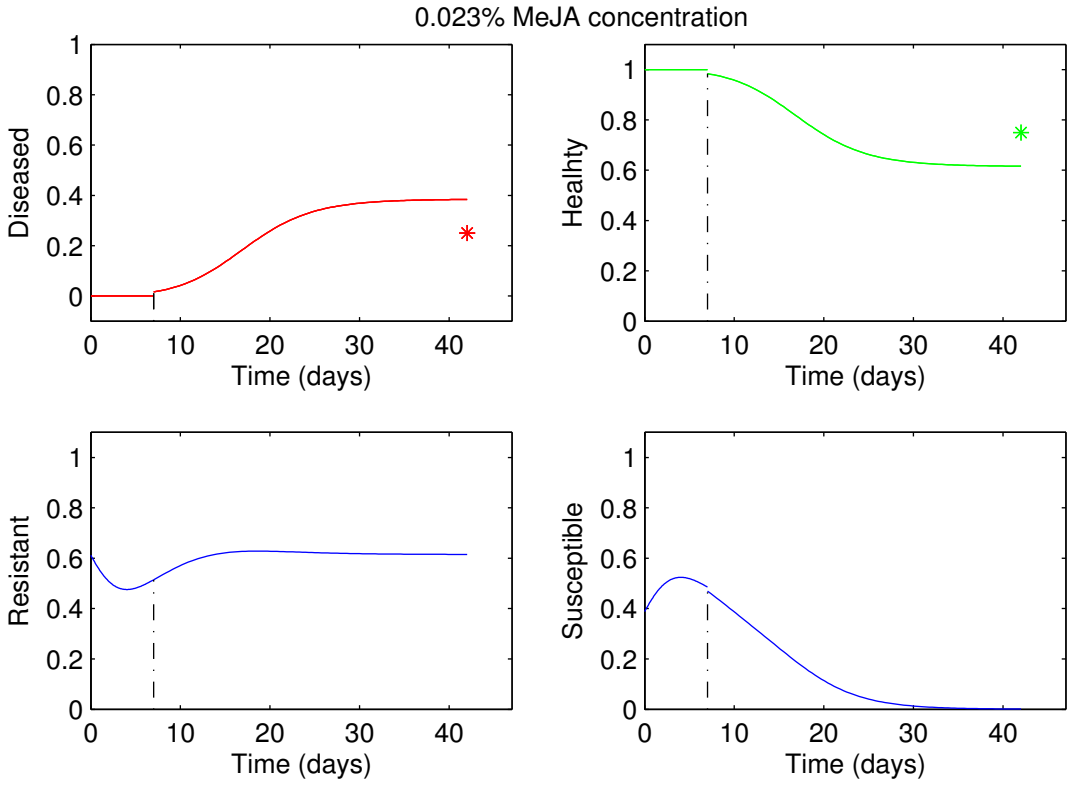

FIGURE 6.3: Solution graphs for each compartment with its elicitor 0.023% concentration. The vertical line (- -) corresponds to the inoculation time $t_p = 7$ days. The marked points are the experimental observations: $*$ (Table 6.2).

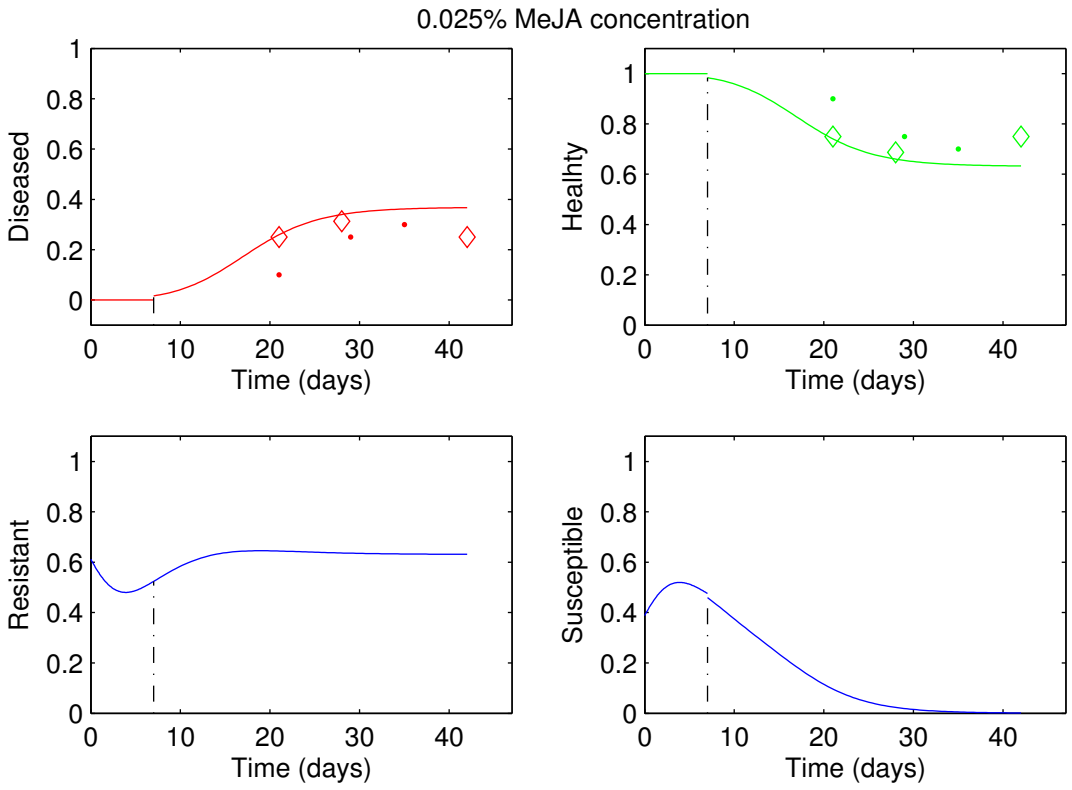

FIGURE 6.4: Solution graphs for each compartment with its elicitor 0.025% concentration. The vertical line (- -) corresponds to the inoculation time $t_p = 7$ days. The marked points are the experimental observations: $\diamond$ (April 2013 data) and $\bullet$ (October 2011 data).

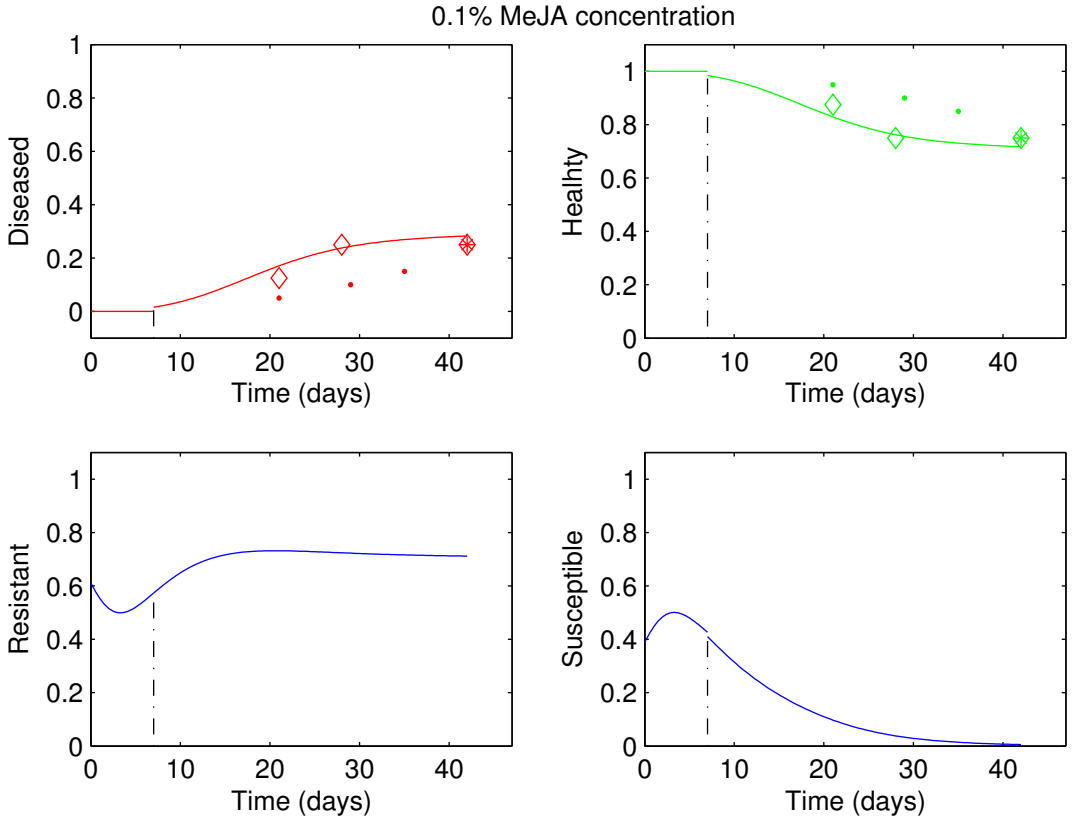

FIGURE 6.5: Solution graphs for each compartment with its elicitor 0.1% concentration. The vertical line (- -) corresponds to the inoculation time $t_p = 7$ days. The marked points are the experimental observations: $\diamond$ (April 2013 data), $\bullet$ (October 2011 data), and $*$ (Table 6.2).

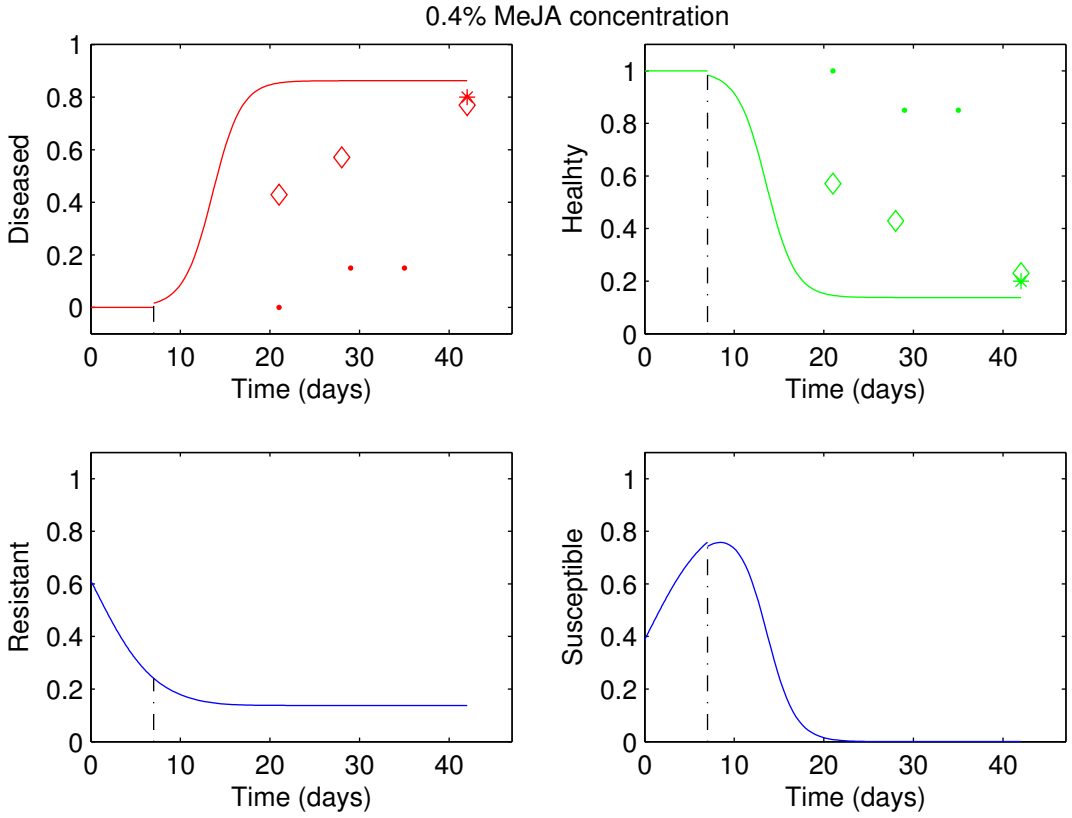

FIGURE 6.6: Solution graphs for each compartment with its elicitor 0.4% concentration. The vertical line (- -) corresponds to the inoculation time $t_p = 7$ days. The marked points are the experimental observations: $\diamond$ (April 2013 data), $\bullet$ (October 2011 data), and $*$ (Table 6.2).

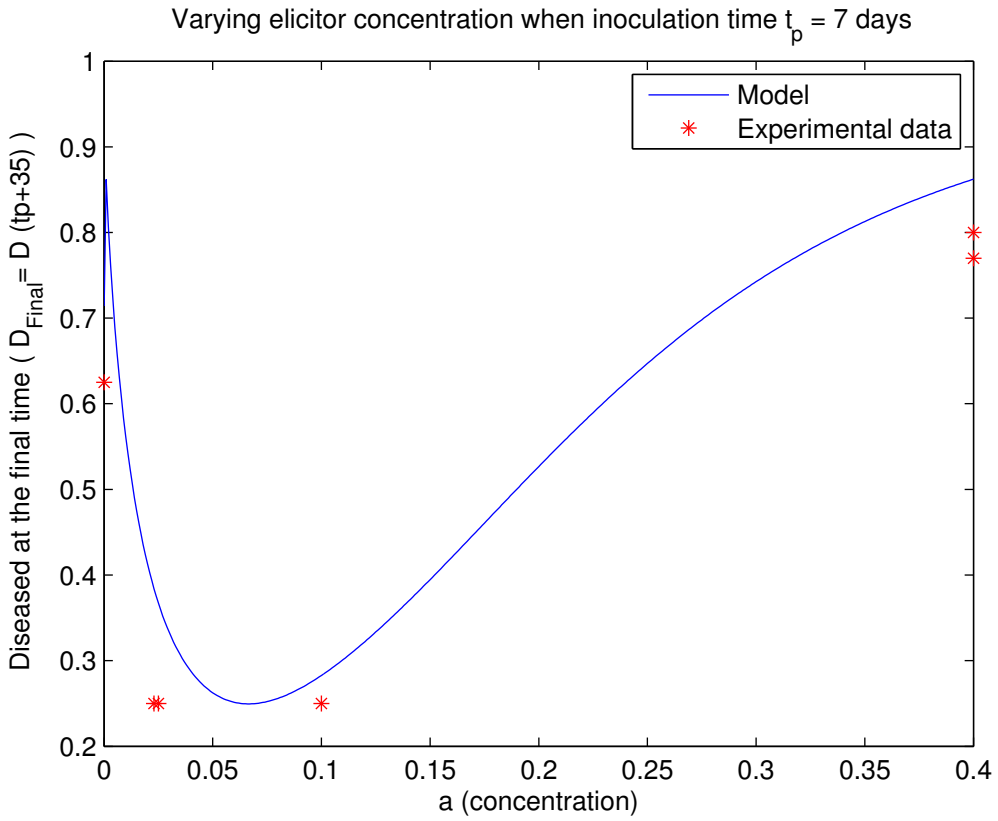

FIGURE 6.7: The proportion of diseased seedlings which were treated (seven days before the pathogen challenge) at the final time $(t_p + 35)$ against the elicitor concentration. The marked points $*$ are the experimental data (from dataset April 2013 and Table 6.2).

The results shown in Figure 6.7 demonstrate that the effect of elicitor MeJA on seedling health is dose dependent. Based on the model simulations, elicitor with concentrations of 0.02% and 0.1% offered a great disease control at a proportion of 0.4 and 0.3 of the whole seedlings population became diseased, respectively. The proportion of diseased seedlings decreases at first, then increases above concentrations of around 0.1%; for example a concentration of 0.4% offers ∼10% disease protection only. In a study by Gould et al. (2009) indicated when a higher elicitor concentration ($> 0.1\%$) is used, there is phytotoxicity in the treated seedlings, and disease incidence is higher. On the other hand, the model simulation shows that if lower concentrations (e.g. $< 0.02\%$) are used, there will be no significant difference in the results compared to the untreated seedlings (those with no disease efficacy).

This numerical experiment also demonstrated that at the lowest dose of elicitor ($\sim 0.067\%$) there was an induced resistance response to the pathogen attack; this finding has important cost benefit implications as knowledge of an "optimal" dose of MeJA would imply increased effectiveness with respect to cost, making it more attractive as a plant protection product. Note that the optimal value obtained from the model's result is close to the value which maximise the function $f(a)$, in the elicitor effectiveness factor.

6.2 Multiple Elicitor Applications

Previous studies have demonstrated that more frequent elicitor applications appeared to be phytotoxic to the seedlings (Gould et al., 2009) though they did suppress disease development (Dinh et al., 2008). It would be beneficial if this experimental observation could be modelled mathematically. Here, the proposed IR model is extended to include a multiple elicitor application; with only two elicitor applications considered in this case study. The elicitors were applied before the pathogen inoculation and the same amount of elicitor used at each time point. This scenario can be described by the following diagram.

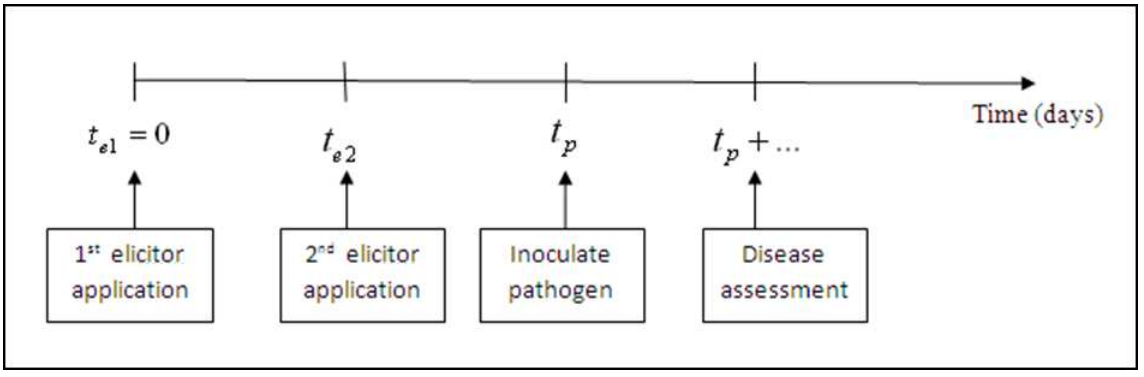

FIGURE 6.8: Schematic timeline for the multiple elicitor applications. Same concentrations (or amount) was applied at each time.

Here, it is assumed that $f(a) = a^r e^{(1-a)}$; therefore the equations for a multiple application will be:

- First application: for $0 < t < t_{e_2}$

$$\frac{dR}{dt} = (f(a)\frac{kt}{t^2 + L^2} - \gamma R)(1 - R) \quad ; R(0) = R_i. \tag{6.9}$$

- Second application: for $t_{e_2} < t < t_p$

$$\frac{dR}{dt} = \left((f(a)\frac{kt}{t^2 + L^2} + f(a)\frac{k(t - t_e)}{(t - t_e)^2 + L^2} - \gamma R\right)(1 - R) \quad ; R(t_{e2}) = R_p. \tag{6.10}$$

- Pathogen inoculation: $t_p < t < T$

$$\begin{aligned} \frac{dR}{dt} &= \left(\left[f(a)\frac{kt}{t^2 + L^2} + f(a)\frac{k(t - t_e)}{(t - t_e)^2 + L^2}\right] - \gamma R\right) \\ &\quad \times(1 - R - D) \qquad ; R(t_p) = R_p, \qquad (6.11) \\ \frac{dD}{dt} &= \beta D(1 - R - D) \qquad ; D(t_p) = D_i. \qquad (6.12) \end{aligned}$$

Note that Equations (6.9)–(6.12) are formulated the same way as those in the single application situation. R_p in Equation (6.10) obtained from Equation (6.9). Here Equation (6.9) describes the first application and Equation (6.10) describes the second application at time t_{e_2}; while Equation (6.11) and Equation (6.12) describe the pathogen inoculation to the seedlings.

It is warmly acknowledged with gratitude that Plant & Food Research Ltd set up a special experiment for this case study (see Table 6.4). The pine seedlings were divided into three groups with different elicitor MeJA concentration. The seedlings were then treated at 7 and 14 days before the pathogen inoculation. That is $t_{e_1} = 0$, $t_{e_2} = 7$ and $t_p = 14$. It must be noted though, that there is no new parameterisation for this study case. The same parameter values in Table 4.3 and the r value stated in the previous section were used for plotting the solution of the Equations (6.9)–(6.12).

Unpublished data sent April 2013			
Elicitor Concentration	Disease Assessment Time		
	$t_p + 14$	$t_p + 21$	$t_p + 35$
1.1mM = 0.025%	0.00	0.188	0.190
4.5mM = 0.10%	0.125	0.438	0.500
18mM = 0.40%	0.778	0.778	0.890

TABLE 6.4: Experimental data on the multiple elicitor applications provided by Plant & Food. The numbers represent the proportion of the diseased seedlings. The pine seedlings were treated with MeJA at 14 days and 7 days before the pathogen inoculation. The number shows the proportion of the diseased pine seedlings.

Figures 6.9 – 6.11 show that the dynamics of these multiple elicitor applications (the red curve) correspond to the percentage concentration when compared to a single application (the blue curve). The marked points in the diagrams are the experimental data as shown in Table 6.4. The numerical computation of the proposed model demonstrates almost the same patterns as observed in the experiment. For a multiple elicitor application at the 0.4% dosage level, the predicted model has the best fit and reproduces the experimental observations, compared to the other percentage concentrations. Unlike the other elicitor concentrations, the error gap is large, which can be attributed to the model's formulation not being appropriate for these experimental observations for these particular concentrations. Moreover, in each figures, the simulations show that a multiple application enhanced the resistance in plants and gave a better disease control compared to a single application.

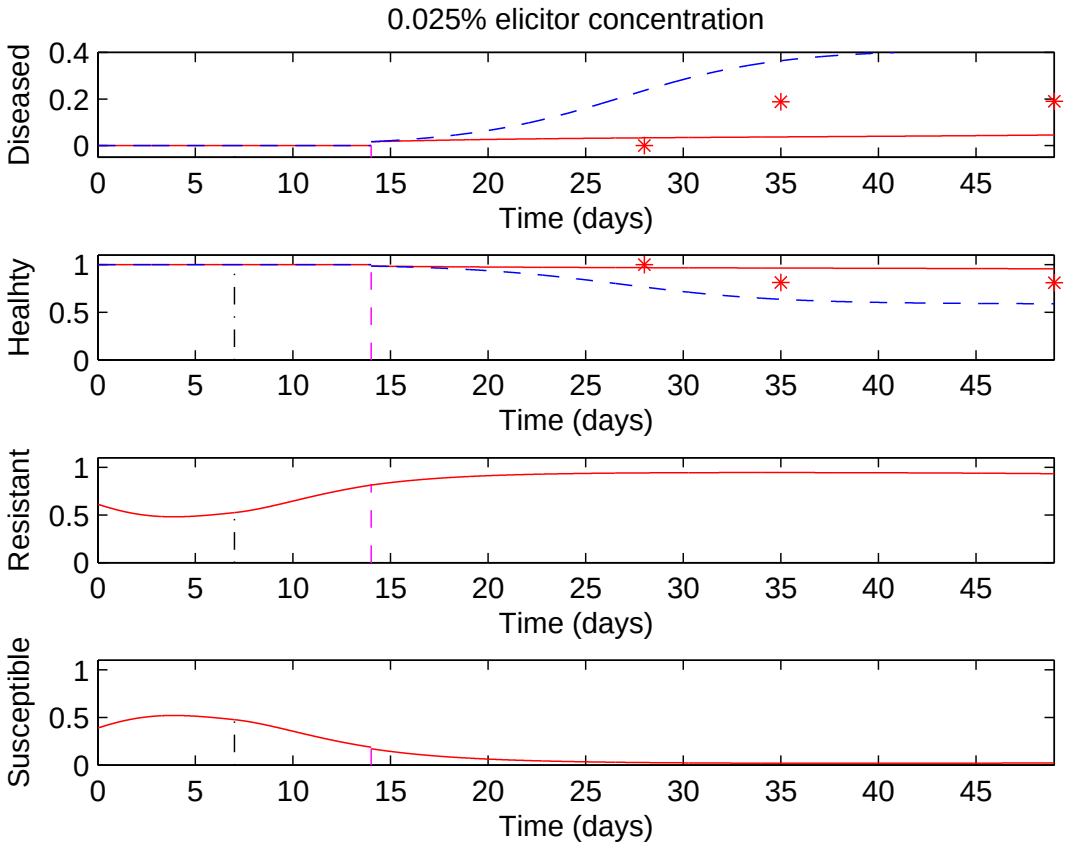

FIGURE 6.9: Solution graphs for multiple application (red curve) and single application (blue) with elicitor concentration 0.025%. The first elicitor application is at $t = 0$ and the second application is at time $t_e = 7$ (described by the vertical line "– .") and the pathogen inoculation at $t_p = 14$ (described by the vertical line "– –").

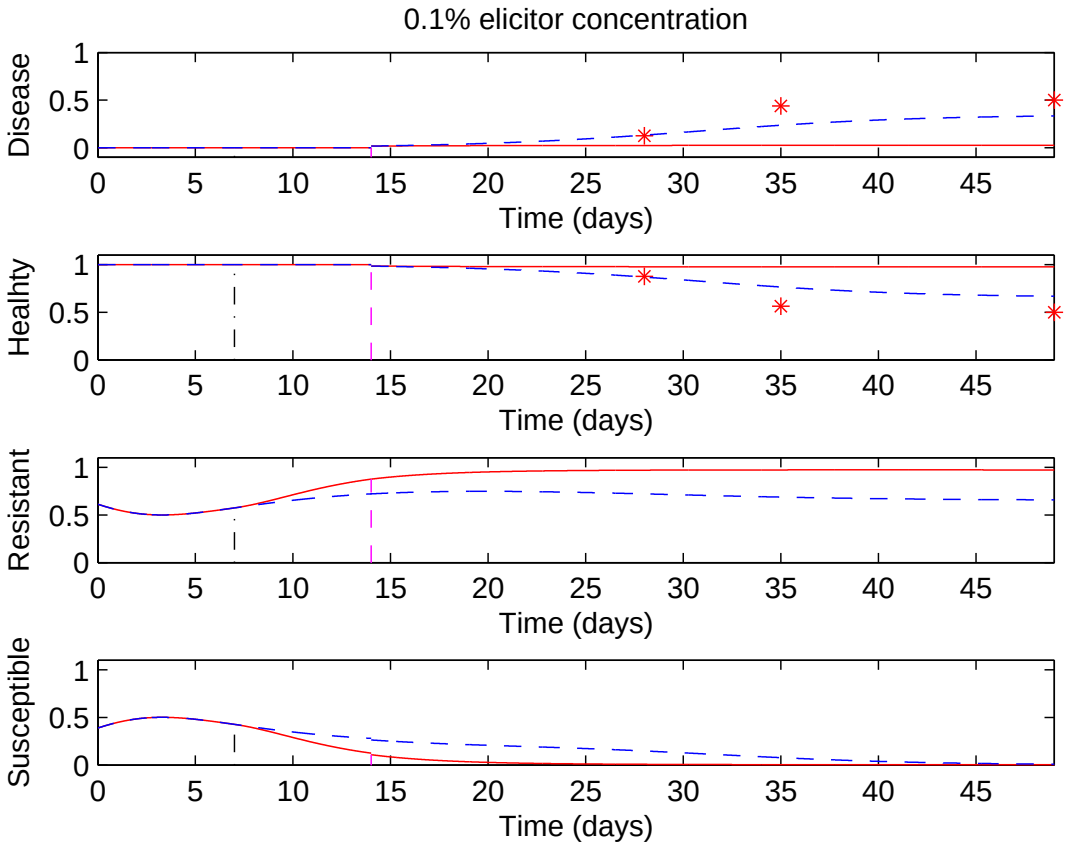

FIGURE 6.10: Solution graphs for multiple application (red curve) and single application (blue) with elicitor concentration 0.1%. The first elicitor application is at $t = 0$ and the second application is at time $t_e = 7$ (described by the vertical line "– .") and the pathogen inoculation at $t_p = 14$ (described by the vertical line "– –").

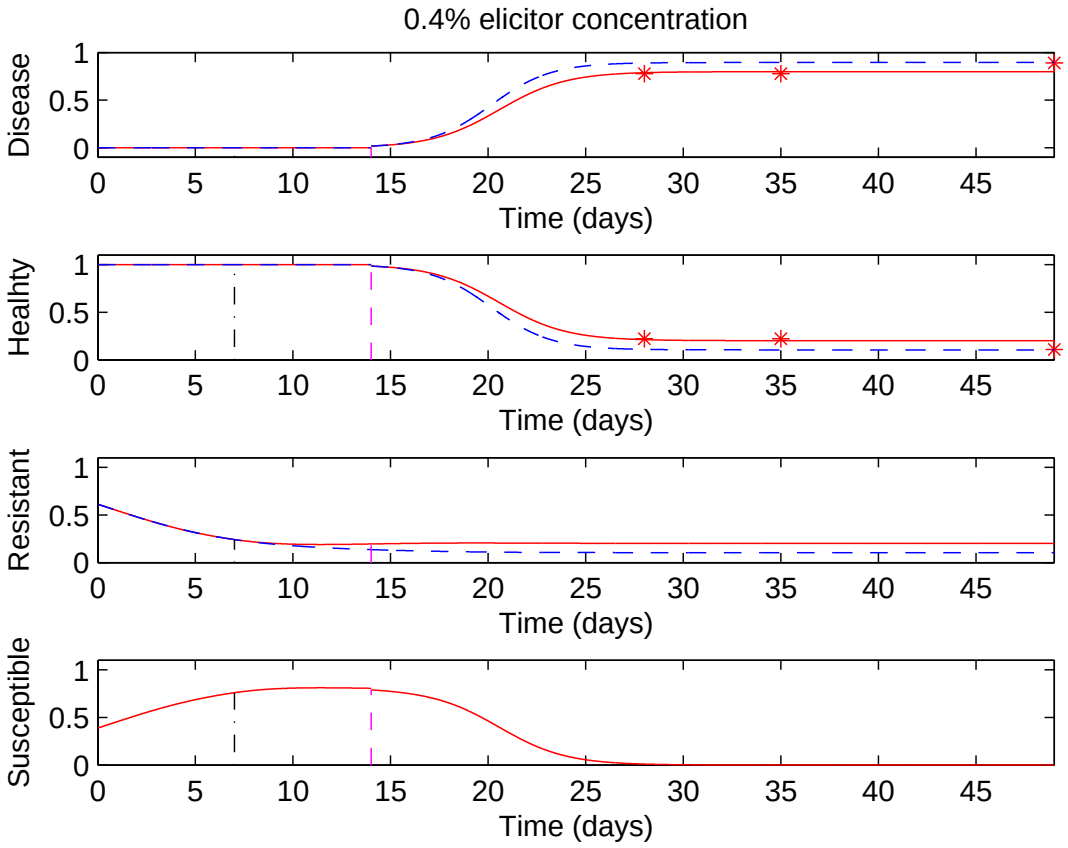

FIGURE 6.11: Solution graphs for multiple application (red curve) and single application (blue) with elicitor concentration 0.4%. The first elicitor application is at $t = 0$ and the second application is at time $t_e = 7$ (described by the vertical line "– .") and the pathogen inoculation at $t_p = 14$ (described by the vertical line "– –").

6.3 Post-Inoculation Elicitor Treatment

Traditionally, elicitor treatment methods have subscribed to the belief that the treatment should be done prior to the pathogen challenge. However, in the real world situation, one can never determine the time of the disease outbreak. Here it would be interesting to extend this proposed IR model to a situation which might be appropriate in the field. The effect of elicitor treatment after a pathogen challenge through a mathematical model is investigated. The assumptions made are:

1. the pathogen is inoculated at $t = 0$

2. the elicitor treatment at $t = t_e$.

Here the proposed treated model is:

- pre-treatment: $0 < t < t_e$

$$\frac{dR}{dt} = -\alpha R(1 - R - D) \quad ; R(0) = R_i \tag{6.13}$$

$$\frac{dD}{dt} = \beta D(1 - R - D) \quad ; D(0) = D_i \tag{6.14}$$

- post-treatment: $t_e < t < T$

$$\frac{dR}{dt} = (\frac{k(t - t_e)}{(t - t_e)^2 + L^2} - \gamma R)(1 - R - D) \quad ; R(t_e) = R_e \tag{6.15}$$

$$\frac{dD}{dt} = \beta D(1 - R - D) \quad ; D(t_e) = D_e \tag{6.16}$$

The pre-treatment formula (Equations (6.13)and (6.14)) describe the seedlings after they have been challenged by the pathogen at $t = 0$. We have assumed they behave like untreated seedlings as in equations (4.9) and (4.10). And, after some time t_e, the seedlings are treated with the elicitor. The post-treatment formulations are given by Equation (6.15) and Equation (6.16) with

$$e(t) = \frac{k(t - t_e)}{(t - t_e)^2 + L^2},$$

where R_e and D_e are obtained from (6.13) and (6.14) respectively at time t_e.

Here, no parameterisation is given for this extended model and, unfortunately, no experimental observations exist to be compared with the model. Therefore, the same parameter values as the previous chapter have been used to plot the solution graph of the equations above (Equation (6.13) – Equation (6.16)). The phase plane in Figure 6.12 illustrates the characteristics of the resistant (R) and diseased (D) compartments. The flows in the diagram indicate the time-evolution of the above dynamical system; the model demonstrates that if the elicitor treatment is done after the pathogen challenge obviously these treated seedlings will be less severely affected

compared to the untreated seedlings. This shows that the elicitor treatment helps the seedlings suppress the pathogen attack and prevents them from becoming severely diseased. Undoubtedly, if the treatment is done immediately after the seedlings are inoculated with pathogens, they will become less diseased. The figure also shows that the trajectories will eventually approach the straight line $R + D = 1$.

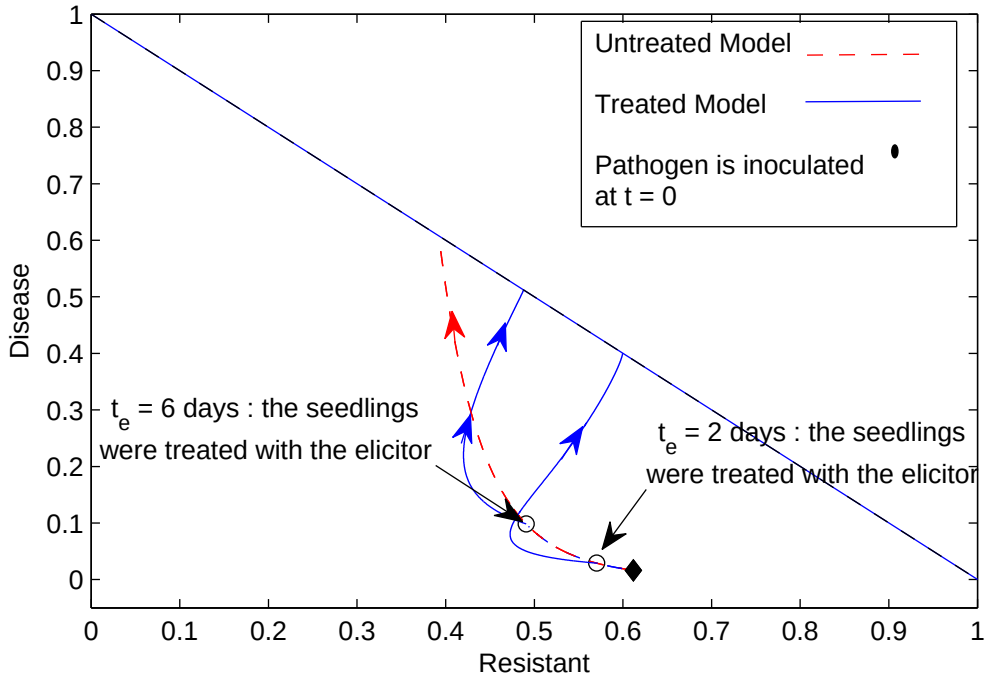

FIGURE 6.12: For this illustration, the seedlings were challenged by the pathogen at time $t = 0$ day, and then 2 days or 6 days later (i.e. $t_e = 2$ ot $t_e = 6$) the seedlings were treated with the elicitor. The blue curve corresponds to the untreated seedlings.

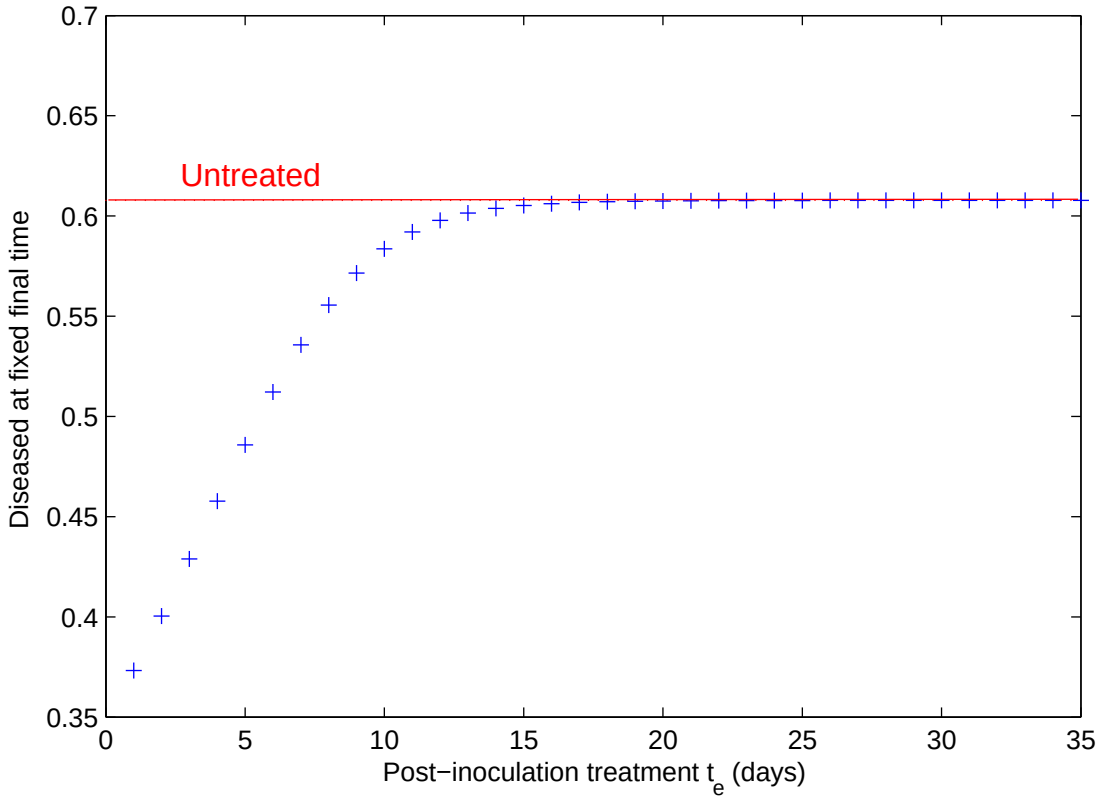

FIGURE 6.13: The proportion of diseased seedlings at fixed final time ($T = t_p$+35) against t_e. The blue marked points (+) correspond to model's outcome.

Figure 6.13 shows that the proportion of diseased seedlings at a final fixed time is increasing with t_e. The model demonstrates that if the treatment is done after 15 days from the pathogen challenge, there is no significant difference in the treatment outcome when compared to the untreated plants.

6.4 Summary

In this chapter, three different case studies extensions of the IR model in Chapter 4 have been presented. These are:

1. the effect of induced resistance due to the elicitor concentration used

2. the effect of induced resistance in a multiple elicitor applications

3. the effect of elicitor treatment after pathogen inoculation.

From the previous IR studies, it is known that there is an effect of different concentrations of elicitor on its capability to induce resistance. The experimental data suggests that this effect is not linearly dependent on the elicitor dose, but is instead sub-linear. This means there is an optimal elicitor concentration that produces the induced resistance at the peak. The effectiveness of a given elicitor concentration is formulated as $a^r e^{(1-a)}$, where a is the scaled dimensionless elicitor concentration and r is the sub-linear effect. This formulation introduces a new parameter r that needs to be parameterised using the same method as in Chapter 3, by comparing a matching experimental data set, by which r is found to be 0.6650. The model matches the experimental observations, where a higher elicitor concentration does not give a significant result compared to the untreated control. From the model, it is demonstrated that at the lowest elicitor concentration tested ($\sim 0.067\%$) there is an induced resistance response to the pathogen attack. This finding has important implications as this "optimal" concentration of MeJA would increase its cost effectiveness making it more attractive as a plant protection product.

The model was also extended to include a regime of elicitor application. Two elicitor applications are considered in this case study, where the applications of elicitor occur on 14 and 7 days before pathogen inoculation. The model was then compared to experimental observations; however, due to a small sample size, the findings might not give the best impression of those experimental observations. Elicitor concentration at 0.4% is the only model simulation that exhibits the characteristics of the observations.

For the last case study, the effect of elicitor treatment after pathogen challenge was investigated. Traditionally, in the greenhouse experiment, elicitor treatment has subscribed to the belief that treatment should occur prior to any pathogen challenge; but, one can never determine the time of the disease outbreak in the real field situation. The assumption made is that the seedlings are in the untreated condition before the treatment, which implies it should be formulated as the untreated system (see Chapter 4). Then, when the seedlings are applied with the elicitor at

time t_e, the seedlings have taken the elicitor effect. The model's simulation shows that it will suppress the disease growth and therefore become less severe compared to the untreated seedlings. While this study case did not confirm the efficacy of post-inoculation treatment, it did partially substantiate that the treatment provides a disease control to the seedlings. Biologically, there is potential for using a plant-defence elicitor to induce resistance to plant disease, which would further enable better plant disease management; instead of using agrochemicals that have the potential for enormous harm to the environment and human beings.

In conclusion, one of the more significant findings to emerge from these case studies is that the model reproduces the experimental observations. The numerical findings from this study provide a new understanding of the efficacy of the elicitor to induce resistance in the plant, which will hopefully benefit the plant pathologist. Therefore, time is saved and the expenditure of doing further experiments is avoided, as the model can be used to predict the outcomes.

Chapter 7

Optimal Strategies and Control

In this chapter optimal control strategies are developed to optimise the continuous application of the elicitor to manage the final disease outcome in a population. The goal of this study is to present a method of control for this class of optimisation problems, developing new strategies with the help of Pontryagin's maximum principle. At this stage no experimental verification of the approach is available, but in view of the model described in the previous chapter, there is a potential practical value in addressing this to show it is feasible and could be implemented in these discussions.

7.1 Continuous Elicitor Application: A Case Study

7.1.1 The Description

The goal is to find a minimal daily elicitor application that will achieve a given disease control level. There are Here a few applications of Pontryagin's maximum principle are presented. First of all, for notational purposes, let the state variables be the following:

- E is the cumulative elicitor effect

- c is the control variable that corresponds to the continuous elicitor application rate
- R represents the resistant compartment
- D represents the diseased compartment.

The process is considered on the time interval $[0, t_f]$ where the final time $t_f \geq 0$ is fixed. Generally, the dynamics underlying the optimal control model is similar to the IR model discussed in Chapter 4. The difference concerns is the term $E(t)$, that is determined by the continuous elicitor application function $c(t)$, a scenario which might be used in the agricultural industry. The minimisation of amount of the elicitor applied is chosen in order to determine the best elicitor application strategy to reduce the cost and to avoid unnecessary application. In previous chapters, the term $e(t)$ was chosen to represent the qualitative effect of a single elicitor application at one time. In other words, $E(t)$ was considered as continuous application effect and do not incorporate the elicitor effect peaking at the later time or delay maximum as in the single application $e(t)$.

In this case study, the objective functional is to minimise the following expression:

$$J\{R, D, E, c\} = \int_0^{t_f} c \; dt$$

where $c(t)$ is a continuously differentiable function.

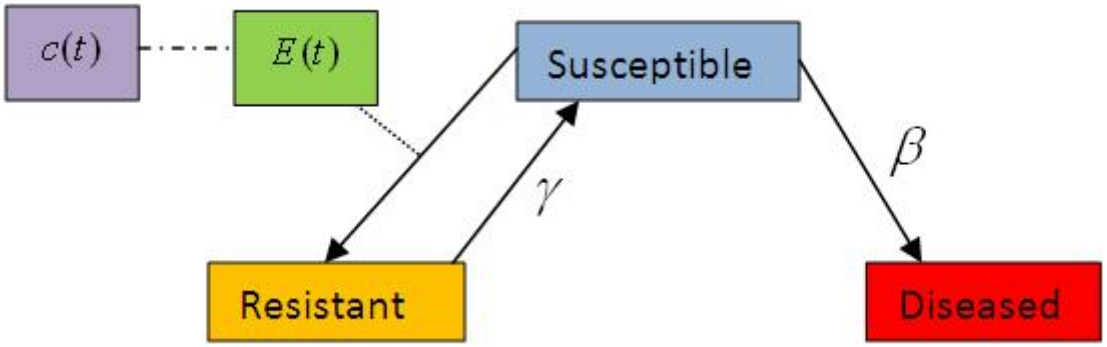

FIGURE 7.1: Schematic diagram for the control of the continuous elicitor application. The elicitor effect is determined by the elicitor applied daily until it reaches the target disease control.

Consider the elicitor effect, $E(t)$, which is dependent on the amount of elicitor applied daily, defined as $c(t)$. Here, $c(t)$ is the application strategy that aids the plant effectiveness in counteracting the pathogen (see Figure 7.1). Mathematically, the cumulative elicitor effect $E(t)$ at time t is given by

$$E(t) = \int_0^t s_0 e^{-\theta(t-\tau)} c(\tau)\, d\tau, \tag{7.1}$$

where θ [days^{-1}] and s_0 [mass^{-1}days^{-1}] are constants. This implies that E has a dimension of days^{-1}. The assumption made here is that discounting the elicitor effect in the future application is simply the reverse process of compounding the elicitor effect on the present elicitor effect, where θ is the discount rate. Here, $c(t)$ is the daily elicitor application in [mass days^{-1}] at time t.

Recall that the equations for this IR model for the treated plants are as described in Section 4.3.1.1, but here change the term $e(t)$ to $E(t)$:

- **Pre-inoculation**: For $0 < t < t_p$

$$\frac{dR}{dt} = (E(t) - \gamma R)(1 - R) \qquad ; R(0) = R_i. \tag{7.2}$$

- **Post-inoculation**: For $t_p < t < t_f$

$$\frac{dR}{dt} = (E(t) - \gamma R)(1 - R - D) \quad ; R(t_p) = R_p, \tag{7.3}$$
$$\frac{dD}{dt} = \beta D(1 - R - D) \quad ; D(t_p) = D_f. \tag{7.4}$$

Then, a successful strategy for the continuous elicitor application needs to be determined in order to get the pre-set "desirable" disease control at the time t_f, say $D(t_f) = D_f$. In other words, what is the least amount of elicitor needed to apply every day to get the best results for protection to the plant to minimise the effect of the pathogen attack. There are other possible alternatives for the optimal control strategy such as minimising the final diseased proportion D_f, but at this stage, the elicitor application strategy to get the pre-specified final disease outcome is taken into account in this thesis.

7.1.2 The Derivation of the Optimal Control System

7.1.2.1 Two-Stage Optimal Control Model

Since in Equation (7.1) $E(t)$ is defined on the time interval of $0 < t < t_f$ but the Equations (7.2)–(7.4) are divided into two different time regimes; that is Equation (7.2) is in $0 < t < t_p$, and Equations (7.3) and (7.4) are in $t_p < t < t_f$. Therefore, these dynamical systems are a two-stage optimal control system.

The dynamics of the first stage in the interval $[0, t_p]$, with $t_p > 0$ denotes the induction time, are modelled by

$$\frac{dR}{dt} = (E(t) - \gamma R)(1 - R) \quad ; R(0) = R_i,$$
$$\frac{dE}{dt} = -\theta E + s_0 c \quad ; E(0) = 0. \tag{7.5}$$

Whereas in the second stage $[t_p, t_f]$, the dynamics involves that of disease D:

$$\begin{aligned} \frac{dR}{dt} &= (E(t) - \gamma R)(1 - R - D) \quad ; R(t_p) = R_p, \\ \frac{dD}{dt} &= \beta D(1 - R - D) \quad ; D(t_p) = D_i \\ \frac{dE}{dt} &= -\theta E + s_0 c \quad ; E(t_p) = E_p. \end{aligned} \tag{7.6}$$

The term $\frac{dE}{dt}$ is obtained from Equation (7.1). Needless to say, the functions $R(t)$, $D(t)$, and $E(t)$ are presumed to be continuous at the transition time t_p. Therefore, R_p and E_p are obtained from Equation (7.5). Here, the pre-set "desirable" disease control at t_f

$$D(t_f) = D_f. \tag{7.7}$$

is given.

Let the control function $c(t)$ be bounded by

$$0 \leq c(t) \leq c_{max}. \tag{7.8}$$

Hence, this optimal control problem consists of determining a piecewise continuous control function $c(t)$ where $c : [0, t_f] \to [0, c_{max}]$ that minimises the objective functional

$$J\{c\} = \int_0^{t_f} c \; dt \tag{7.9}$$

subject to the constraints in Equation (7.5), Equation (7.6) and Equation (7.8). Using the same necessary conditions of Pontryagin's maximum principle, the Hamiltonian for both stages can be obtained. Let the Hamiltonian for the first stage be $\mathcal{H}_1$ and the second stage be $\mathcal{H}_2$.

$$\mathcal{H}_1 = c + \lambda_R(E - \gamma R)(1 - R) + \lambda_E(-\theta E + s_0 c) \tag{7.10}$$

$$\begin{aligned} \mathcal{H}_2 = {} & c + \lambda_R(E - \gamma R)(1 - R - D) + \lambda_D \beta D(1 - R - D) \\ & + \lambda_E(-\theta E + s_0 c) \end{aligned} \tag{7.11}$$

Here the λ_R, λ_D, and λ_E are the adjoint variables. Thus, the adjoint equations can be obtained for both stages.

- The first stage : $0 < t < t_p$

$$\begin{aligned}
\frac{d\lambda_R}{dt} &= -\frac{\partial \mathcal{H}_1}{\partial R} \\
&= -\lambda_R[(-\gamma)(1-R) + (E-\gamma R)(-1)] \\
&= \lambda_R(E + \gamma(1-2R)). \qquad (7.12) \\
\frac{d\lambda_E}{dt} &= -\frac{\partial \mathcal{H}_1}{\partial E} \\
&= -\lambda_E[\theta(-1)] - \lambda_R[(1-R)(1)] \\
&= \lambda_E\theta - \lambda_R(1-R). \qquad (7.13)
\end{aligned}$$

- The second stage : $t_p < t < t_f$

$$\begin{aligned}
\frac{d\lambda_R}{dt} &= -\frac{\partial \mathcal{H}_2}{\partial R} \\
&= -\lambda_R[(-\gamma)(1-R-D) + (E-\gamma R)(-1)] - \lambda_D\beta D(-1) \\
&= \lambda_R(E + \gamma(1-2R-D)) + \lambda_D\beta D. \qquad ; \lambda_R(t_f) = 0. \quad (7.14) \\
\frac{d\lambda_D}{dt} &= -\frac{\partial \mathcal{H}_2}{\partial D} \\
&= -\lambda_R(E-\gamma R)(-1) - \lambda_D\beta[(1-R-D) + D(-1)] \\
&= \lambda_R(E-\gamma R) - \lambda_D\beta(1-R-2D). \qquad (7.15) \\
\frac{d\lambda_E}{dt} &= -\frac{\partial \mathcal{H}_2}{\partial E} \\
&= -\lambda_E[\theta(-1)] - \lambda_R[(1-R-D)(1)] \\
&= \lambda_E\theta - \lambda_R(1-R-D). \qquad ; \lambda_E(t_f) = 0. \quad (7.16)
\end{aligned}$$

Note that there is no terminal constraint for D as it is fixed. Now, from both Hamiltonians $\mathcal{H}_1$ (Equation (7.10)) and $\mathcal{H}_2$ (Equation (7.10)) the optimality condition can be obtained

$$\frac{\partial \mathcal{H}_1}{\partial c} = \frac{\partial \mathcal{H}_2}{\partial c} = 1 + \lambda_E. \qquad (7.17)$$

Observe the difficulty in obtaining the analogues $\frac{\partial \mathcal{H}_1}{\partial c} = \frac{\partial \mathcal{H}_2}{\partial c} = 0$ for continuous control. This means there must exist a *switching function*

$$\phi = 1 + \lambda_E, \tag{7.18}$$

which determines an optimal control that minimises the Hamiltonians according to

$$c^*(t) = \begin{cases} c_{max} & \text{if } \phi(t) < 0, \\ 0 & \text{if } \phi(t) > 0, \\ \text{singular} & \text{if } \phi(t) = 0 \quad \forall t \in I_s \subset [0, t_f]. \end{cases} \tag{7.19}$$

From Lenhart & Workman (2007), a *singular control* is characterised by the condition $\phi(t) = 0$ over a subinterval $I_s \subset [0, t_f]$. If $\phi(t) = 0$ is not sustained over an interval of time, then the optimal system becomes a "*bang-bang control problem*". The instance of the optimal control system switching between 0 to c_{max} or vice-versa is called *switch times*.

These conditions allow the optimal system to have discontinuities, and the optimal control system derived above is of bang-bang type.

7.1.2.2 One-Stage Optimal Control Model

In this section, a one-stage optimal control model is formulated. For this purpose, take for simplicity $t_p = 0$, meaning the pathogen and the elicitor were introduced simultaneously at the initial $t = 0$. Therefore, the optimal control system is defined by

$$\text{minimise} \qquad J\{c\} = \int_0^{t_f} c \, \mathrm{d}t \tag{7.20}$$

subject to:

$$\begin{aligned}
\frac{dR}{dt} &= (E-\gamma R)(1-R-D) \qquad ; R(0)=R_i \\
\frac{dD}{dt} &= \beta D(1-R-D) \qquad (7.21)\\
\frac{dR}{dt} &= -\theta E + s_0 c \qquad ; E(0)=0 \qquad (7.22)
\end{aligned}$$

with boundary conditions the same as (7.7); and the same condition for $c(t)$ as in Equation (7.8). Therefore, the Hamiltonian will be

$$\mathcal{H} = c + \lambda_R(E-\gamma R)(1-R-D) + \lambda_D \beta D(1-R-D) + \lambda_E(-\theta E + s_0 c), \quad (7.23)$$

where the λ_R, λ_D, and λ_E are the adjoint variables. Following the same procedure, the adjoint equations are determined by

$$\begin{aligned}
\frac{d\lambda_R}{dt} &= -\frac{\partial \mathcal{H}}{\partial R} \\
&= -\lambda_R[(-\gamma)(1-R-D) + (E-\gamma R)(-1)] - \lambda_D \beta D(-1) \\
&= \lambda_R(E + \gamma(1-2R-D)) + \lambda_D \beta D \qquad ; \lambda_R(t_f)=0, \qquad (7.24)\\
\frac{d\lambda_D}{dt} &= -\frac{\partial \mathcal{H}}{\partial D} \\
&= -\lambda_R(E-\gamma R)(-1) - \lambda_D \beta[(1-R-D) + D(-1)] \\
&= \lambda_R(E-\gamma R) - \lambda_D \beta(1-R-2D), \qquad (7.25)\\
\frac{d\lambda_E}{dt} &= -\frac{\partial \mathcal{H}}{\partial E} \\
&= -\lambda_E[\theta(-1)] - \lambda_R[(1-R-D)(1)] \\
&= \lambda_E \theta - \lambda_R(1-R-D) \qquad ; \lambda_E(t_f)=0. \qquad (7.26)
\end{aligned}$$

Note that no terminal constraint is given for $\lambda_D(t_f)$ as $D(t_f)$ is fixed. If the optimality condition is applied to Equation (7.23), then the same function as in Equation (7.17) is obtained; that is, there is a switching function $\phi = 1 + \lambda_E$ and same arguments as in Equation (7.19) holds. Here, it can be concluded that this one-stage optimal control system is of bang-bang type too.

According to H. Maurer (personal communication, March, 2013), an expert in optimal control theory, generally, discretisation and large-scale nonlinear programming (NLP) methods are capable of determining the accurate optimal control structure. The bang-bang control problem also can be solved by using these two methods. Commonly the Applied Modelling Programming Language (AMPL) is used with Interior Point Optimizer (IPOPT) command to solve optimal control system with bang-bang control problem (Laboratories, 2013; Laird & Wächter, 2013; Fourer et al., 2003). Although the AMPL student version can be downloaded free online, it is limited to a number of variables and the tool IPOPT is not available in this student version. The full version is expensive and it was not possible to obtain the AMPL license at this stage. Unfortunately, this bang-bang optimal control example cannot be solved in MATLAB since it is difficult to determine the switching time analytically.

However, the bang-bang control problem can be illustrated as in Figure 7.2. It shows that the optimal control is bang-bang with only one switching time t_s and the control $c(t)$ structure is changing at time, t_s, determined by Equation (7.19). The control is restricted to between a lower bound ($c(t) = 0$) and an upper bound ($c(t) = c_{max}$). This suggests that if it is desired to have a pre-set number of diseased seedlings in the final time, the solution is to apply an amount elicitor dosage until the unique switching point t_s, and turn it off when the desired level of disease control is reached.

It is simply a straightforward ODE system to solve this proposed optimal system and find the switching time t_s analytically. Although the system can be simplified (by a few assumptions being made) to determine t_s, there might be a risk of missing the optimal switching time; which may affect the outcome. Thus, a simple modification is made to the objective functional, J, in the next section.

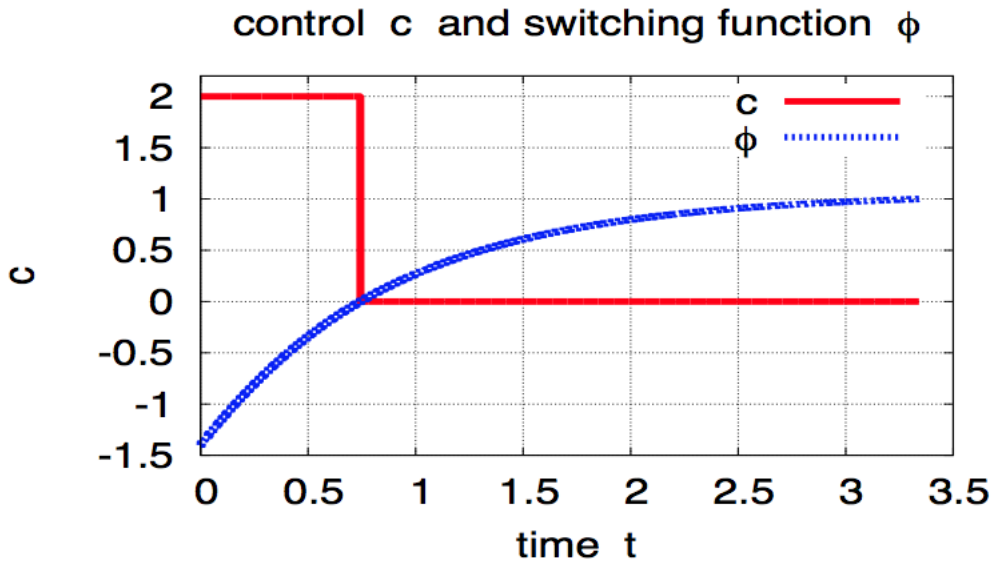

FIGURE 7.2: ϕ is the switching function determined from $\lambda_E(t)$. This illustration of the bang-bang type control problem was plotted using arbitrary parameter values. It was shown in the diagram, the regime of elicitor application, represented by control variable c, is switched off after certain of time (refer to Equation (7.19)).
This figure is courtesy of Prof. Helmut Maurer using AMPL software.

7.2 Example: Control $c(t)$ with Quadratic Term

In this section, an illustration of the optimal control for this IR model (for the one-stage problem) is presented by defining the objective functional as

$$\text{minimise} \qquad J\{c\} = \int_0^{t_f} c^2 \; dt. \tag{7.27}$$

Here, the objective functional is a L^2-norm space with a quadratic term for the control $c(t)$. Although the function c is more likely to be more appropriate than c^2 from an agricultural or forestry perspective. By changing the power of c it will eventually modify the system to an ordinary optimal control system. This is shown in the arguments below.

By minimising the Equation (7.27) subject to

$$\begin{aligned}
\frac{dR}{dt} &= (E-\gamma R)(1-R-D) && ; R(0)=R_i, && (7.28)\\
\frac{dD}{dt} &= \beta D(1-R-D) && ; D(0)=D_i, \quad D(t_f)=D_f, && (7.29)\\
\frac{dE}{dt} &= -\theta E + s_0 c && ; E(0)=0. && (7.30)
\end{aligned}$$

Using Pontryagin's maximum principle, the Hamiltonian can be defined as

$$\mathcal{H} = c^2 + \lambda_R(E-\gamma R)(1-R-D) + \lambda_D \beta D(1-R-D) + \lambda_E(-\theta E + s_0 c). \quad (7.31)$$

Then, the adjoint equations for this system are

$$\begin{aligned}
\frac{d\lambda_R}{dt} &= -\frac{\partial \mathcal{H}}{\partial R}\\
&= -\lambda_R[(-\gamma)(1-R-D)+(E-\gamma R)(-1)] - \lambda_D\beta D(-1)\\
&= \lambda_R(E+\gamma(1-2R-D)) + \lambda_D\beta D. && ; \lambda_R(t_f)=0. && (7.32)\\
\frac{d\lambda_D}{dt} &= -\frac{\partial \mathcal{H}}{\partial D}\\
&= -\lambda_R(E-\gamma R)(-1) - \lambda_D\beta[(1-R-D)+D(-1)]\\
&= \lambda_R(E-\gamma R) - \lambda_D\beta(1-R-2D). && && (7.33)\\
\frac{d\lambda_E}{dt} &= -\frac{\partial \mathcal{H}}{\partial E}\\
&= -\lambda_E[\theta(-1)] - \lambda_R[(1-R-D)(1)]\\
&= \lambda_E\theta - \lambda_R(1-R-D) && ; \lambda_E(t_f)=0. && (7.34)
\end{aligned}$$

Note that there is no transversality condition for λ_D as the system imposed a fixed end-point on the state variable for D. Also observe that the adjoint equations in Equations (7.32)–(7.34) are the same as in Equations (7.24)–(7.26). However, the difference of the Hamiltonians in Equation (7.31) and Equation (7.23) is the power of the function c.

Using the Hamiltonian in Equation (7.31), the optimality condition implies that

$$\frac{\partial \mathcal{H}}{\partial c} = 2c + \lambda_E s_0 = 0,$$
$$\text{and so the optimal solution is } c^* = -\frac{s_0}{2}\lambda_E. \tag{7.35}$$

Furthermore, the Hamiltonian in Equation (7.31) satisfies the concavity condition as in Equation (3.18):

$$\frac{\partial^2 H}{\partial c^2} = 2$$

which is $\frac{\partial^2 H}{\partial c^2} > 0$ at c^*. It can be concluded that c^* (Equation (7.35)) is the optimal control function for the optimal control system above (Equations (7.27)–(7.30)).

Therefore, the optimal control problem strategy is obtained by solving the optimal system, which consists of six ODEs and its boundary conditions:

$$\begin{aligned}
\frac{dR}{dt} &= (E - \gamma R)(1 - R - D) && ; R(0) = R_i \\
\frac{dD}{dt} &= \beta D(1 - R - D) && ; D(0) = D_i, \quad D(t_f) = D_f \\
\frac{dE}{dt} &= -\theta E + s_0 c && ; E(0) = 0 \\
\frac{d\lambda_R}{dt} &= \lambda_R(E + \gamma(1 - 2R - D)) + \lambda_D \beta D && ; \lambda_R(t_f) = 0 \\
\frac{d\lambda_D}{dt} &= \lambda_R(E - \gamma R) - \lambda_D \beta(1 - R - 2D) && \\
\frac{d\lambda_E}{dt} &= \lambda_E \theta - \lambda_R(1 - R - D) && ; \lambda_E(t_f) = 0.
\end{aligned}$$

This optimality system is solved by interpreting the system as a boundary-value problem (BVP). The "bvp4c" command in MATLAB is the numerical procedure used to compute the solution. This MATLAB built-in tool ,"bvp4c", is a finite difference code that implements the three-stage Lobatto IIIa formula.

To solve for, and plot, the solution of this optimality system, the same parameter values were used as in Table 5.6, in particular R_i, D_i, β, γ. The other parameter

values were chosen arbitrarily for illustrative purpose:

$$\begin{aligned} D_f &= 0.3483, \\ \theta &= 0.05, \\ s_0 &= 0.1. \end{aligned}$$

At the beginning there was a struggle to compute this BVP. The most difficult part of the solution of BVP is to provide an initial estimation to the solution. In order to direct the "bvp4c" for the solution of interest, it is necessary to assist the solver by informing it with a guess. However, coming up with a sufficiently good guess can be the most challenging part of solving a BVP (Gökhan, 2011). Therefore, a good set of initial guesses for variables $(R, D, E, \lambda_R, \lambda_D, \lambda_E)$ was needed to run "bvp4c". Since the values for $\lambda_R(0), \lambda_D(0)$ and $\lambda_E(0)$ are unknowns, these values were chosen arbitrarily as zeros. However, the "bvp4c" computation does not converge to a unique solution and every time the initial guess was changed BVP seems to have multiple solutions. This shows that the convergence for a unique solution depends on the initial guess function. To solve this problem, an iterative method to the solution was executed. The solution of the initial guess function with $(R, D, E, \lambda_R, \lambda_D, \lambda_E) = (R_i, D_i, 0, 0, 0, 0)$ was then recorded and used as the initial guess function for the "bvp4c". With this approach, the "bvp4c" solver computed to a unique solution and this solution was then compared with the solution computed by AMPL courtesy of Prof. Helmut Maurer. It was pleasing to see the BVP's result matched AMPL's result. The advantage of AMPL is that one does not have to define the initial guess and work out analytically the adjoint equations in order to solve the optimal control problem.

Figures 7.3 to 7.9 show the simulation for this optimal control problem. In Figures 7.3 and 7.4, the computations illustrate that both compartments R and D tend to reach a plateau after 40 days. By this time the disease has stopped progressing, therefore there is no need to apply the elicitor again (see Figure 7.5). This figure shows the optimal strategy for elicitor application, $c(t)$, required to achieve the desirable disease control, fixed as D_f. This numerical result indicates that initially (when $t = 0$) a considerable amount of elicitor is needed before a sharp decline, reaching a local minimum at day 25. The total amount of elicitor is calculated as

$J\{c\} = \int_0^{100} c^2 \, dt = 1.1290$ (units). Although, after 40 days, while no elicitor is applied to the plants, the elicitor's effect is still available in the plant (Figure 7.6).

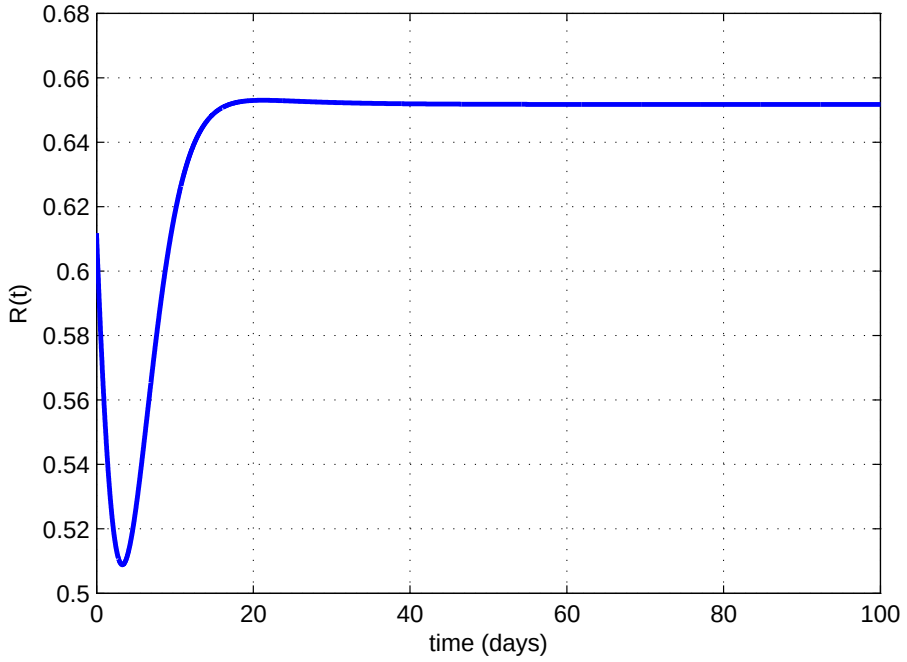

FIGURE 7.3: Dynamical solution for $R(t)$ in Equation (7.28). The solution shows that from the initial time $t = 0$, the proportion of the resistant plants drop then increase back to reach a steady state (almost).

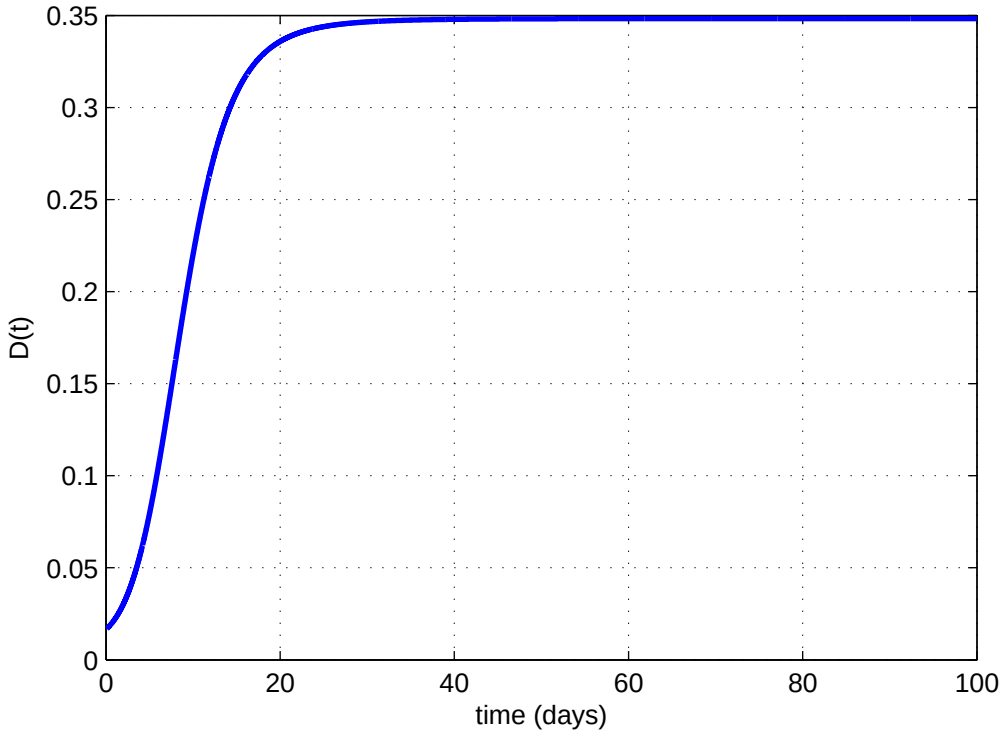

FIGURE 7.4: Dynamical solution for $D(t)$ in Equation (7.29). The solution shows the behaviour of the disease growth is similar to the logistic growth curve. Initially the proportion of the diseased plant increases then reaches its plateau after 40 days.

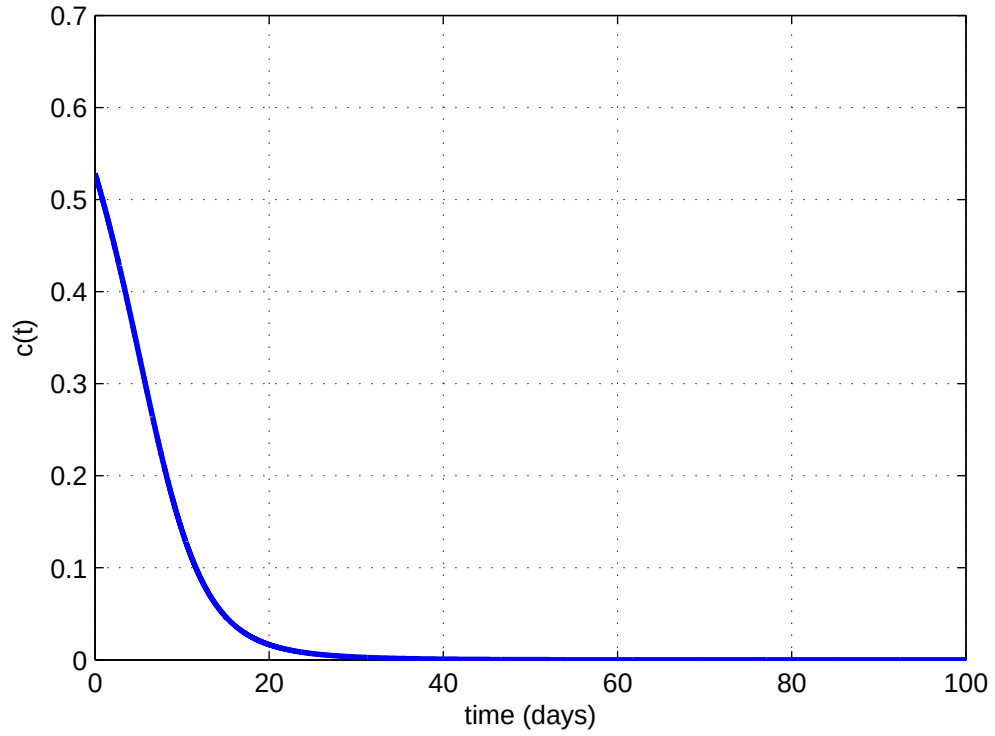

FIGURE 7.5: Dynamical solution for $c(t)$ in Equation (7.35). It shows the optimal strategy for a daily elicitor application $c(t)$ to achieve the pre-set desirable proportion of diseased seedlings at the final time called D_f. The numerical result shows that at the initial time ($t = 0$), a large amount of elicitors has to be applied and later decreased.

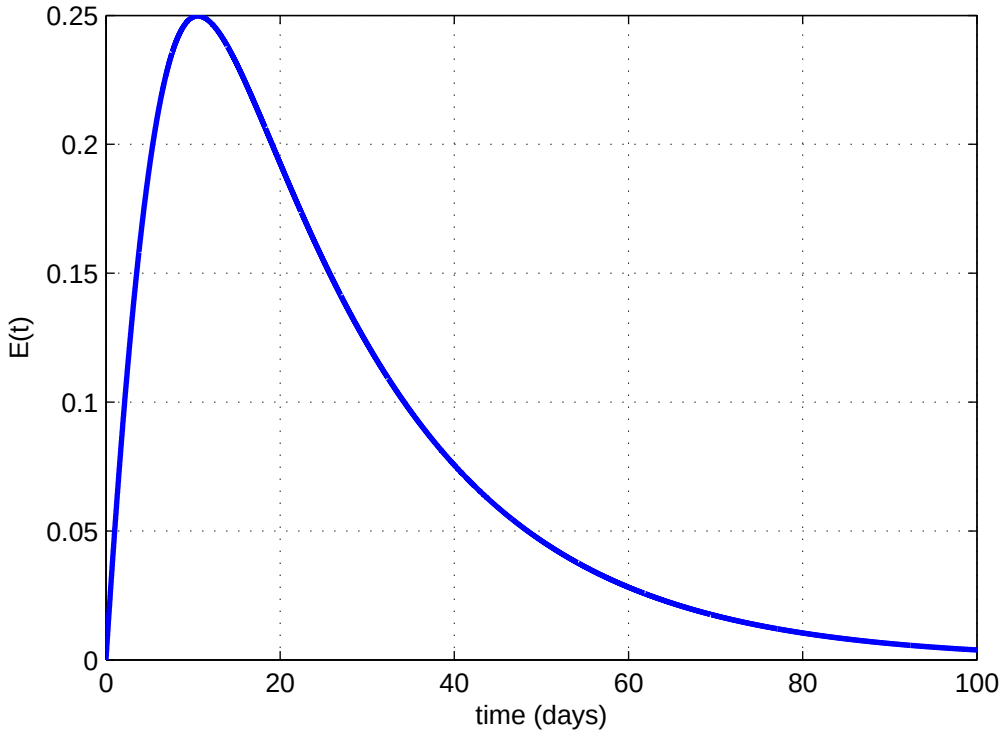

FIGURE 7.6: Dynamical solution for $E(t)$ in Equation (7.30). This describes the cumulative elicitor effect which corresponds to the elicitor application everyday (see also Figure 7.5 how daily application changes this cumulative elicitor effect).

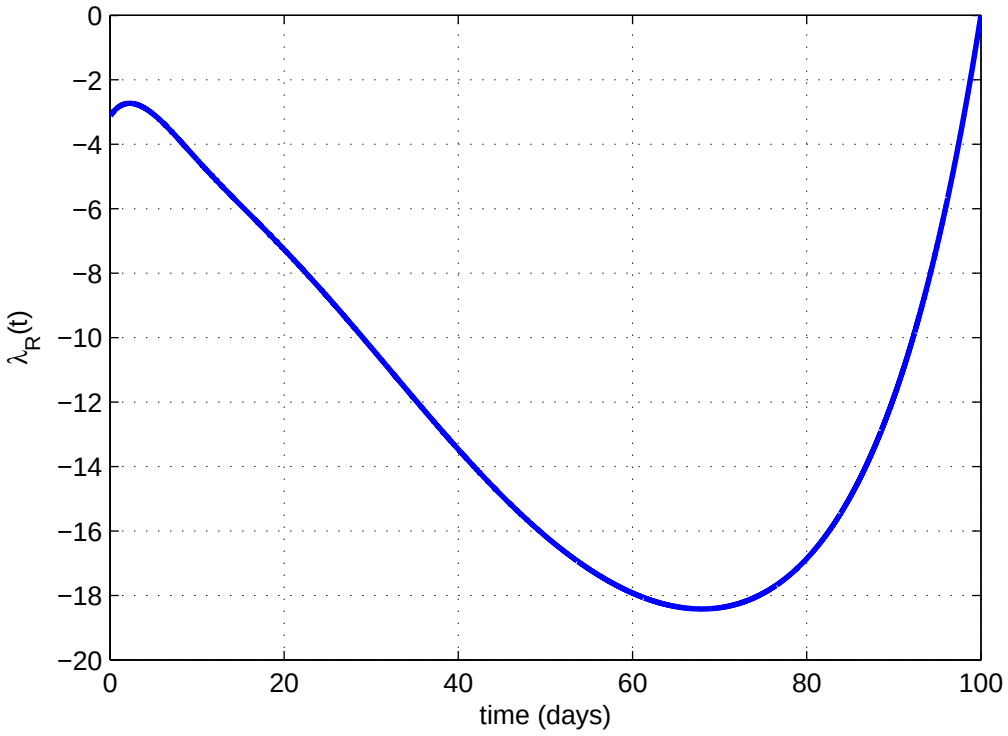

FIGURE 7.7: Dynamical solution for $\lambda_R(t)$ in Equation (7.32).

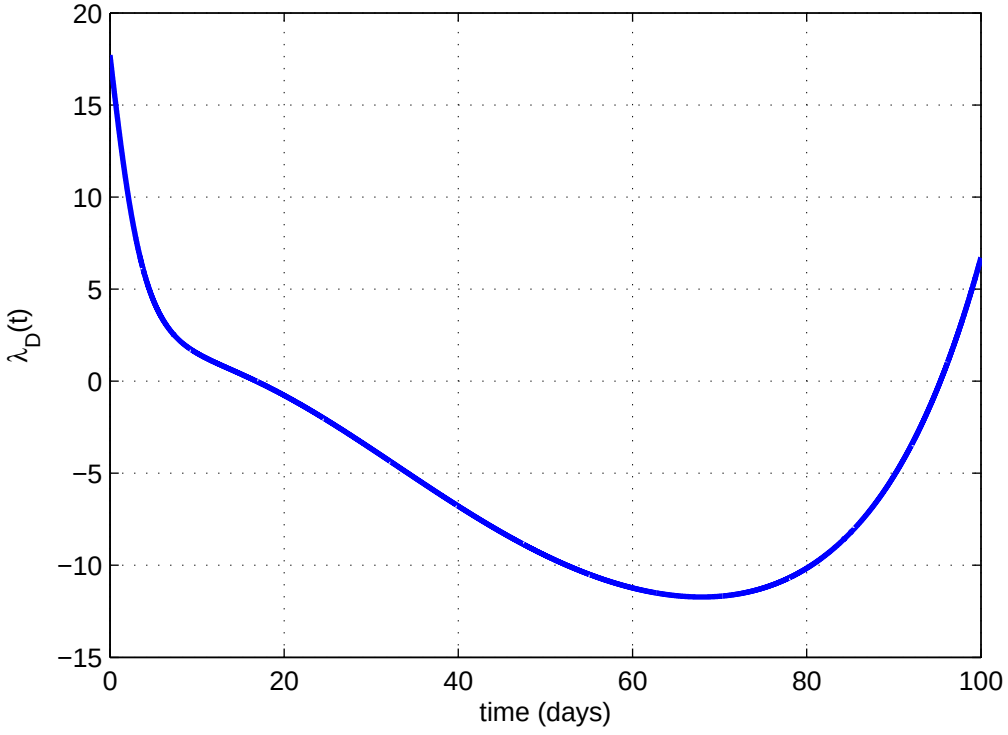

FIGURE 7.8: Dynamical solution for $\lambda_D(t)$ in Equation (7.33).

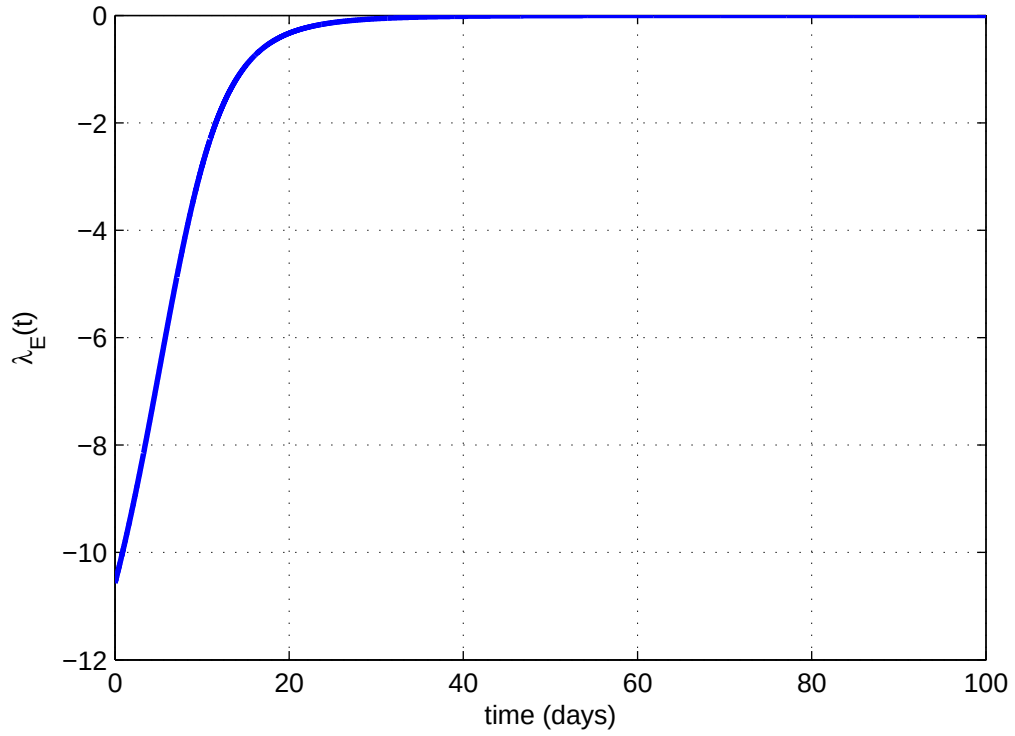

FIGURE 7.9: Dynamical solution for $\lambda_E(t)$ in Equation (7.34).

7.3 Summary

In this chapter, an application of Pontryagin's maximum principle has been presented. The IR model in Chapter 4 is extended to apply this well-known method where a continuous elicitor application is considered, here defined by $c(t)$. The goal is to determine the best strategy for $c(t)$ that will give the pre-specified disease control at the final observation time called D_f. The derivation of this optimal system, with the objective functional as $J\{c\} = \int_0^{t_f} c\ dt$ has led to a bang-bang control problem which is interesting in itself. Unfortunately, there is no facility to compute this bang-bang control problem . However, for learning purposes, it is still valuable to compute this optimal system with a modified objective functional. The objective functional is defined as $J\{c\} = \int_0^{t_f} c^2\ dt$, where c is in the quadratic term. It is also assumed that the infection and the treatment were introduced at the same time;

that is $t_p = 0$, which leads to a simple one-stage optimal control system. This modification changes the bang-bang control system to the ordinary control problem. The modified optimal control system was solved by setting the system as the boundary value problem. Therefore in this case, the system can be computed in MATLAB using "bvp4c".

Although no experimental observations have been compared with this optimal control system, it gives insight into how this continuous elicitor application can still provide disease control for the plants (omitting the fact that there is a possibility of phytotoxicity in the plants). In reality, it is not necessary to apply the protection agent (such as fungicides) every day; commonly protection agents are applied to the plant according to a calendar-based (e.g. every 7 to 14 days) schedule, to control a plant disease. However, a daily application for an existing infection makes more sense. Growers may be able to control the amount of the elicitor applied daily to possibly eliminate unnecessary applications. The numerical computations show that after some time ($t = 40$) the disease will stop progressing and therefore no elicitor application will be needed (see Figures 7.4 and 7.5).

Chapter 8

Conclusion

8.1 Thesis Summary

In the past, the efficacy of induced resistance (IR) to control plant diseases has typically been studied experimentally, whether in the fields or in greenhouses. The objective of this thesis was to develop a generic mathematical model of IR to have a better understanding of the behaviour of IR, which sometimes cannot be gained from an experiment. Building on the approach of Jeger et al. (2009) and Xu et al. (2010) in previous modelling of biological control systems, the compartmental SIR model was applied for the potential of using a plant-defence elicitor to induce resistance to plant disease. Several assumptions on the biological background were made in order to simplify the biological process associated with IR. The developed model was generic and can be used for any combination of plant-elicitor-pathogen scenarios; which of course will have different parameters. The numerical results from this IR model lead to a potentially powerful tool for quantifying the development of more potent elicitors and strategies for their application.

The case study used in this thesis was on the effect of elicitor, methyl jasmonate (MeJA) on the resistance of pine seedlings (*Pinus radiata*) by the causal agent of pine stem canker and tip dieback (*Diplodia pinea*). The experimental data given were in two components only; diseased and healthy. However, the IR model had the advantage of quantifying the proportion of the plants that were susceptible and

resistant, when observations were unable to determine these two components. This experimental data was fitted to the model to estimate the unknown parameters, and the ordinary least-squares method is used for the parameter estimation. The estimated parameters were then used to analyse the dynamical IR model and extended IR model to several case studies.

From the phase plane (Figure 5.17), the model enables the likely long-term effect of the disease to be determined. The attracting steady states are dependent on the initial conditions and not, as is usually the case, asymptotically stable. Moreover, the model was capable of determining the optimal induction time t_p which leads to a minimisation of the long-term effect for elicitor application before the inoculation of the plants by the pathogens. The model was also capable of determining the optimal elicitor concentration to provide IR for the maximum effect. This IR model was then extended to multiple elicitor applications; it was shown in the model simulation that a weekly elicitor application gives a better disease control compared to a single application. Besides that, numerical results show that if the elicitor was applied after pathogen inoculation, then the treated plants were less severely affected compared to the untreated plants. Another interesting outcome from this thesis was the implementation of Pontryagin's maximum principle to the IR model. For this case study, a continuous elicitor application was considered, and the goal was to determine the best application strategy in order to get the most desirable disease control. Although daily elicitor application might cause phytotoxicity to the plants, this daily application strategy is reasonable for plants that may be already infected. The results from this numerical experiment gave the optimal application strategy, and thus will help farmers avoid unnecessary application.

In conclusion, this new IR model has the potential to be implemented as a decision support tool for the management of plant diseases, which involves an assessment of the risk and economic cost critical for commercial operations (Gent et al., 2011).

8.2 Further Research

Some suggestions for future research following this thesis include:

- Consider a different plant-elicitor-pathogen system. At this stage the model has only been considered for *Pinus radiata*-MeJa-*Diplodia pinea*. Therefore a new parameterisation needs to be determined if the model to be used to analyse a different system.

- Include a delay time on the elicitor effect. In this thesis it was assumed that the elicitor has an immediate effect once applied to the plants.

- More data for elicitor concentrations to estimate accurately for parameter r. Results from this thesis (Section 6.1) can be more robust if more data points are considered. It has to be admitted that only a small number of data points were considered in the parameter estimation.

- Explore more on the multiple applications strategy. At this stage the model only considered two elicitor applications before the pathogen inoculation. The model can be further explored to consider a single application before and after the pathogen inoculation. Possible questions include: how does this change the efficacy of elicitor to induced resistance?

- Experimentation with the bang-bang control type. In Chapter 7, bang-bang control type was discussed but the analysis was not completely covered. Further analysis needs to be done and a possible paper might come from this numerical experiment. This could be in collaboration with Prof. Helmut Maurer, an expert on optimisation and optimal control theory.

Bibliography

Abdul Latif, N. S., Wake, G. C., Reglinski, T., & Elmer, P. A. (2014). Modelling induced resistance to plant disease. *Journal of Theoretical Biology*, *347*, 144–150.

Abdul Latif, N. S., Wake, G. C., Reglinski, T., Elmer, P. A. G., & Taylor, J. T. (2013). Modelling induced resistance to plant disease using a dynamical system approach. *Frontiers Plant Science*, *4*.

Agrios, G. N. (2005). *Plant Pathology*. San Diego, California: Academic Press.

Boltyanskii, V. G., Gamkrelidze, R. V., & Pontryagin, L. (1956). Towards a theory of optimal processes. *Reports Acad. Sci. USSR*, *110*.

Bonello, P., Gordon, T. R., Herms, D. A., Wood, D. L., & Erbilgin, N. (2006). Nature and ecological implications of pathogen-induced systemic resistance in conifers: A novel hypothesis. *Physiological and Molecular Plant Pathology*, *68*, 95–104.

Boughton, A. J., Hoover, K., & Felton, G. W. (2006). Impact of chemical elicitor applications on greenhouse tomato plants and population growth of the green aphid, *Myzus persicae*. *Entomologia Experimentalis et Applicata*, *120*, 175–188.

Chester, K. C. (1933). The problem of acquired physiological immunity in plants. *Quaterly Review Biology*, *8*, 129–154.

Cipollini, D., & Heil, M. (2010). Cost and benefits of induced resistance to herbivores and pathogens in plants. *CAB Reviews: Perspective in Agriculture, Veterinary Science, Nutrition and Natural Resources*, *5*, 1–25.

Clark, C. W. (1990). Optimal control theory. In *Mathematical Bioeconomics: The Optimal Management of Renewable Resources*, (pp. 88–95). United States of America: John Wiley & Sons.

Dinh, S. Q., Joyce, D. C., Irving, D. E., & Wearing, A. H. (2008). Effects of multiple applications of chemical elicitors on *Botrytis cinerea* infecting geraldton waxflower. *Australasian Plant Pathology*, *37*, 87–94.

El Modafara, C., Elgaddaa, M., El Boutachfaitib, R., Abouraichaa, E., Zehhara, N., Petitb, E., El Alaoui-Talibia, Z., Courtoisb, B., & Courtoisb, J. (2012). Induction of natural defence accompanied by salicylic acid-dependant systemic acquired resistance in tomato seedlings in response to bioelicitors isolated from green algae. *Scientia Horticulturae*, *138*, 55–63.

Elmer, P. A. G., & Reglinski, T. (2006). Biosuppresion of *Botrytis cinerea* in grapes. *Plant Pathology*, *55*, 155–177.

Eyles, A., Bonello, P., Ganley, R., & Mohammed, C. (2010). Induced resistance to pests and pathogens in trees. *New Phytologist*, *185*, 893–908.

Fitza, K., Myburg, A., Payn, K., & Naidoo, S. (2011). Induced resistance and associated defence gene responses in *Pinus patula*. In *IUFRO Tree Biotechnology Conference 2011: From Genomes to Integration and Delivery*. Bahia, Brazil.

Forster, G. A., & Gilligan, C. A. (2007). Optimizing the control of disease infestations at landscape scale. *PNAS*, *104*, 4984–4989.

Fourer, R., Gay, D. M., & Kernighan, B. W. (2003). *AMPL: a modelling language for mathematical programming*. United States of America: Duxbury Press, Brooks-Cole Publishing Company.

García-Mier, L., Guevara-González, R. G., Mondragón-Olguín, V. M., Verduzco-Cuellar, B., & Torres-Pacheco, I. (2013). Agriculture and bioactives: Achieving both crop yield and phytochemicals. *International Journal of Molecular Sciences*, *14*, 4203–4222.

Gent, D. H., De Wolf, E., & Pethybridge, S. J. (2011). Perceptions of risk, risk aversion, and barriers to adoption of decision support systems and integrated pest management: an introduction. *Phytopathology*, *101*, 640–643.

Gibbs, B. P. (2011). *Advanced Kalman filtering, least-squares and modelling*. New Jersey, USA: John Wiley & Sons, Inc.

Gilligan, C. A., & van den Bosch, F. (2008). Epidemiological models for invasion and persistence of pathogen. *Annual Review of Phytopathology*, *46*, 385–418.

Godard, J.-F., Ziadi, S., Monot, C., Le Corre, D., & Siluè (1999). Benzothiadiazole (bth) induces resistance in cauliflower (brassica *oleracea* var *botrytis*) to downy mildew of crucifers caused by *Peronospora parasitica*. *Crop Protection*, *18*, 397–405.

Gökhan, F. S. (2011). Effect of the guess function & continuation method on the run time of matlab bvp solvers, matlab - a ubiquitous tool for the practical engineer.
URL www.intechopen.com/articles/show/title/effect-of-the-guess-function-continuation-method-on-the-run-time-of-matlab-b

Gould, N., Reglinski, T., Northcott, G. L., Spiers, M., & Taylor, J. T. (2009). Physiological and biochemical responses in *Pinus radiata* seedlings associated with methyl jasmonate-induced resistance to *Diplodia pinea*. *Physiological and Molecular Plant Pathology*, *74*, 121–128.

Gould, N., Reglinski, T., Spiers, M., & Taylor, J. T. (2008). Physiological trade-offs associated with methyl jasmonate - induced resistance in *Pinus radiata*. *Canadian Journal of Forest Research*, *38*, 677–684.

Graves, R. N. (2010). A method to accomplish the optimal control of continuous dynamical systems with impulse controls via discrete optimal control and utilising optimal control theory to explore the emergence of synchrony (phd. dissertation, university of tennessee, united states).
URL http://trace.tennessee.edu/utk-graddiss/801

Hammerschimdt, R. (2007). Introduction: Definitions & some history. In D. Walters, A. Newton, & G. Lyon (Eds.) *Induced resistance for plant defence: A sustainable approach to crop protection*, (pp. 1–8). Singapore: Blackwell Publishing.

Hill, R. A., Eden, M. A., Cutler, H. G., Elmer, P. A. G., Reglinski, T., & Parker, S. R. (1999). Practical natural solutions for plant disease control. In H. G. Cutler, & S. J. Cutler (Eds.) *Biologically active natural products: Agrochemicals*, (pp. 201–208). USA: CRC Press LLC.

Hindumathy, C. K. (2012). The defense activator from yeast for rapid induction of resistance in susceptible pearl millet hybrid against downy mildew disease. *International Journal of Agriculture Sciences*, *4*, 196–201.

Holopainen, J. K., Heijari, J., Nera, A. M., Vuorinen, M., & Kainulainen, P. (2009). Potential for the use of exogenous chemical elicitors in disease & insect pest management of conifer seedlings production. *The Open Forest Science Journal*, *2*, 17–24.

Huang, C.-H., & Vallad, G. E. (2012). Effect of application frequency and reduced rates of acibenzolar-s-methyl on the field efficacy of induced resistance against bacterial spot on tomato. *Plant Disease*, *96*, 221–227.

Issues, P. (2011). Agriculture.
URL http://www.pollutionissues.com/A-Bo/Agriculture.html

Jacometti, M. A., Wratten, M., & Walter, M. (2010). Review: Alternatives to synthetic fungicides for *Botrytis cinerea* management in vineyards. *Australian Journal of Grape & Vine*, *16*, 154–172.

Jeger, M. J., Jefferies, P., Elad, Y., & Xu, X. M. (2009). A generic theoretical model for biological control of foliar plant disease. *Journal of Theoretical Biology*, *256*, 201–214.

Johnson, M. L., & Faunt, L. M. (1992). Parameter estimation by least-squares methods. *Methods in Enzymology*, *210*, 1–37.

Keener, J., & Sneyd, J. (1998). *Mathematical Physiology*. United States of America: Springer-Verlag New York Inc.

Kermack, W. O., & Mckendrick, A. G. (1927). A combination to the mathematical theory of epidemics. *Proceeding of the Royal Society of London*, *115*, 700–721.

Kessel, G. J. T., Köhl, J., Powell, J. A., Rabbinge, P., & van der Werf, W. (2005). Modelling spatial characteristics in the biological control of fungi at leaf scale: Competitive substrate colonisation by *b*otrytis cinerea and the saprophytic antagonist *u*locladium atrum. *The American Phytopathological Society*, *95*, 439–448.

Kuć, J. (2000). Developments and future of induced systemic resistance in plants. *Crop Protection*, *19*, 859–861.

Laboratories, B. (2013). Ampl: a modelling language for mathematical programming.
URL http://www.ampl.com

Laird, C., & Wächter, A. (2013). Ipopt home page.
URL https://projects.coin-or.org/Ipopt

Lenhart, S., & Workman, J. T. (2007). *Optimal control applied to biological model*. United States of America: Taylor & Francis Group.

Liu, Y. H., Liu, D. L., An, M., Fu, Y. L., Zeng, R. S., Luo, H., Wu, & Pratley, J. (2009). Modelling tritrophic interactions mediated by induced defence volatiles. *Ecological Modelling*, *220*, 3241–3247.

Lyon, G. D., & Newton, A. C. (1997). Do resistance elicitors offer new opportunities in integrated disease control strategies? *Plant Pathology*, *46*, 636–641.

Mandal, S. (2010). Induction of phenolics, lignin and key defines enzymes in eggplant (*Solanum melongena* l.) roots in response to elicitors. *African Journal of Biotechnology*, *9*, 8038–8047.

McSpadden Gardener, B. B., & Fravel, D. R. (2002). Biological control of plant pathogens: Research, commercialisation, and application in the usa.
URL http://www.plantmanagementnetwork.org/pub/php/review/biocontrol/

Moorman, G. W. (2013). Pine diseases.
URL http://extension.psu.edu/pests/plant-diseases/all-fact-sheets/pine-diseases

Moreira, S. L., Xoaquín, & Zas, R. (2009). Defensive responses of *Pinus pinaster* seedlings to exogenous application of methyl jasmonate: Concentration effect and systemic response. *Environmental and Experimental Botany*, *67*, 94–100.

Muilerman, H. (2011). New revolutionary regulation enters in force...but will europe abandon its bad old habits.
URL http://www.pan-germany.info/News/PR/110614.html

Ndeffo Mbah, M. L., & Gilligan, C. A. (2013). Optimal control of disease infestations on a lattice. *Mathematical Medicine and Biology*.
URL doi:10.1093/imammb/dqt012

Nicholson, R. L., & Hammerschmidt, R. (1992). Phenolic compounds and their role in disease resistance. *Annual Review of Phytopathology*, *30*, 369–389.

Nix, S. (2013). The deadly coniferous tree diseases.
URL http://forestry.about.com/od/forestdiseases/p/con_dis_worst.htm

Pathak, S., & Maiti, A. (2012). Pest control using virus as control agent: A mathematical model. *Nonlinear Analysis: Modelling and Control*, *17*, 385–418.

Pieterse, C. M. J., L.-Reyes, A., Van der Ent, S., & Van Wees, S. C. M. (2009). Networking by small-molecule hormones in plant immunity. *Nature Chemical Biology*, *5*, 308–316.

Pimentel, D. (2002). Agricultural chemicals and the environment. In R. Lal, D. O. Hansen, N. Uphoff, & S. Slack (Eds.) *Food Security and Environmental Quality in the Developing World*, (pp. 205–213). Boca Raton, FL: CRC / Lewis Publisher.

Polking, J. C. (2009). Ode software for matlab.
URL http://math.rice.edu/~dfield/

Pontryagin, L., Boltyanskii, V. G., Gamkrelidze, R. V., & Mishchenko, E. F. (1962). *The Mathematical Theory of Optimal Processes*. New York, USA: Wiley-Interscience.

Radman, R., Saez, T., Burke, C., & Keshavarz, T. (2003). Elicitation of plants and microbial cell systems. *Biotechnology and Applied Biochemistry*, *37*, 91–102.

Rafikov, M., & de Holanda Limeira, E. (2012). Mathematical modelling of the biological pest control of the sugarcane borer. *International Journal of Computer Mathematics*, *89*, 390–401.

Reglinski, T., Dann, E., & Deverall, B. (2007). Integration of induced resistance in crop production. In D. Walters, A. Newton, & G. Lyon (Eds.) *Induced resistance for plant defence: A sustainable approach to crop protection*, (pp. 201–228). Singapore: Blackwell Publishing.

Reglinski, T., & Dick, M. (2005). Biocontrol of forest nursery pathogens. *NZ Journal of Forestry*, *November*, 19–26.

Reglinski, T., Elmer, P., Vanneste, J., Hoyte, S., Wurms, J., K. Taylor, Parry, F., Ah Chee, A., Yu, J., Cornish, D., Stewart, A., Hill, R., & Stark, C. (2011). Control of psa using beneficial microbes and elicitors. In *2011 Momentum Kiwifruit Conference*. TECT Arena, Tauranga, New Zealand.

Reglinski, T., Stavely, F. J. L., & Taylor, J. T. (1998). Induction of phenylalanine ammonia lyase activity and control of *Sphaeropsis sapinea* infection in *Pinus radiate* by 5-chlorosalicylic acid. *European Journal of Forest Pathology*, *28*, 153–158.

Reglinski, T., Taylor, G., J. Northcott, Ah Chee, A., Rodenburg, N., & Hill, R. (2012). Differential effects of biotic and abiotic elicitors on defence and physiology in *Pinus radiata*. In *FOA - MAF 10th Annual Forest Biosecurity Workshop*. Bio-Protection Research Centre, Canterbury, New Zealand.

Reglisnki, T., Rodenburg, N., Taylor, J. T., Ah Chee, A., Spiers, T. M., & Hill, R. A. (2012). *Trichoderma atroviride* promotes growth and enhances systemic resistance to *Diplodia pinea* in radiata pine (*Pinus radiata*) seedlings. *Forest Pathology*, *42*, 75–78.

Schaffer, W. M. (1983). The application of optimal control theory to the general life history problem. *The American Naturalist*, *121*, 418–431.

Soylu, S., Baysal, O., & Soylu, E. M. (2003). Induction of disease resistance by the plant activator acibenzolar-s-methyl (asm) against bacterial canker (*c*lavibacter michiganensis subsp. *m*ichiganensis) in tomato seedlings. *Plant Science*, *165*, 1069–1075.

Strange, R. N., & Scott, P. R. (2005). Plant disease: A threat to global security. *Annual Review of Phytopathology*, *43*, 83–116.

Teniente, L. M., Pacheco, I. T., Chavira, M. M. G., Velazquez, R. V. O., Ruiz, G. H., Oliver, A. M., & Gonzàlez, R. G. G. (2010). Use of elicitor as an approach for sustainable agriculture. *African Journal of Biotechnology*, *9*, 9155–9162.

Thakur, M., & Sohal, B. S. (2013). Role of elicitors in inducing resistance in plants against pathogen infection: a review. *ISRN Biochemistry*.

Underwood, N. C. (1998). The timing of induced resistance and induced susceptibility in the soybean - mexican bean beetle system. *Oecologia*, *114*, 376–381.

Underwood, N. C. (1999). The influence of plant and herbivore characteristics on the interaction between induced resistance and herbivore population dynamics. *The American Naturalist*, *153*, 282–294.

Van Loon, L. C. (1997). Induced resistance in plants and the role of pathogenesis-related proteins. *European Journal of Plant Pathology*, *103*, 753–765.

van Maanen, A., & Xu, X.-M. (2003). Modelling plant disease epidemics. *European Plant Disease Epidemics*, *109*, 669–682.

Vanderplank, J. E. (1982). *Host-pathogen interaction in plant disease*. New York, USA: Academic Press.

Vivas, M., Martín, J. A., Gil, L., & Solla, A. (2012). Evaluating methyl jasmonate for induction of resistance to *Fusarium oxysporum*, *F. circinatum* and *Ophiostoma novo-ulmi*. *Forest System*, *21*, 289–299.

Walters, D. (2009). Introduction. In D. Walters (Ed.) *Disease control in crops: Biological and environmentally friendly approaches*, (pp. 1–6). Singapore: Blackwell Publishing.

Walters, D., Walsh, D., Newton, A., & Lyon, G. (2005). Induced resistance for plant disease control: Maximizing the efficacy of resistance elicitors. *Phytopathology*, *95*, 1368–1373.

Walters, D. R. (2010). Induced resistance: Destined to remain on the sidelines of crop protection? *Phytoparasitica*, *38*, 1–4.

Walters, D. R. (2011). *Plant defense: Warding off attacks by pathogens, herbivores, and parasitic plants*. Singapore: Blackwell Publishing.

Walters, D. R., Ratsep, J., & Havis, N. D. (2013). Controlling crop disease using induced resistance: Challenges for the future. *Journal of Experimental Biology*, (pp. 1–18).

Whittle, A. J., Lenhart, S., & Gross, L. J. (2007). Optimal control for management of an invasive plant species. *Mathematical Biosciences and Engineering*, *4*, 101–112.

Xiao, Y., & van den Bosch, F. (2003). The dynamics of an eco-epidemics model with biological control. *Ecological Modelling*, *168*, 203–214.

Xu, X. M., Salama, N., Jeffries, P., & Jeger, M. J. (2010). Numerical studies of biocontrol efficacies of foliar plant pathogens in relation to the characteristics of a biocontrol agent. *Phytopathology*, *100*, 814–821.

Zadoks, J. C., & Schein, R. D. (1979). *Epidemiology and Plant Disease Management*. New York, USA: Oxford University Press.